INFORMATION TO USERS

This manuscript has been reproduced from the microfilm master. UMI films the text directly from the original or copy submitted. Thus, some thesis and dissertation copies are in typewriter face, while others may be from any type of computer printer.

The quality of this reproduction is dependent upon the quality of the copy submitted. Broken or indistinct print, colored or poor quality illustrations and photographs, print bleedthrough, substandard margins, and improper alignment can adversely affect reproduction.

In the unlikely event that the author did not send UMI a complete manuscript and there are missing pages, these will be noted. Also, if unauthorized copyright material had to be removed, a note will indicate the deletion.

Oversize materials (e.g., maps, drawings, charts) are reproduced by sectioning the original, beginning at the upper left-hand corner and continuing from left to right in equal sections with small overlaps. Each original is also photographed in one exposure and is included in reduced form at the back of the book.

Photographs included in the original manuscript have been reproduced xerographically in this copy. Higher quality 6" x 9" black and white photographic prints are available for any photographs or illustrations appearing in this copy for an additional charge. Contact UMI directly to order.

UMI®

Bell & Howell Information and Learning
300 North Zeeb Road, Ann Arbor, MI 48106-1346 USA
800-521-0600

Mechanism of the onset of detonation in blast initiation

by

Kiumars Mazaheri Body

Department of Mechanical Engineering
McGill University
Montreal, Quebec, Canada

A thesis submitted to the
Faculty of Graduate Studies and research
in partial fulfillment of the requirement for the degree of
Doctor of Philosophy

May 1997

Abstract

The problem of blast initiation of gaseous detonation has been studied by focusing on the onset of detonation, i.e. the development of a pressure pulse during the quasi-steady period which leads to an abrupt acceleration to form a self-sustained detonation. This study has been carried out by numerical simulation of the one-dimensional Euler equations in a planar geometry. For the chemical kinetics model, a single-step Arrhenius law was assumed. It was found that for the critical energy required to initiate a detonation, the onset starts with the development of a pressure pulse between the reaction front and the shock front. The formation of the pressure pulse was attributed to the rapid energy release in the long induction length during the quasi-steady period. It was observed that within the framework of the present analytical model of a single-step Arrhenius rate law without losses, it is difficult to define a precise value for the critical initiation energy. However, the abrupt increase in the run up distance when the initiation energy reaches some critical range can be used to define the critical initiation energy. The present results show that initiation process has the same mechanism for both stable and unstable detonations. However, for unstable detonations when the activation energy is very high, no unique value can be defined for the critical initiation energy. It was found that analytical models based on the Zeldovich criterion cannot predict the critical initiation energy over the full range of activation energies considered in this study. This is because the Zeldovich criterion does not consider any dynamic effects during the quasi-steady period. Comparing previous research on initiation which used other initial conditions and the "blast initiation" which was studied in the present work, it was concluded that the onset of detonation during the quasi-steady period has the same mechanism for "deflagration to detonation transition" and "direct initiation". The role of hot spots in detonation onset was also studied. A single temperature perturbation was used to generate a hot spot. It was observed that the effect of the hot spot is mainly a gasdynamics effect. Hot spots promote onset through a multi-step shock merging mechanism. An optimum perturbation amplitude which can facilitate the initiation faster has been identified.

Résumé

Le problème de l'initiation des détonations gaseuses par onde de choc est étudié, en mettant l'emphase sur la formation de la détonation, i.e. le développement d'un pic de pression dans la période quasi-statique, et son accélération marquée pour former une détonation auto-soutenue. Cette étude consiste en l'analyse numérique des équations de Euler de dimension 1, dans une géométrie planaire. Une loi d'Arrhenius simple est utilisée comme modèle de cinétique chimique. Il est observé que pour l'énergie critique requise pour initier une détonation, la formation débute avec le développement d'un pic de pression entre le front de réaction et le front du choc. La formation de ce pic de pression est attribuée à un fort dégagement d'énergie au sein de la longue zone d'induction chimique dans la période quasi-statique. Il est aussi observé que dans le cadre du présent modèle numérique de la loi de réaction d'Arrhénius en une étape et sans pertes, il est difficile de définir de façon précise l'énergie d'initiation critique. Cependant, l'accroissement marqué dans la distance de formation lorsque l'énergie d'initiation atteint une certaine plage critique peut être utilisé pour définir l'énergie d'initiation critique. Les présents résultats démontrent que le mécanisme d'initiation est le même pour les détonations stables et instables. Par contre, pour les détonations instables, lorsque l'énergie d'activation est très élevée, aucune valeur unique ne peut être définie pour l'énergie d'initiation critique. Il est aussi demontré que les modèles analytiques basés sur le critère de Zeldovich ne peuvent pas prédire l'énergie critique d'initiation pour toutes les énergies d'activation considérées dans cette étude. Ceci est dû au fait que le critère de Zeldovich ne considère aucun effet dynamique dans la période quasi-statique. En comparant d'autres travaux portant sur différentes conditions initiales, à celui-ci portant sur l'initiation par onde de choc, il est conclu que la formation de la détonation est régie par le même mécanisme, qu'il s'agisse d'une transition à partir d'une déflagration, ou d'une initiation directe. Le rôle des points chauds dans la formation de la détonation est aussi étudié. Une perturbation de température singulière est utilisée pour générer un point chaud. Il est observé que l'effet des points chauds est principalement relié à la dynamique des gaz. Les points chauds favorisent la formation de la détonation par un mécanisme de convergence de chocs en plusieurs étapes. Une valeur optimale de l'amplitude de perturbation pouvant accélérer le processus de formation est identifiée.

Dedicated to:

The unfulfilled dream of my late father

and

the ever-lasting love and support of my mother.

Acknowledgments

This work would not be complete without recognizing the essential contributions of several individuals. I am especially indebted to:

My wife and my sons, for their understanding and patience during a time of constant "non-existence" and "unusual neglect."

My supervisor, Prof. John H. Lee, from whose keen physical insight I have gained so much. I would like to thank him for his invaluable guidance throughout the course of this work.

Dr. Randy Chue, for his invaluable encouragement, friendship, and many discussions throughout the course of this work.

Sincere thanks are due to Prof. R. Baliga, from whom I have learned a great deal, not only from his excellent teaching of CFDHT, but also from his love of science.

I gratefully acknowledge fruitful scientific exchanges with Prof. R. Knystautas, Prof. J. Shepherd, Prof. A. Dremin, Prof. A. Bourlioux, Dr. F. Zhang, and Dr. L. He during different stages of this work.

The assistance and encouragement from all members of the Shock Wave Physics Group, past and present, and from Mr. Raymond Comeau during my stay at McGill is gratefully acknowledged. I thank Prof. D. Frost for his understanding in providing the computer facilities.

My special thanks go to: Dr. Andrew Higgins for his editorial comments and very stimulating discussions during the preparation of the final version of the thesis, Mr. Jean-

Philippe Dionne who supplied the French version of the Abstract, and Ms. Michele Shemie for her assistance with different aspect of this work.

I would like to extend my appreciation towards my past teachers, the late Prof. F. Ghahremani and Prof. M. Molki, for their encouragement and advice which have had an invaluable role in the continuation of my scientific career.

My heartfelt thanks go to my late father, my dear mother, and my sisters and brothers; I am deeply indebted to them for their encouragement and support throughout my academic life.

Last, but far from least, I express my thanks to the Ministry of Culture and Higher Education of the Islamic Republic of Iran for making my post-graduate studies possible by awarding me a scholarship and to their special advisor Dr. R. Hosseini for his sincere dedication to his job. I understand that my training abroad has been very costly to my country, specially during this difficult economic time.

Table of Contents

List of Figures

List of Tables

Nomenclature

C	Chemical source term
CFL	Courant-Friedrichs-Lewy condition
CJ	Chapman-Jouguet detonation
D	detonation velocity
d_c	critical tube diameter
D_{CJ}	Chapman-Jouguet detonation velocity
DDT	Detonation to Deflagration Transition
e	total internal energy
E_a	activation energy
E_c	critical initiation energy
E_o	initiation energy
E_s	source energy
F	flux vector
f	factor of overdriven (defined as: $(D/D_{CJ})^2$)
G	Geometry source term
hrl	half reaction length
I	numerical constant in blast theory (used in Eq. 3.1)
J, and j	geometry index (0, 1, and 2 for planar, cylindrical and spherical geometries, respectively)
K_j	geometry factor (1, 2π, and 4π for planar, cylindrical and spherical geometries, respectively)
L_c	Characteristic length for non-dimensionalization (half reaction zone thickness of ZND detonation)

M	Mach number
M^*	shock critical strength (Mach number)
M_S	shock Mach number
M_{sh}	shock Mach number
n	time index
p	pressure
p_o	initial pressure
P_{sh} and p_{sh}	shock pressure
Q	heat release per unit mass of the reactant
R	specific gas constant
R^*	shock critical radius
R_S	shock radius
S	Source term
SWACER	Shock Wave Amplification by Coherence Energy Release
t	time
T	temperature
t_c	characteristic time for non- dimensionalization
T_{sh}	shock temperature
U	vector of conservative variables
u	particle velocity
w	reaction rate
x	distance
X_{sh} and x_{sh}	shock location
ZND	Zeldovich-von Neuman-Doring detonation

Greek symbols:

κ	non-dimensional pre-exponential factor in Arrhenius law
κ	detonation front curvature
Δ	induction length
τ	induction time
γ	specific heats ratio
ρ	density
λ	detonation cell size
β	reaction progress variable (β=1 for reactants and β=0 for products)

Subscripts:

L	Left
R	Right
o	initial condition, unburnt mixture properties
CJ	Chapman Jouguet properties
sh	shock condition

Chapter 1

Introduction

1.1. Background

In general, a combustible mixture can support two modes of combustion: deflagration and detonation. In the deflagration regime, in the limit it can burn as a laminar flame at a typical velocity of the order of about 0.5 m/s, or it may accelerate to a turbulent flame where velocity can be orders of magnitude higher. The other extreme is the detonation mode, in which a detonation wave propagates at about 2000 m/s amplifying the pressure by a factor of 20 across the wave. It is interesting to note that a diverse variety of propagation mechanisms are responsible for the observed four orders of magnitude change in wave velocity. While the propagation of a laminar deflagration is governed by the molecular diffusion of heat and mass from the reaction zone to the unburned mixture, the propagation of a detonation depends on the adiabatic shock compression of the unburned mixture. To support a detonation at such high speed, the rate of transformation of energy in the reaction zone must be very high. The combustible gas immediately ahead of the reaction front must be heated to such a high temperature as to permit a high reaction rate in the reaction front. This thesis deals with the second mode, i.e. gaseous detonation waves. Detonation is defined as a combustion-supported shock wave with significant pressure and density rise across the wave. The main characteristic of detonation waves is the coupled motion of the shock front and the reaction zone behind it.

The earliest theory regarding detonation waves is the classical Chapman-Jouguet (CJ) theory [Fickett and Davis 1979]. This theory permits the calculation of the average static parameters of detonation (i.e. detonation velocity, pressure rise across the wave, etc.) which agree surprisingly well with experimental observations. The CJ theory is based on thermodynamic equilibrium and does not require a knowledge of the chemical rate processes. Hence, it cannot predict the rate-dependent detonation parameters (i.e., initiation energy, critical tube diameter, etc.). The CJ theory states that the flow downstream of the wave is sonic relative to the shock (this is also called the CJ criterion).

Another important theory of detonations is the Zeldovich-von Neuman-Doring (ZND) theory. This theory considers a one-dimensional steady structure for detonation waves, which consists of a normal shock wave followed by an induction zone and subsequently by a reaction zone. The termination of the reaction zone is the CJ or sonic plane, where the equilibrium states are as predicted by the CJ theory. Experimentally, laminar ZND structure is seldom observed for a self-sustained detonation, since it is unstable to small perturbations. However, this model permits a length or time scale to be determined from the chemical kinetics. The ZND reaction length is typically more than one order of magnitude smaller than the effective reaction zone length of real detonations.

Besides these classic theories, numerous theoretical, experimental, and computational research has been performed in the past four decades on the different aspects of gaseous detonations. Despite these efforts, there is no quantitative theory as yet capable of predicting the parameters of gaseous explosions from first principles based on the thermo-chemical properties of a mixture. For example, it is unclear what minimum energy is required for the initiation of detonation, or under which conditions a detonation wave may transit through a small opening into a big reservoir. Furthermore, whether it is possible or not to detonate a

certain mixture cannot be determined a priori. Among the dynamic parameters of detonation, the minimum energy required for the direct initiation of a detonation in a given explosive has long been considered as perhaps the most direct means of determining the explosive sensitivity by researchers. On the other hand, the initiation process in the critical condition involves all the chemical-gasdynamic interactions observed in self-sustained detonations. Since the propagation of an unstable pulsating detonation is believed to be a process of continuous failure and re-initiation, understanding the initiation problem may be a key to the understanding the propagation mechanism of detonation waves.

The main objective of this thesis is to contribute towards the understanding of the initiation process focusing on the chemical-gasdynamic interactions in the reaction zone. In a broader context, the motivation of this work is to add to the understanding of the dynamics of propagating detonation waves.

1.2. Initiation of detonation waves

Generally, there are two modes of initiation. The combustible mixture can be ignited by a low energy source and burn as a slow flame. Under appropriate conditions, it will accelerate and undergo a transition to detonation. This process is referred to as deflagration to detonation transition (DDT). During DDT the mechanism of the propagation of combustion wave changes from molecular diffusion to convective turbulent transport and autoignition by adiabatic shock compression. In the final phase of DDT, the shock-flame complex is observed to propagate at about half the CJ detonation velocity for a certain period of time, which terminates with the abrupt onset of a detonation wave. This regime of propagation is called the quasi-steady regime. The ignition source plays no role in the DDT process. Com-

prehensive reviews on DDT have been published by Lee *et al.* [1980], Shepherd *et al.* [1992], and Sichel [1992].

The second mode of initiation, direct initiation, is also referred to as the fast mode of generating a detonation wave, where the detonation is formed instantaneously via the rapid deposition of a large amount of energy in a small volume of the combustible mixture. If a sufficient amount of energy is released by the igniter, rapid autoignition takes place behind the generated blast wave and the reaction-coupled shock quickly becomes a CJ detonation. For direct or blast initiation, the energy of the source is the sole parameter that governssucess or failure of detonation initiation. When the critical initiation energy[1] is deposited in a mixture, initially a highly overdriven detonation is formed, where the shock front and the reaction front (the flame) are coupled and move together. Then, the wave decays to a strength about half the CJ velocity in which the shock and the reaction front are decoupled. For a period of time, much longer than the chemical induction time, the shock propagates almost steadily. This so-called quasi-steady period is terminated with an abrupt acceleration of the shock front to an overdriven detonation wave. Finally, the overdriven wave decays to a self-sustained detonation wave. If the initiation energy is slightly smaller than this critical value, the decoupling continues and the shock eventually decays to an acoustic wave.

It is observed that both modes of initiation can be divided in two phases. In DDT the first phase is characterized by laminar and then turbulent flame acceleration and formation of a shock-flame complex. In direct initiation the first phase involves the rapid decay of the blast wave to a sub-CJ velocity where shock front and reaction front are decoupled. The shock-reaction front complex in both DDT and in the critical regime of direct initiation propagates in a quasi-steady period, which terminates with abrupt onset of a detonation wave. Therefore, DDT and direct initiation differ only in the initial phase. The final phase or the so-

[1] The critical initiation energy is defined as the minimum energy required to generate a detonation.

called quasi-steady regime which terminates with the abrupt formation of detonation is common in both process. The initial stage of the turbulent flame acceleration process in DDT is extremely complex. On the other hand, the initial stage of direct initiation is much more amenable to theoretical description. However, the key process of the initiation of a detonation wave is the final transient development of the shock-reaction zone complex. The present study has been focused on the final stage of the onset of detonation. Particularly, the mutual interaction of gasdynamics and chemical kinetics will be studied in detail.

1.3. Previous works

The theoretical description of the initiation problem consists of showing the coupling between the shock wave and the chemical reaction occurring behind it. Due to the complex nature of the interaction of gasdynamics and the chemistry of combustion in detonation structure, an analytical solution of this problem presents formidable difficulties, unless one introduce some simplifying assumptions.

The first theoretical consideration for the gasdynamics of spherical detonations was analyzed by Jouguet, Taylor, and Zeldovich, which is known as the JTZ model. According to this model, a spherical detonation front propagates at a constant CJ velocity irrespective of the magnitude of the initiation energy, even in the limit of zero initiation energy. The possibility of zero initiation energy threw considerable doubt on the validity of this theory. Considering the initiation energy, Lee [1965] proposed the "reactive blast wave" model, which assumed the reaction zone is a discontinuity (infinite reaction rate). Although this model had provided a good solution for strongly overdriven detonations, obviously it was not able to predict any rate-dependent phenomenon such as the various degrees of coupling occurring in

an initiation process. The infinite reaction rate assumption destroys the coupling mechanism between gasdynamics and chemical kinetics. Therefore, models based on this assumption cannot describe a number of important experimental observations such as the existence of a critical energy for direct initiation. However, by considering a finite rate for the chemical reaction, the set of non-linear gasdynamics-chemical kinetics equations should be solved simultaneously, which is mathematically very difficult (if possible at all). In principle this can be achieved by using the numerical approaches. In 1970, Bach and Lee [1970-b] proposed a phenomenological model. In their model, the coupling between the shock and the reaction front was modeled by a so-called effective chemical energy, which depended on the local shock strength, the shock radius, and on the induction zone thickness. However, since this model ignored the effect of chemical kinetics on gasdynamics, it was not capable of predicting the transition process and the critical condition. These limitations led Kyong [1972] to use numerical simulation to analyze the initiation problem. Due to the poor numerical method used at that time, this simulation could not provide much more information than Bach-Lee model. The main objective of these works had been to predict the shock trajectory in the initiation process. Although the above works were relatively successful in predicting the initial phase of direct initiation, the quasi-steady period and the abrupt onset of detonation were not explored by them. This was due to the fact that the complex coupling of gasdynamics and chemical reaction during the second phase of initiation does not lend itself to simple phenomenological modeling.

The first work to predict the critical initiation energy was the pioneering study of Zeldovich *et al.* [1956]. They stated that for successful initiation, the shock should have a minimum strength (i.e., CJ strength) when it has propagated a distance at least of the order of the chemical induction length. They proposed a criterion which is still the framework of many current theories. This criterion shows the dependence of the critical initiation energy, E_c, to

chemical induction length, Δ, (i.e., $E_c \sim \Delta^3$ for spherical detonations). Since in this criterion the constant of proportionality is missing, it has been the subject of further research.

In the framework of strong blast theory, Lee [1966] recast the Zeldovich criterion to a form for quantitative determination of critical energy. If the induction length is determined based on a steady structure for the detonation wave, the critical energy calculated based on Lee's formulation of the Zeldovich criterion is found be three orders of magnitude less than the experimental values. However, the correct order of magnitude of the critical initiation energy is obtained if an experimentally determined reaction zone thickness is used instead of the steady reaction zone thickness [Lee 1977]. In middle of 70's several models were proposed to calculate the critical initiation energy which included the effect of the finite rate of chemical reactions through experimental length or time scales. These models all were based on the Zeldovich initiation theory. They all have stated that for successful initiation, by the time the blast has decayed to some critical strength (say, M^*), the shock radius must not be less than a certain critical value (i.e., R^*). This critical value is specified by a balance between initiation energy and the chemical heat release. The difference between these models is in the way the critical condition is defined. Among them more popular are the kernel model of Lee *et. al* [1976], the Sichel model [1977], hydrodynamic thickness model of Edwards [1976], and chemical energy model of Korobeinikov [1972]. A comprehensive review of these models and a comparison to experiment has been published by Benedick *et al.*[1986].

For the onset of a detonation wave in the critical regime, a re-establishment or amplification process in the quasi-steady period is necessary. The models discussed above, based on an energy balance in the first phase of initiation, do not consider the re-establishment process. Therefore, a prediction of the different degrees of coupling cannot be expected from

them. On the other hand, the critical strength of the shock which is required in these models is mainly arbitrary and based on ad hoc assumptions. This drawback has limited the usefulness of these models to a certain range of fuel-air mixtures. Nevertheless, these models are the only available means for estimating the correct order of magnitude of the critical initiation energy.

Recently, a new criterion has been proposed by He and Clavin [1994], to predict the critical initiation energy for a curved detonation. He-Clavin formulation is an extension of the ZND model for a curved detonation. In the framework of square-wave model, they derived a relationship between the detonation velocity, D, and the front curvature, κ. Their formulation is based on the quasi-steady motion of the detonation front. They showed that there exists a maximum detonation front curvature above that no steady propagation of detonation is possible. Then, using the strong blast theory, they correlated this critical condition to the critical initiation energy. The critical initiation energy calculated with this theory is about one order of magnitude higher than the value calculated by a numerical simulation of the full unsteady problem. This is the first theory which predicts the critical initiation energy, only based on the thermo-chemical properties of mixtures. Nevertheless, the main drawback of the previous models still persists in this theory. The essence of the initiation criterion is similar to the kernel model. Indeed, only a different kernel size and shock strength in critical condition are proposed by He and Clavin.

Since the critical energy is a quantitative measure of detonability, there have been numerous experimental works in the past forty years devoted to measuring and cataloguing it for different mixtures [Bull 1979, Benedick *et al.* 1982, 1984, Lee 1977, Matsui and Lee 1979, etc.]. Many researchers have tried to correlate it to some characteristic length of detonation structure such as cell size, critical tube diameter, etc. [Lee *et al.* 1982, Desbordes

1986, Benedick *et al.* 1986]. Among those experimental studies only a few contributed towards the understanding of the physical processes involved in transition region. Among them is the observation of the three regimes of initiation based on the amount of the initiation energy. These three regimes have been called Supercritical, Critical, and Subcritical regimes by Bach et al. [1969]. According to their experiments, when the critical initiation energy is deposited in the media, the generated shock decays first to a sub-CJ strength. Then, for a while the structure moves with a quasi-steady velocity about half CJ strength. In this period the shock and the reaction front are decoupled. At the end of this quasi-steady period, local explosion occurs suddenly in the reaction zone which forms a "detonation bubble". This bubble grows and captures the shock front and forms a detonation wave. The basic mechanism of formation and amplification of the local explosion leading to detonation re-establishment was not clear in their experiment. In an effort to elucidate the mechanism of the formation and amplification of a strong shock Lee *et al.* [1978] carried out an investigation on the photochemical initiation of detonation. They proposed SWACER as the mechanism for the formation of a detonation wave in an originally shockless mixture. The Shock Wave Amplification by Coherent Energy Release (SWACER) mechanism is based on the principle that the time sequence of chemical energy release is such that it is coherent with the shock wave it generates, thus adding strength to the shock wave as it propagates. In their experiment, the key feature which led to the amplification was an appropriate sequence of energy release due to a spatial gradient of induction time. Later, Knystautas *et al.* [1979] suggested the same mechanism for the initiation of spherical detonation by a hot turbulent gas jet. Whether or not the same mechanism is responsible for the shock amplification in the quasi-steady period in direct initiation should be addressed.

The success of some correlations based on the detonation cell size in early and middle of 80's [Lee 1984], led many researchers to utilize this length scale to propose new models

for the initiation problem. Among them are Cell Energy Method of Vasiliev et al. [1980], and Surface Energy Model of Lee [1984]. However, later discoveries regarding the dependence of cell regularity on the detonation instability threw some doubt on the extent of the validity of these models [Lee 1991]. The later research of Moen *et al.* [1986], Shepherd [1986], and Lee [1991, 1993] suggested that the dynamic parameters of detonation depend not only on the cell size, but also on the degree of cell regularity which is directly related to the stability of detonation waves. All research up to the middle of the 80's confirmed the universality of the so-called 13 λ correlation between critical tube diameter and the detonation cell size [Lee 1984]. Later studies had revealed that this correlation is valid only for mixtures with high activation energy. Moen *et al.* [1986] demonstrated the breakdown of the $d_c = 13\ \lambda$ correlation for mixtures with high Argon dilution. They found that for C_2H_2 - O_2 with 75% Argon dilution, $d_c = 24\ \lambda$ and later Shepherd *et al.* [1986] reported that for C_2H_2 - O_2 with 80% Argon dilution, $d_c = 20\text{-}30\ \lambda$. For mixtures with high Argon dilution, the cell pattern is found to be highly regular. The link between cell regularity and activation energy was first brought in by Ulyanitski [1981], who observed that mixtures with low activation energies have more regular structure. Reviewing the recent advances in the dynamic structure of detonation waves, Lee [1991, 1993] has suggested that the $d_c = A\ \lambda$ correlation must include a stability parameter. Lee [1993] pointed out two different detonation failure mechanisms for the critical diameter problem. These two failure mechanisms are characteristics of unstable and stable detonations, respectively. For highly irregular structure, the mechanism of ignition is due to hot spots. Thus, failure is due to the inability to form explosion centers in the failure wave, when it has penetrated to the tube axis (mild explosion category). On the other hand, for high Argon diluted case, failure is due to the excessive curvature of the entire detonation front (strong ignition category). Therefore, according to Lee [1993], the breakdown of $d_c = 13\ \lambda$ correlation is due to a different mechanism of re-initiation for stable and unstable

detonations. The existence of two failure mechanisms is consistent with the Oppenheim's classification of ignition. According to Oppenheim [Meyer and Oppenheim 1971], the demarcation line between two regimes of ignition is associated with the temperature sensitivity of the induction time. These results suggest that the critical initiation energy or the direct initiation process may also be affected by the degree of stability of the detonation. As mentioned above, some initiation models, such as the Surface Energy Model of Lee [1984], have explicitly utilized the $d_c = 13\ \lambda$ correlation to determine the critical initiation energy. Therefore, the critical initiation energy and the initiation process may depend on the detonation instability. This fact necessitates a study on the effect of the instability on the initiation process.

Another class of research, which is gaining importance today, is the numerical simulation of the governing gasdynamics-chemical kinetics equations. The first numerical simulation of detonation is the pioneering work of Fickett and Wood [1966]. They showed the oscillatory propagation of the detonation front by numerical simulation of one-dimensional Euler equation. Since then, a large body of research has been performed using the computational approach, with only very few of them emphasizing the physical aspects of the initiation problem. Among them the numerical simulation of the development of gaseous detonations in a non-uniformly preheated mixture by Zeldovich *et al.* [1970, 1988] is particularly interesting. Investigating the process of shock amplification prior to the formation of a self-sustained detonation, they showed that a temperature gradient in a special range may cause the spontaneous formation of a detonation wave. According to Zeldovich *et al.* [1988], if the arrival of a weak pressure wave at a fixed location coincides with the beginning of fast ignition, the pressure wave amplification may be expected. The coupling mechanism between the waves of chemical heat release and the pressure waves is closely connected with the gradient of local properties which affect the rate of reaction such as temperature and reac-

tant radicals. When the pressure wave becomes strong enough to cause vigorous chemical reaction, the mixture will detonate. This is indeed the essence of the SWACER mechanism.

Taki and Fujiwara [1984] showed that an attenuating one-dimensional detonation may be re-established by an explosion in the induction region due to density disturbances prescribed in induction domain. However, in their numerical simulation the mechanism of natural re-establishment of the detonation after the decaying phase was not explored.

One of the most systematic numerical studies of the initiation problem is due to Clarke and coworkers. In a series of numerical studies [Clarke *et al.* 1986, 1989, 1990, Singh and Clarke 1992, Sileem and Kassoy 1990], they investigated the detonation initiation process for different means of generating the precursor shock. The initiation shocks in their works were created via a heat source from a wall [Clarke *et al.* 1986, 1990], the generation of a strong shock by a piston [Clarke and Singh 1989, Singh and Clarke 1992], and heat addition from a thin layer adjacent to the wall for a finite period of time [Sileem and Kassoy 1990]. Due to the initial condition, their works correspond to the "slow" mode of the formation of detonation or DDT. However, the emphasizes of these works have been on the second phase of initiation which is common in both modes of initiation. Clark *et al.* [1986] followed the history of events that are initiated by the addition of a large amount of heat power through a solid surface at x=0. They showed that a strong shock is established following deposition of the energy at the wall. The shock becomes the trigger to switch on vigorous chemical activity in its wake. Their calculations suggested that a detonation always forms upon deposition of power, no matter how little energy is deposited. They also observed [1990] that the reduced reaction rate results in formation of a detonation behind the precursor shock, and not by acceleration of the reaction front which overtakes the front. Sileem *et al.* [1991], concluded that the essential feature of detonation onset is the development of a reaction front in the gas that

has been conditioned by the lead shock. Singh and Clarke [1992] concluded that despite different methods of generating the precursor shock (i.e., different initial conditions), the appearance of a so-called "triplet" is a common feature in the formation of a self-sustained detonation. The "triplet" is a combination of the shock wave, the unsteady reaction domain behind the shock, and the quasi-steady fast flame (deflagration) downstream of that. Not only the appearance of the "triplet", but also the subsequent events (i.e., the formation of a pressure pulse and its amplification to an overdriven detonation) appears to be the same for the three different initial conditions used. It is expected that the same trend will be observed in the second phase of blast initiation in critical regime. Clarke *et al.* [1986, 1990] also pointed out that the diffusion does not play a role in the propagation of the triplet and the amplification process. This conclusion reduces the numerical modeling of the initiation process to simulation of the Euler equations. The studies of Clarke and his coworkers were restricted to only the observation of the initiation process for different initial conditions. They did not explore the physical mechanism involved in the mutual gasdynamic-chemical kinetic interaction in the quasi-steady period which causes the amplification process. On the other hand, since the initial conditions were different from "direct initiation" as it is defined (for example by Lee 1977), their work cannot be correlated to the problem of the critical initiation energy.

In a more recent work, using numerical simulation, He [1996] reproduced the three regimes of initiation for cylindrical detonations. He showed that the He-Clavin initiation criterion [He *et al.* 1994] is not valid for highly unstable detonations. He-Clavin criterion is based on the curvature effect for a quasi-steady detonation. It appears that the front curvature is not an adequate parameter to characterize the direct initiation process. Numerical simulation shows that the acceleration to detonation in quasi-steady period occurs when the leading shock has decayed to very low velocities, well below the value of minimum detonation velocity at the maximum curvature point predicted by the He-Clavin theory. The formation and

propagation of gaseous detonations are mainly characterized by the "unsteady" gasdynamics-chemical kinetics interaction behind the leading shock in the so-called quasi-steady period. The curvature effect can intensify the unsteadiness in the initiation process, due to faster expansion, but its effect should be studied in the framework of an unsteady analysis.

1.4. Objective of the present work

Despite considerable research, at the present time there still is no model capable of predicting the initiation energy without using of some experimental data. The lack of a unique characteristic length or time scale to model the complex nonlinear interaction of gasdynamics and chemical kinetics within the structure of detonation waves, prevents current models from being quantitatively correct. The current models can only predict the correct order of magnitude of the critical initiation energy for some fuel-air mixtures. A better understanding of the initiation process may lead to a correlation between physical parameters, different length scales involved in the problem, and the critical initiation energy.

In the critical regime of initiation when the blast decays to a sub-CJ value, the coupling between the reaction front and the shock front breaks down. The formation of a detonation, consequently, depends on the re-establishment process. This process, which occurs during the quasi-steady period, has not been considered in any of the current initiation models. Therefore, it is necessary that the re-establishment process in the quasi-steady period be examined thoroughly. The principle objective of the present research is to elucidate the onset of detonation in the second phase of the critical initiation regime when the blast has decayed to a sub-CJ strength. In particular, the questions that should be addressed are: What is the mechanism of the re-establishment of a detonation after the decoupling has occurred in the

first phase of blast initiation? What is the role of the shock front? And what is the role of the chemical kinetics in the re-establishment process? By answering these questions, the reason why the current initiation models are limited to a certain range of mixtures and why they can predict only the order of magnitude of the critical initiation energy will be understood.

One common assumption in many initiation models is the so-called quasi-steady assumption. This assumption stems from the fact that before the abrupt onset of detonation at the end of quasi-steady period, the detonation front has an almost constant velocity. On the other hand, experimental observations indicate that the onset in the critical regime is due to the formation and explosion of a so-called detonation bubble [Lee 1977] which is an unsteady phenomenon. Furthermore, numerical simulations of initiation (e.g., Clarke *et al.* 1986, 1990) show the generation and amplification of a pressure pulse in the quasi-steady period prior to the abrupt amplification of the shock front, which is an inherently unsteady event. The role of the unsteadiness in the so-called quasi-steady period is another missing factor in initiation models which will be addressed in the present study.

As mentioned in the previous section, detonation instability has a certain effect in some dynamic parameters of detonations. It is suspected that it may have some important effects on the initiation process. As part of the objective of the present study, the effect of the "detonation instability" on the initiation process in the quasi-steady period will be investigated.

Another missing link in the initiation problem is a possible correlation between different modes of initiation (i.e., DDT and "blast initiation"). Clarke and coworkers have demonstrated the similarity between the onset for three different initial conditions (see Section 1.3). However, none of their work was on "blast initiation" as it is defined in literature (e.g., Lee 1977). In this study, using numerical simulation of the "blast initiation" in the critical regime,

the onset in the second phase of blast initiation will be compared with the results of the other initial conditions to find any possible universality of the initiation problem.

Experimental observations of the direct initiation of detonations in a homogeneous explosives have revealed that the onset of detonation develops from discrete hot spots. The hot spots are formed from various gasdynamics fluctuations such as turbulence and shock-boundary layer interactions. Due to the random nature of hot spots, the detailed gasdynamics process of the development of the detonation from hot spots has not been clarified yet. It is only known that "hot spot" refers to a local high temperature region which promotes the reaction rate. Therefore, another important question, which will be addressed after exploring the amplification process, is the effect of hot spots on direct initiation.

1.5. The method of study

Due to the unsteady nature of the transition process in second phase of the initiation process and the equal importance of gasdynamics and chemical kinetics in this process, the mathematical solution of the governing equation, even in the simplest form, is very difficult (if possible at all). The simplest model which may be proposed for this process is the one-dimensional Euler equations and a one-step Arrhenius reaction rate model. This simple model consists of a set of highly non-linear partial differential equations. It seems that the only possible approach to study the detail flow structure is the numerical simulation of these equations. On the other hand, the short review of some of the numerical simulations in previous section showed the capability of numerical simulation and one-dimensional analysis to reproduce many aspects of the highly transient and unstable events of the initiation and propagation of gaseous detonations. The description of the chemical rate process can range

from a single-step Arrhenius rate law to the full set of kinetics rate equations for all the elementary kinetics steps. For a qualitative study of the physics of the problem, a single-step rate law suffices. The major disadvantage of a single-step Arrhenius law is that the induction and reaction processes cannot be varied independently. Furthermore, the different geometries (i.e., spherical, cylindrical, and planar) do not seem to offer any qualitative differences. Of course, with the high capacity and fast computing power of a new generation of computers, and the recent invention of high resolution numerical schemes, the numerical simulation of multidimensional detonations, even with detailed chemistry, is now feasible [Oran 1987]. However, using simple models helps researchers to understand many aspects of the initiation process which cannot be extracted from the tremendous amount of information resulting from a multi-dimensional simulation with detailed chemistry. Therefore, throughout this work, a high resolution numerical code has been developed, which was then employed to elucidate the details of the non-linear gasdynamics-chemical kinetics interactions in the unsteady structure of gaseous detonations.

1.6. Scope and outline of the present work

In this thesis the problem of direct or blast initiation of gaseous detonation waves has been analyzed via numerical simulation of the governing gasdynamics chemical kinetics equations. This study is limited to a one-dimensional planar geometry. A one-step Arrhenius law has been used as the chemical kinetic mechanism. Therefore, no quantitative result comparable with the experimental data can be expected from the present work. Specifically, the mechanism of re-establishment of the detonation front in the critical regime of initiation and its dependence on different parameters are addressed. The thesis is divided into six chapters,

including this Introduction.

In Chapter 2, the details of the numerical code which has been developed by the author is presented. This code is a combination of some numerical schemes in the category of higher-order Godunov method. The governing equations of the problem and the non-dimensionalizing procedure also are presented in this chapter.

The three regimes of initiation have been simulated numerically in Chapter 3 for stable detonations. The problem of the generation of a pressure pulse and its amplification in the so-called quasi-steady period are addressed in this chapter. The correlation between different parameters involved in the initiation process, and the initiation for different values of source energy are also discussed. Specifically, the problem of the existence of a critical initiation energy in the framework of a loss-less model has been investigated in this chapter. In the last section of this chapter, the similarity of the onset by different initial conditions is discussed.

Activation energy is the main parameter which controls the instability of one-dimensional detonations [Chue 1993]. By increasing the activation energy beyond the stability limit, the initiation problem for unstable detonations is studied in Chapter 4. Then, the initiation processes for stable and unstable detonations are compared.

All the calculations mentioned above are initialized for homogeneous mixtures. On the other hand, experimental observations of direct initiation in homogeneous explosives have revealed that the onset of detonation develops from discrete hot spots. Due to the random nature of hot spots, the detailed process of the development of detonation from hot spots is not clear. In a numerical simulation, hot spot formation and its effect on the initiation can be controlled by introducing a single temperature perturbation in the media. This simulation is discussed in Chapter 5. Introducing a disturbance in the quasi-steady period can also promote

the amplification process in the blast initiation problem, which helps to better understand the critical initiation problem.

Finally Chapter 6 is the conclusion of this study. This chapter will also refer to the contribution of the present work to the current knowledge of initiation of detonation waves and some recommendations for future research in this field.

Chapter 2

General Consideration

2.1. Introduction

The purpose of this chapter is to describe all the necessary tools and information utilized in the studying the main problem. The main problem is the numerical simulation of the blast initiation of gaseous detonations. The essential role of simulation is to provide numerical experiments performed in exactly the same physical conditions that are of the interest of the researcher. Therefore, in this chapter, the analytical requirements for the numerical experiment, as well as the numerical code itself, are explained.

2.2. Analytical model

It is well recognized that the essential mechanism responsible for the highly non-linear structure observed in detonation waves can be expressed by a simple model. This model consists of the one-dimensional reactive Euler equations with the Arrhenius law as the chemical reaction mechanism. There are three assumptions in this model. The first assumption is 'one-dimensional' analysis. The main features of the direct initiation are manifested in its longitudinal direction. The numerical simulation of two-dimensional and three-dimensional detonation structure is possible at the present time [Oran 1987], although it is

very computationally intensive. However, there are still important questions which can be addressed by one dimensional analysis. The one-dimensional simulation provides a simpler environment which is needed to understand the basic longitudinal events. In fact, this is the main advantage of the computer simulation, which allows the experiment to be performed in the desired, idealized way. Therefore, although the presence of transverse waves are a necessity for detonation propagation [Lee 1991], they are intentionally neglected in these calculations. The effect of transverse waves on direct initiation has not been studied systematically yet. Edwards *et al.* [1978], investigating the critical initiation regime, reported that they did not observe transverse waves in the quasi-steady period. However, further investigation is needed to clarify the effect of transverse waves on direct initiation.

The second assumption is the neglecting of diffusion. This assumption is widely discussed by many researchers (e.g., Clarke *et al.* 1986, 1990). Indeed, the diffusion time scales are much slower than the chemical and gasdynamics time scales in the initiation process. Therefore the diffusion term can be dropped from the Navier-Stokes equations.

The last assumption is the use of a single-step Arrhenius model for chemical kinetics. Here, again the main reason is to avoid un-necessary complications to the simulation. On the other hand, numerical simulation with the detailed chemistry is very time consuming. Although no real chemical reaction can be modeled by a single irreversible reaction, the Arrhenius law provides the sensitivity of the heat release to the shock temperature and the activation energy in the reaction zone which is observed with more detailed chemistry. The major disadvantage of a single-step Arrhenius law is that the induction and reaction processes cannot be varied independently

The equations of inviscid gasdynamics (i.e., Euler equations) in a fixed frame can be

written in the following non-dimensional form:

$$\frac{\partial U}{\partial t}+\frac{\partial F}{\partial x}=S-JG \tag{2.1}$$

where,

$$U=\begin{pmatrix}\rho\\ \rho u\\ \rho e\\ \rho\beta\end{pmatrix},\quad F=\begin{pmatrix}\rho u\\ \rho u^2+p\\ u(e+p)\\ \rho u\beta\end{pmatrix},\quad S=\begin{pmatrix}0\\ 0\\ 0\\ -\rho w\end{pmatrix},\text{ and }\quad G=\begin{pmatrix}\rho u/r\\ \rho u^2/r\\ u(e+p)/r\\ \rho u\beta/r\end{pmatrix}$$

J = 0, 1, and 2 corresponds to planar, cylindrical and spherical geometry respectively. Here, S and G are, respectively, the source terms due to combustion and geometry. ρ,u, and p are density, particle velocity, and pressure, respectively. β is the reaction parameter which varies between 1 (for unburnt reactant) and 0 (for product), and e is the internal energy per unit mass which is defined as:

$$e=\frac{p}{\rho(\gamma-1)}+\frac{u^2}{2}+Q\beta \tag{2.2}$$

where, Q is the heat release per unit mass of reactant. γ is the ratio of specific heats which is assumed to be constant in these calculations. w is the reaction rate which follows the Arrhenius rate law:

$$w=k\beta\exp(-\frac{E_a}{RT}) \tag{2.3}$$

where E_a is the activation energy, R is the specific gas constant, and T is the absolute temperature. The dependent variables are non-dimensionalized with respect to the unburnt mixture properties. Density is non-dimensionalized with ρ_O , and pressure with γp_O. For the velocity, the sound speed of the unburned mixture, C_O, is used as the reference. The charac-

teristic length scale, L_c, is the length passed by a fluid particle to travel from the leading shock to a position where $\beta = 0.5$ in a ZND structure, the so-called half-reaction length (hrl). This length scale is calculated for a mixture with $Q/RT_o = 50$, $E_a/RT_o = 25$, and $\gamma=1.2$. Hence, the length scale does not change for different mixtures. The characteristic time scale, t_c, is the half-reaction zone length divided by the sound speed in the fresh mixture (i.e., $t_c=L_c/C_o$). The pre-exponential factor in the Arrhenius law is scaled as : $\kappa = k\, L_c/C_o$. Note that the dimension of k in the original Arrhenius law is 1/time. The mixture is assumed to behave like an ideal gas which has the following non-dimensional equation of state:

$$p = \rho T \tag{2.4}$$

2.3. The physical model

When a large quantity of energy E_o is suddenly deposited into a reactive gas mixture within a small size, the gas expansion generates a very strong blast wave and a highly overdriven detonation is formed instantaneously. As the blast wave expands, its intensity decreases. Experimental observations [Lee 1977] show that the transition of this overdriven detonation to a self-sustained CJ detonation is possible only when the deposited energy is larger than a critical value E_c. To study the initiation problem, the propagation of a strong blast wave in a combustible gaseous mixture has been simulated computationally in the present work.

As the initial condition, the point blast model where the early time phenomenon is essentially the decay of a strong blast wave governed by the similarity solution of Taylor [1950] has been utilized. The subsequent decay of the blast wave where chemical reaction comes into play is described by numerical simulation. For a strong blast wave with the shock

Mach number M_S at the location R_S with respect to the center of initiation, the initiation energy is obtained from

$$\frac{E_0}{p_0} \cong R_s^{j+1} \gamma k_j M_s^2 I$$

where, "I" is a function only of γ and should be calculated from the similarity solution of the strong blast wave, p_0 is the pressure of the fresh mixture, and (j, k_j) is (0, 1), (1, 2π), and (2, 4π) for the planar, cylindrical and spherical geometries, respectively. In planar geometry, E_0/p_0 the non-dimensional initiation energy has the same form as the so-called explosion length. Thus, it is non-dimensionalized with half reaction length.

2.4. Numerical method

The essential role of simulation is to provide numerical experiments performed in exactly the same physical conditions that are of interest to the researcher. Because of this, today numerical simulation plays a significant role in dealing with very complex phenomena such as the dynamic structure of unstable detonations. Recent numerical schemes can provide a great deal of information which is very costly to capture with experimental tools, if possible at all.

Over the last 40 years a great number of numerical schemes have been devised for the simulation of compressible gasdynamics. In recent years, a number of new shock-capturing schemes, often called high resolution schemes, have been proposed. Among them are FCT, MUSCL, ENO, and PPM methods. There are several excellent review articles which compare these schemes from different point of views. Interested readers are referred to those articles, particularly the paper of Yang et al. [1992] and the Ph.D. thesis of Bourlioux [1991].

After comparing different schemes, they recommended PPM as the best in overall performance. Therefore, in the present work, PPM is chosen as the main gasdynamics solver. The details of this method are explained in Appendix A.

In analyzing the initiation and propagation of pulsating detonation, the tracking of the shock front has an essential role. In the past twenty years, several methods have been developed to track the front and other discontinuities in flow field. For our purpose, the simplest one is conservative front tracking of Chern and Colella [1987], which has been utilized in the present study.

Due to the presence of length scales on the order of the induction length, it is necessary to use very fine meshes in the simulation of detonation waves. On the other hand, far from reaction zone the effective length scales are much larger than the induction length. Since all reactions are completed in a narrow region close to the shock, it is more economical to use fine meshes only in this region and coarse grids elsewhere. To fulfill this requirement, a simple version of the "Adaptive Mesh Refinement" of Berger and Colella [1989] has been utilized to have an effective and economical representation of the small length scales involving the stiff chemistry near the front. In particular, two sets of uniform grids have been used to discretize the computational domain. The entire domain is covered by coarse grids, and fine meshes are superimposed on coarse grids in the vicinity of front. The details of the shock tracking as well as the mesh refinement strategy which were adopted in this numerical simulation are explained in Appendix A.

One of the most successful simulations of one-dimensional detonations has been due to Bourlioux [1991]. Bourlioux examining different numerical methods, made an outstanding combination of the three numerical schemes explained above. Here, the Bourlioux approach is followed closely. This combination, proved to be very effective at the capturing of differ-

ent discontinuities in the wave structure.

To set up the algorithm, following Sod [1977], Bourlioux [1991], and He [1993], a time splitting method has been used to remove the source terms from the system of equations (2.1). The basic idea behind this splitting method is to resolve any physical process according to its corresponding time scale [Oran 1987]. On the other hand, this fractional scheme has the advantage that the equations preserve their conservative form in cylindrical and spherical geometries, which is a pre-requisite for many numerical methods. The fractional strategy proceeds as follows. First the system:

$$U_t + F(U)_x = 0 \tag{2.5}$$

which represents the one-dimensional equations of gasdynamics in Cartesian coordinates, is solved. The solution of Eq. 2.5 is used as the initial conditions for the system of ordinary differential equations for the geometrical source terms;

$$U_t = -JG \tag{2.6}$$

Finally, the solution of Eq. 2.6 is used as the initial conditions to solve:

$$U_t = S \tag{2.7}$$

the equation for the source term due to chemical heat release. The basic algorithm is of the following form:

$$U^{n+2} = L_H^{\Delta t} L_G^{\Delta t} L_C^{\Delta t} L_C^{\Delta t} L_G^{\Delta t} L_H^{\Delta t} U^n \tag{2.8}$$

where $L_H^{\Delta t}$ shows the numerical solution of the hyperbolic Eq. 2.5. C, and G refer to the geometry and chemical source terms, respectively.

2.4. Code validation

In this section the results of calculations for some test problems, obtained with the code based on the above numerical methods, are presented. These test problems include two inert flows, namely the Sod problem and the Lax problem, the simulation of planar pulsating detonation, the initiation of cylindrical detonation, and the propagation of stable ZND detonation. The outstanding features of the above mentioned numerical methods were shown with several examples in the Ph.D. thesis of Bourlioux [1991]. The objective of these tests is to show the reliability of the code developed by the author.

2.4.1. The Sod problem

The shock tube problem which was used by Sod [1978] to test a number of methods for solving the equations of compressible flow, has become a standard test problem. The initial conditions for this problem consist of two semi-infinite states separated by a diaphragm at time t=0. The left and right states are set to the following conditions:

$$\text{For } x<50.0, \quad \begin{bmatrix} \rho_L \\ u_L \\ p_L \end{bmatrix} = \begin{bmatrix} 1.0 \\ 0.0 \\ 1.0 \end{bmatrix}, \text{ and for } x>50.0, \quad \begin{bmatrix} \rho_R \\ u_R \\ p_R \end{bmatrix} = \begin{bmatrix} 0.125 \\ 0.0 \\ 0.1 \end{bmatrix}$$

with $\gamma = 1.4$. The result of a numerical simulation of Sod's problem at time t=25 obtained from this code is compared with exact solution in Fig. 2.1. The capability of the present code to capture shock and other discontinuities is quite good. To test the grid dependency, the calculations were repeated with 50, 100, and 200 grid point. Figure 2.1 shows that the calculation with 200 grid points is converged to the exact solution. This calculation has been

performed in a constant mesh domain.

2.4.2. The Lax problem

This is also a shock tube problem similar to Sod's, but with one of the two semi-infinite states used as initial conditions is not at rest. The initial conditions are as follows:

$$\text{For } x<50.0,\ \begin{bmatrix}\rho_L\\ u_L\\ p_L\end{bmatrix}=\begin{bmatrix}0.445\\ 0.698\\ 3.528\end{bmatrix},\ \text{and for } x>50.0,\ \begin{bmatrix}\rho_R\\ u_R\\ p_R\end{bmatrix}=\begin{bmatrix}0.5\\ 0.0\\ 0.571\end{bmatrix}$$

with $\gamma = 1.4$. Figure. 2.2 compares the exact solution of Lax problem with a simulation with 200 grid points at time t=15. The agreement is very good.

2.4.3. The pulsating detonation

The ability of a code to capture the stability characteristics near a stability boundary and also in highly unstable cases has been recognized as a measure of a code's abilities [Bourlioux *et al.* 1990,, He *et al.* 1993]. This test has been performed for a mixture with heat release $Q/RT_O = 50$ and $\gamma = 1.2$, while E_a/RT_O, the reduced activation energy, varies between 24.5 and 29.5. In most cases shown here $\Delta x = L_c/2$ for coarse grids and $\Delta x = L_c/10$ for fine grids, where L_c is the half reaction length. (For $E_a/RT_O = 28.5$ and 30, $\Delta x = L_c/4$ and $\Delta x = L_c/20$ have been used for coarse and fine grids, respectively.)

Figure 2.3 shows the shock pressure history for E_a = 24.5 and 25; two stable cases. Thus, the perturbation produced in the transition region of initiation is damped easily. $E_a = 25.5$, is the stability boundary for this mixture. Figure 2.4 shows the propagation of detonation at the stability boundary for two cases with different initiation energies. It is

clearly seen that after a transition period which depends on the initiation energy, the wave eventually propagates in an unstable manner. The oscillation here is very mild and resembles the sinusoidal oscillation of a linear oscillator. The period of oscillation is 12.8, very close to the result of linear stability analysis [Lee and Stewart 1990]. The degree of instability is increased with activation energy [Chue 1993]. For $E_a/RT_o = 26$ the amplitude of oscillation is greater than the previous case, but the period is almost the same (Fig. 2.5-a). For $E_a/RT_o = 27.5$ a new mode of oscillation is observed. Here higher modes appear (Fig. 2.5-b), and the period of oscillation is twice the simple mode. If we continue to increase the activation energy even higher modes will emerge. As Fig. 2.6-a shows for $E_a/RT_o = 28.5$ a period tripling is observed. For $E_a/RT_o = 29.5$, the propagation is completely irregular. Even after a very long time no repeated oscillation is observed in the range of calculations performed here (Fig. 2.6-b). All the above results are very close to the similar calculations which have been performed by Chue [1993], and He *et al.* [1995]. Chue and He used the ZND profile as the initial condition in their simulations, while here a blast wave has been used as the initiator.[2] Nevertheless, detonation propagation characteristics (e.g. the period and amplitude of oscillation), after the initial transients have passed, should be the same, as they are.

2.4.4. The direct initiation of a cylindrical detonation

The next test problem is the blast initiation of a diverging detonation. Figure 2.7 shows the initiation and long term propagation for a cylindrical detonation near the stability limit for three different initiation energies. The three regimes of initiation (i.e. Supercritical, Critical, and Subcritical regimes) are observed. This problem will be discussed thoroughly in next chapters. The only published result for the same case is due to He [1996]. This result is in close agreement with He's results.

---

[2] Longting He has extensively used the blast wave to initiate cylindrical and spherical detonation waves, but in the cases we used as the reference for comparison he used the ZND profiles as initial condition.

2.4.5. The propagation of a steady ZND detonation

This test is taken from Bourlioux [1991]. The ZND solution for the degree of over-driven $f = 1.1$, $\gamma = 1.4$, $E_a/RT_o = 10$, and $Q/RT_o = 10$ has been computed by the present code. The half reaction length of the same mixture is used as the length scale here. The initial condition consists of one shock discontinuity separating the uniform pre-shock state from a constant U_L state corresponding to the ZND solution at the end of the reaction zone (i.e. $\beta \rightarrow 0$). The leading shock velocity after the formation of ZND wave is compared with the theoretical solution in Fig. 2.8 for a very long time. To test the grid convergency, the calculations with three different grids are compared with the exact value. It is observed that with 10 grid points per half reaction length the result of the simulation has converged to the exact solution. The correct capturing of the leading shock strength (i.e., the von Neuman spike), and keeping it constant for quite a long time, can be accounted as the reliability of the code.

2.5. Conclusion

In this chapter some recent numerical schemes were implemented to construct a computational tool capable of simulating the highly non-linear interaction between gasdynamics and chemical kinetics in the unstable structure of gaseous detonation waves. The reliability of this code has been tested with several benchmark problems. This code has been used to study the mechanism of blast initiation of gaseous detonations for a wide range of the activation energy in a planar geometry.

Chapter 3

The onset of detonation waves in blast initiation

3.1. Introduction

The phenomenon of direct or blast initiation has been well established in the 60's. Using an "instantaneous point source" such as a laser spark, it was found that for a given mixture there exists a critical energy below which the blast decays to an acoustic wave (Fig. 3.1-a). Far above this critical energy, the strong blast decays asymptotically to a CJ detonation (Fig. 3.1 b). For a range of source energies around the critical energy, the blast first decays to a sub-CJ strength before it accelerates back to the CJ velocity. The duration of the sub-CJ period depends on the initiation energy. At the critical value, the blast decays to about half the CJ value and the shock remains at this velocity for a short duration until an abrupt transition to detonation occurs in the form of localized explosion centers developed in the quasi-steady reaction zone (Fig. 3.1-c). As stated in Chapter 1, current initiation models can predict only the correct order of magnitude of the critical initiation energy for a limited range of Fuel-Air mixtures. To have a better understanding about the drawbacks of those models, one typical model will be analyzed and compared with the result of numerical simulation of the complete unsteady gasdynamics-chemical kinetics governing equations.

The qualitative behavior of a blast decaying to a sub-CJ value and its acceleration to CJ detonation can be seen from the following simple consideration of energy conservation. This energy balance is the essence of many phenomenological initiation models (e.g., the Kernel model of Lee *et al.* 1976). At any instant in time when the blast is located at R_S (Fig. 3.2) and the reaction front at R_S-Δ (where Δ is the induction length), the conservation of energy for planar geometry simplifies to the following form [Lee 1977]

$$M_s^2 = \frac{1}{I}\left[\frac{E_0}{C_0^2 R_s(t)} + \frac{Q}{C_0^2}\left(1 - \frac{\Delta}{R_s}\right)^{11}\right] \tag{3.1}$$

where M_S is the blast Mach number, E_O is the initiation energy, C_O denotes the speed of sound in unburnt mixture, and Q is heat release per unit mass of the reactant. For a strong blast (γ = 1.2 and planar geometry) I has a value of 2.622. When it decays to low velocities in the quasi-steady period, according to Kernel model, "I" is calculated from its final CJ value:

$$I = \frac{Q}{C_0^2\, M_{CJ}^2} \tag{3.2}$$

In the early period of blast decaying, when the blast is strong, the first term in Eq. 3.1 dominates and the shock strength M_S^2 decays like $1/R_S$. "Δ" becomes significant for low shock strengths near the autoignition limit (at about half of the CJ velocity). When the blast radius, R_S, becomes large the first term vanishes and since $R_S >> \Delta$, the shock Mach number goes to a constant value (i.e., the CJ value). Figure 3.3 shows the shock strength versus its radius as given by the energy conservation Eq. 3.1. The decaying phase of the blast is shown, as well as the increasing strength of the shock wave, driven by the liberation of chemical energy. The sum of these two sources is also shown as a dashed line. It is seen that this simple energy balance can reproduce the qualitative behavior of the leading shock in the critical regime; the shock decays to a sub-CJ value before acceleration to form a CJ detonation. In Fig. 3.4-a the result of a numerical simulation using the code described in Chapter 2 is

shown. The same problem as Fig. 3.3 is again considered (the same mixture properties and source energy). The solution in Fig. 3.4, however, can be viewed as the exact solution of the governing unsteady equations of the coupled gasdynamics and chemical kinetics. The simulation predicts successful initiation for the same source energy as Fig. 3.3. However, the sub-CJ period is more pronounced and of longer duration than estimated in Fig. 3.3. The onset of detonation is also accompanied by an overshoot in shock strength. If the source energy is reduced from 1765 to 1614, the blast wave continues to decay to an acoustic wave and no initiation is observed (Fig. 3.4-b). If we construct a plot of the shock strength predicted by the energy equation according to the simple model (Eq. 3.1) for a subcritical case (i.e., E_0/P_0=1000), the result (see Fig. 3.5) is not that different than the earlier plot for critical initiation (Fig. 3.3). In fact comparing Figs. 3.3 and 3.5, it is difficult to identify a feature which would introduce one result a successful initiation and the other a failure. But when the complete coupled gasdynamics and combustion equations are solved, we observe very different result. In fact since no chemical kinetics involved in this model, it cannot predict the different degree of coupling between the shock front and the reaction front. This drawback causes that those phenomenological models such as the Kernel model predict only the correct order of magnitude of the critical initiation energy. This prediction is based on a criterion which is usually imposed by the researcher based on experimental observation. For instance in Kernel model, the shock Mach number in the critical condition is considered to be about the autoignition value (M_S^*). The critical condition is defined as the condition in that two terms of Eq. 3.1 are equal. Then, given this autoignition strength, M_S^*, and an experimental induction length, Δ, the critical initiation energy may be calculated from Eq. 3.1. To gain enough insight regarding the initiation problem the details of the gasdynamics-chemical kinetics interaction during the initiation process should be investigated in the critical regime of initiation. The key process of the initiation of a detonation wave is the final transient development

of the shock-reaction zone complex. In this chapter our attention is focused on this final stage of the so-called "onset" of detonation phenomenon. In particular, the mutual interaction of gasdynamics and chemical kinetics is studied in detail. This study has been performed by numerical simulation of the governing gasdynamics-chemical kinetics equations in a one-dimensional planar geometry. All investigations in this chapter corresponds to stable detonations. According to linear stability analysis [Lee and Stewart 1990], for a mixture with Q/RT_o=50 and γ = 1.2, if the reduced activation energy E_a/RT_o is lower than 25.5, the self-sustained detonation will propagate at a constant (i.e., CJ) velocity. The problem of the onset of unstable detonations will be studied in Chapter 4. The details of the governing equations and numerical methods have already been described in Chapter 2.

3.2. Results

3.2.1. The three regimes of initiation

The numerical simulations of the three regimes of initiation are shown in Fig. 3.6. In this figure the leading shock pressure (P_{sh}) is plotted as a function of the shock radius (x_{sh}). This figure corresponds to a mixture with Q/RT_o = 50, E/RT_o = 24, and γ = 1.2. The dotted line shows the non-dimensional pressure at the von-Neuman spike of the corresponding self-sustained CJ detonation. The three curves correspond to subcritical, critical, and supercritical initiation regimes, where the non-dimensional initiation energies (i.e., E_o/P_o) are 1614, 1765, and 3415, respectively. In the early times of blast wave propagation, the shock pressure decays rapidly as in a strong non-reactive blast wave (i.e., $M_s \sim 1/R_s$). If the initiation energy is below a critical value, it is found that the blast wave progressively decays to an acoustic wave. This regime is referred to as the Subcritical regime. On the other hand, if the initiation

energy greatly exceeds the critical value, the blast decays asymptotically to a strength of the CJ value, forming a self-sustained detonation wave at x=50. This regime is called supercritical initiation. Near the critical initiation energy, the phenomenon is more interesting. The decaying process slows down when shock reaches about x=30. A simple energy balance shows that this point is very close to the location where the total chemical heat release is equal to the value of the initiation energy, i.e.,

$$\frac{E_0}{P_0} \cong \Delta x\, Q \qquad \Rightarrow \qquad \Delta x \cong 35$$

Then, for a short period, the shock front propagates at an almost constant velocity. This phase of the blast initiation is called the quasi-steady period. For future reference, the beginning of the quasi-steady period shall be defined as the location where the initiation energy equals the total chemical heat release. The end of the quasi-steady period is considered as the location with the same shock strength as the beginning point. The quasi-steady period is terminated by an abrupt acceleration of the shock front to form an overdriven detonation wave. This overdriven detonation then decays asymptotically to a self-sustained CJ wave. This regime of initiation is called the critical regime of initiation. The three regimes of initiation first were observed experimentally by Bach *et al.* [1969]. The terminology for the initiation process in the critical regime is defined in Fig. 3.7. The quasi-steady period is shown as the distance between x=30 and 115. The shock pressure varies between 19 and 24 in this interval, corresponding to the shock Mach number between 4.6 and 5.3. Two important parameters in the critical initiation regime are the shock "overshoot" and the "run up distance". The degree of "overshoot" in shock pressure at the end of the quasi-steady period is measured with respect to the shock pressure of the corresponding ZND detonation. In Fig. 3.7, the maximum pressure is about 65 which is approximately twice the corresponding steady ZND detonation. Another important parameter in the critical initiation regime is the run up distance. The dis-

tance between the center of initiation and the location of the maximum shock pressure shall be referred as the run up distance. The run up distance corresponding to this case is about 130. This distance is an indication of how far from the center of ignition a detonation wave is formed. The acceleration after the quasi-steady period from p_{sh}=24 to p_{sh}=65 occurs in a distance of about 15. This rate of change of the shock pressure is comparable with the early decay of the blast wave over the same pressure range. It is interesting to compare the rate of the change of the shock pressure in three phases, the early decaying, the quasi-steady period, and the rapid acceleration phase. $\Delta P_{sh}/\Delta x$ will be about 3.2, 0.12[1] and 2.7, in these three phases respectively. Due to the very small rate of the change of Psh in the second phase (i.e., 0.12), it has been called the quasi-steady period. The quasi-steady velocity of the leading shock during the quasi-steady period does not imply a steady flow structure behind the shock, an assumption made in previous analysis of the initiation problem (e.g., Lee 1977, Edwards 1976). In fact the flow structure will be shown to be very transient during the quasi-steady period later in this chapter.

More insight about the difference between the three regimes of initiation can be gained by studying the relative motion of the reaction front with respect to the leading shock which will be referred to as the "coupling" phenomenon in this text. In general a self-sustained detonation wave is characterized by its unique coupling between the reaction zone and the shock front. The point of the maximum heat release which is very close to the location of the maximum temperature gradient, shall be defined as the reaction front. The relative motion of these two fronts can be investigated from temperature profiles. The temperature profiles for the three regimes are shown in Figs. 3.8 and 3.9. Figure. 3.8-a shows the temperature profiles at several subsequent times during the blast decaying of the subcritical regime. The temperature is plotted versus the distance from the point of initiation in this figure. Each profile in-

[1] For the quasi-steady period the value of this parameter corresponds to the distance between the minimum state and the end of this phase.

volves two sharp temperature rises. The first jump (from the right of each profile) corresponds to the shock front. Then, for a short distance from the shock, the temperature remains almost constant. This distance corresponds to the chemical induction zone. After this length, the second fast temperature rise is observed. This sharp temperature rise is due to the rapid chemical heat release. The distance between the shock front and the point of maximum reaction rate will be defined as the induction length of the chemical reaction. As an example, for the last profile in Fig. 3.8-a, the shock is located at about x=145, and the reaction front is around x=122. Therefore, the distance between two fronts, (i.e., the induction length), at this moment is about 23. It is clearly observed that, in the early time after initiation, when the blast is still strong, the two fronts are coupled. As the blast propagates, the distance between two fronts progressively increases. At the other extreme, for the supercritical initiation, Fig. 3.8-b shows a different behavior. In this regime, it is observed that even after x=130 two fronts are coupled. This coupled motion of the two fronts is, in fact, the main characteristic of a self-sustained stable detonation.

The coupling phenomenon is more interesting in the critical regime. In this regime, which is shown in Fig. 3.9, the decoupling is started when the shock reaches about x=28. Then, the distance between two fronts increases (Figs. 3.9-a and 3.9-b). Near the end of the quasi-steady period, the distance between two fronts decreases and the shock begins to accelerate. This can be seen in Fig. 3.9-c after x=115. Finally, two fronts become completely coupled at about x=125.

Some very important observations regarding the time evolution in the quasi-steady period can be made from the analysis of the pressure profiles. The pressure profiles for the critical regime are plotted in Fig. 3.10. The location of the reaction front is also pointed by an arrow in some of the pressure profiles. Figure. 3.10-a shows the pressure profiles up to

x_{sh}=65. It is observed that the shock pressure as well as the pressure gradient at the shock are decreasing as the shock moves forward. When the shock reaches about x=81 (Fig. 3.10-b), the pressure gradient at the shock is almost zero. At the same time, it is observed that in the region between the reaction front (shown by an arrow) and the shock a pressure pulse begins to develop (Fig. 3.10-b about x=77). As the structure moves, the amplitude of the pressure pulse increases. When shock is located at x=86, the maximum pressure is not at the shock anymore; the maximum pressure corresponds to the pressure pulse instead. It can be seen that the distance between the reaction front and the peak pressure is decreasing as the complex moves. As the strength of the pressure pulse increases, the shock front accelerates.

The relative motion of the peak pressure, the reaction front, and the shock front are shown in a wave diagram in Fig. 3.11, where the location of these waves are plotted versus time. Until x=87, the distance between the shock and the reaction front increases. On the other hand, up to this moment (i.e., t=15) the maximum pressure is at the shock. After that the maximum pressure occurs at the pressure pulse. Then, the reaction front and the pressure pulse converge to each other after t=17. At x=120 these two are almost coupled. Eventually, the leading shock has been captured about x=128 by the reaction front-pressure pulse complex.

As it was seen, unlike the quasi-steady motion of the shock front, the structure behind the shock is not steady in the so-called quasi-steady period. The quasi-steady motion of the shock front in the quasi-steady period has led many researchers to the assumption that the flow structure behind the shock is also quasi-steady state (e.g., Lee 1977, Edwards 1976). In fact, the dynamic aspects of the development of the pressure pulse in the quasi-steady regime has been hidden by the static (i.e., steady) behavior of the leading shock. The effect of the chemical kinetics on the pressure pulse amplification in quasi-steady regime is studied in

next section.

3.2.2. The amplification of the pressure pulse

To understand the reason of the fast amplification of the pressure pulse, its interaction with the chemical kinetics should be studied. The description of the chemical rate process can range from a single step Arrhenius rate law to the full set of kinetics rate equations for all the elementary kinetics steps. For a qualitative study of the physics of the problem, a single step rate law is enough for the present study. The major disadvantage of a single step Arrhenius law is that the induction and reaction processes cannot be varied independently.

When a particle crosses the shock, its induction time mainly depends on the shock temperature. This can be expressed by the Arrhenius kinetics model, i.e.,

$$\tau = A \exp(\frac{E_a}{T_{sh}}) \tag{3.3}$$

According to this relation, the temperature sensitivity of the induction time is much higher at the low temperatures. The temperature sensitivity can be obtained from Eq. 3.3 by differentiation, as:

$$\frac{-d\tau}{dT_{sh}} = \frac{E_a \tau}{T_{sh}^2} \tag{3.4}$$

It is seen that both induction time and its sensitivity to temperature are function of activation energy. Figures. 12-a and b show the variation of 'τ' and '$-d\tau/dT$' with temperature (i.e., 1/T) for various values of the reduced activation energy (E_a/RT_o). The general characteristics of the curves is a very sharp increase in 'τ' and '$-d\tau/dT$' when temperature drops to some critical value. The value of this critical temperature increases with activation energy. The varia-

tion of these two parameters with shock temperature in the critical regime corresponding to Fig. 3.7, calculated by numerical simulation, can be seen in Fig. 3.13-a and b. Point A in this figure corresponds to x_{sh}=25, where the shock pressure is about 30. Point B corresponds to the minimum shock strength in the quasi-steady period. It is seen that the induction time is increased by a factor of about three between A and B. On the other hand, when the leading shock reaches to x_{sh}=120 (i.e., point D, where shock is highly overdriven), the induction time reduced to 0.2. This means about 30 times reduction with respect to the minimum state ($\tau_B \cong 6$). The variation of the sensitivity parameter with temperature is shown in Fig. 3.13-b. It is clearly seen that at lower temperatures the sensitivity of the induction time to temperature is very high. Thus, a small increase in shock temperature causes large decrease in the induction length or increase of the reaction rate. Due to low reaction rate in induction zone, the condition of shocked particle does not change too much before crossing the pressure pulse. However, after crossing the pressure pulse, the temperature and reaction rate of the particle increases which in turns strengthens the pressure pulse. The next shocked particle is passed by a stronger pressure pulse. The mutual interaction of the pressure pulse and the chemical heat release at the reaction front, eventually caused the rapid amplification of the pressure pulse and the onset of a detonation. This is the essence of the Shock Wave Amplification by Coherent Energy Release (SWACER) mechanism of Lee [1978]. One important factor which hastens the amplification in the present case is the presence of the leading shock. The compression waves that are emitted from the pressure pulse toward the leading shock strengthen it. Due to the strong dependency of the reaction rate on shock temperature, a particle processing by a stronger shock will be further advanced in the induction process before encountering the pressure pulse. A small increase in shock temperature, decreases the induction time significantly which is equivalent to a significance increase in the rate of heat release. The increase in reaction rate, in turns, increases the strength of the pressure pulse.

Thus a positive feedback cycle is formed behind the shock. A difference is observed between the present case and the shock amplification in the temperature gradient field of Zeldovich et al. [1970] and the induction gradient field (due to the gradient of free radicals) of Lee et al. [1978]. In those cases the induction period profile were prescribed a priori. In the current problem, there is an evolution of the gradient field due to a positive feedback shock receives from behind.

For further consideration of the quasi-steady period, the initiation processes in the critical regime for some activation energies (the same heat release per unit mass and the same γ) are shown in Fig. 3.14. Three curves correspond to the reduced activation energies E_a/RT_o = 15, 20, and 24. The most pronounced effect of the activation energy is in the differences between run up distances, which is much longer for mixtures with higher activation energies. This effect is the result of two factors. One, the longer induction length for higher activation energies which necessitates a longer distance to be traveled by the pressure peak to catch up the front. Second, the average reaction rate is lower for the higher activation energies, this causes a longer time for the amplification of the pressure pulse before coupling with the reaction front. The average reaction rates in the quasi-steady period are 1.52, 0.96, and 0.68 for E_a/RT_o = 15, 20, and 24, respectively.

In Fig. 3.14, it is also observed that the minimum shock strength in the quasi-steady period is lower for smaller activation energies. This is due to the fact that for low activation energies the reaction rate is quite significant even at low temperatures. The corresponding shock temperature (i.e., T_{sh}/T_o) for the above activation energies are 1.5, 2.1, and 2.55, respectively. However, the interesting point is the very close value of the sensitivity parameter (i.e., $d\tau/dT_{sh}$) for these three cases. The value of this parameter at the minimum state in the quasi-steady period is 22.13, 21.1, and 22.9 for E_a/RT_o = 15, 20, and 24 respectively. It ap-

pears that more important than the shock strength or the activation energy is the value of the sensitivity parameter in the quasi-steady period. In other words, the initiation blast in the critical initiation regime always decays to a strength so that this parameter retains an almost constant value in the quasi-steady period.

The three regimes of initiation as defined in Fig. 3.6 were studied in last sections. The value of subcritical initiation energy in this figure is 1614 while the supercritical initiation corresponds to E_0/p_0=3415. It is seen that there is a wide range of initiation energy between these two regimes. In next section the initiation process for other initiation energies will be studied.

3.3. The role of the initiation energy

According to the Chapman-Jouguet theory, the only stable self-sustained shock-reaction zone complex is the CJ detonation. From purely gasdynamic considerations, it can be shown that all shock initiated reactions are unstable except when the complex moves with CJ velocity (Toong, 1983). It is a well recognized fact that heat addition drives a one-dimensional subsonic flow behind a shock to the sonic condition, which is the equilibrium (i.e., the stable) condition for a shock initiated reaction complex (i.e., the CJ condition). Therefore, in the framework of the present model[2], all shock-reaction complexes other than CJ detonation are "unstable" and will eventually transit to a CJ detonation.

The above discussions have some very important implications. The most important conclusion is that, regardless of the value of the initiation energy, any blast initiation can initiate a detonation wave. This problem will be studied in next section. Here, it is necessary to

[2] To realize the above argument, two important properties of the present analytical model should be taken into consideration. a - Reaction rate ~ $\exp(E_a/RT)$, this means finite exothermic reaction at any temperature. b - The gasdynamics model (i.e., the Euler equations) contains no dissipative losses.

distinguish between two types of instability. The "detonation instability" refers to the oscillatory change in the detonation front velocity. In the framework of the present model, the key parameter which determines the detonation instability is the reduced activation energy E_a/RT_0. According to linear stability analysis [Lee and Stewart 1990], for a mixture with $Q/RT_0=50$, and $\gamma=1.2$, if the reduced activation energy is higher than 25 the detonation will be unstable. Another instability, which introduced in this section, is the inherent instability of any sub-CJ shock-exothermic reaction complex, which seeks the only stable case allowed, CJ detonation. In this text this second type will be referred to as "shock-reaction zone instability", or just "instability".

3.3.1. Is there any lower limit for initiation energy?

In previous section it was concluded that, regardless of the value of the initiation energy, any shock initiated reaction complex can initiate a detonation wave. In this section, this problem will be studied via the numerical simulation of the governing unsteady gasdynamics-chemical kinetics equations.

In section 3.2.1, it was observed that when the initiation energy is less than the critical value, the reaction front decouples from the shock front (Fig. 3.8-a). Although the structure has been decoupled for a long time, it is expected that a detonation will be formed later. To further clarify this problem, the evolution process (i.e., the p_{sh}-x_{sh} curve) with different initiation energies are plotted in Fig. 3.15. This figure is indeed an extension of Fig. 3.6 to a wider range of initiation energies. Different Curves correspond to different initiation energies. Curve 5 represents the initiation process for the case referred to as the critical initiation in Fig. 3.6. The non-dimensional initiation energy per unit area, Eo/Po, for this case is 1764. The initiation energies for Curves 6, 7, and 8 are 1711, 1703, and 1695 respectively. How-

ever, it is observed that for these initiation energies a detonation has also been formed. For Curve 9 which corresponds to initiation energy about 1600 no formation of detonation was observed for the time of calculation. Now, one question that arises is which curve really corresponds to the critical initiation energy. This question will be answered later in this chapter. Now, some properties of Fig. 3.15 will be examined in detail.

It is useful to correlate the run up distance and the overshoot to the initiation energy. For simplicity only Curves 1-5 of Fig. 3.15 are considered for this analysis. It is seen that by increasing the initiation energy, both run up distance and the amount of the overshoot are reduced. In the supercritical regime, almost no overshoot is observed. It has already been observed that when the leading shock decays to a sub-CJ value a pressure pulse is formed between two fronts. In general, when a pressure pulse-reaction front complex is formed behind the shock, its amplification depends on the property of particles crossing the pressure pulse. The particle which crosses the pressure pulse has already been processed by the shock front. Indeed, this particle re-processes by the pressure pulse, hence, its reaction rate is very high. Whenever the "pressure pulse-reaction front" complex captures the shock its amplification ceases, since now it processes a cold mixture. Thus, a longer quasi-steady period (for the same mixture) causes a higher final amplification. That is the reason for higher overshoot of Curve 5 with respect to Curves 2-4 which correspond to higher initiation energies.

In Fig. 3.15 there is also a qualitative difference between initiations with initiation energies higher than 1764 (i.e., Curve 5) and those with lower initiation energies. For example in Curve 7, a pressure jump occurs at about x_{sh}=185, before acceleration to an overdriven wave which started at x_{sh}=235. Therefore, in contrast to Curve 5, here the build up of the front occurs in two steps. The details of the evolution process can be better studied via a wave diagram. Figure 3.16 demonstrates a wave diagram which involves the propagation of

the reaction front, the shock front, and the path of the maximum pressure. This wave diagram corresponds to Curve 8 of Fig. 3.15. It is observed that before Xsh ≅ 160 the maximum pressure is located at the shock. When shock reaches at this point, the peak pressure moves to a point between the shock and the reaction front (i.e., point P1 in Fig. 3.16). It is seen that the pressure pulse decouples from the reaction zone, hence, it has not been amplified to a high value. As a result when it hits the shock at x=170, it cannot amplify the shock front too much. A small amplification of the shock front due to this pressure wave can be seen as point A in Curve 8 of Fig. 3.15. After merging of the pressure pulse with the shock front, for a while the maximum pressure would be at the shock, however, the shock front continues to decay. It is observed that when shock arrived at Xsh ≅ 190, the peak again moves from the shock to another pressure pulse at P2. For a while the pressure pulse moves in phase with the reaction front. Again, the pressure pulse decouples from the reaction front at about x≅205 and merges with the shock at Xsh ≅ 225. This merging appears as a jump in shock pressure at point B in Fig. 3.15. This procedure, which includes: 1- the formation of a pressure pulse between two fronts, 2- the limited amplification of the pressure pulse, and 3- its merging with the leading shock, occurs several times before the final onset of a detonation wave. An important point to note here is that, despite the formation of several pressure pulses (e.g., at points P1 and P2 in Fig. 3.16), they could not be amplified enough to form a detonation wave. It appears that for rapid amplification of the pressure pulse a special condition is needed which had not been met before the formation of the pressure pulse at point P3 (Fig. 3.16). According to Zeldovich et al. [1970], for the onset of detonation in a non-uniformly heated mixture, the temperature gradient should be in a "certain" range. No quantitative criterion has been proposed for this "certain" gradient range by Zeldovich et al. It seems that when the first pressure pulse is formed, the temperature gradient behind the shock is not proper for the rapid amplification of the pressure pulse. After each merging a temperature wave (i.e., a contact discontinuity) is

reflected from the shock front towards the reaction front. The temperature wave increases the temperature and changes the temperature gradient between two fronts. After several shock merging, eventually the appropriate temperature gradient has been formed between two fronts.

It was already shown that the chemical kinetics is very sensitive to temperature. The effect of this sensitivity can be seen in Fig. 3.15 in the difference between evolution processes corresponding to Curves 6, 7, and 8. Where, a small change in shock temperature at x=100 has caused a great difference in amplification process. This conclusion can be generalized to all Curves in Fig. 3.15. It is seen that when the minimum shock temperature is higher than a critical value, (say the value correspond to the minimum state of Curve 5), a big difference in minimum shock temperature does not cause a major difference in evolution process. On the other hand, when shock has decayed to a lower strength, small changes in shock strength (or temperature) cause a large difference in evolution process. Nevertheless, when the shock temperature is too low, the appropriate mechanism (e.g., the shock merging mechanism) has been set up naturally to help the transition from an unstable situation to a stable one. The mechanism of shock merging phenomenon to initiate a detonation will be discussed again in Chapter 5.

Next, the results of another series of computational experiments, where the activation energy is reduced to $E_a/RT_o=15$ will be examined. The initiation processes (i.e., the P_{sh}-X_{sh}) with different initiation energies for this case are plotted in Fig. 3.17. It is observed that, when the shock is very week, the onset is characterized by a sudden change in shock pressure to a very high value. It seems that the leading shock has been received no information (i.e., no pressure wave) from behind before to be captured with the pressure pulse. More insight regarding this abrupt change in shock strength may be obtained by studying the flow profiles.

Some pressure and reaction rate profiles corresponding to E_o/p_o=115 of Fig. 3.17 are plotted in Figs. 3.18-a and 3.18-b respectively. In Fig. 3.18-a it can be seen that, an overdriven detonation is formed far behind the leading shock at x= 130. On the other hand, Fig. 3.18-b shows that, the acceleration to detonation has occurred in the vicinity of the reaction front which has a great distance from the leading shock. This observation has the important implication that initiation phenomenon in this case is not occurring in the vicinity of the shock front. It is instead due to pressure pulse generation and amplification process in the vicinity of the reaction front, no matter how far from the original shock front it may be. Adiabatic heating associated with the pressure pulse can induce reactions to occur more rapidly and when the energy release is coupled to the propagating waves, rapid acceleration occurs which may result in the formation a of detonation.

Comparing Fig. 3.15 with Fig. 3.17, it can be seen that when the shock is very slow, its role is essential for mixtures with high activation energy. This is due to low rate of reaction for high activation energies which prevents the fast rate of heat release. Hence, some other mechanism is needed to prepare the region behind the shock for rapid wave amplification. The merging of the pressure pulse with the shock front generates a contact surface which increases the temperature in the reaction zone and prepares the condition for the onset of detonation.

The present results contradict with the experimental observation that a distinct value for the critical initiation energy exists, below which no detonation occurs. To understand the reason of this contradiction, two factors should be noted to; the present single-step rate law and the effect of heat loss which is ignored in the present gasdynamics model (i.e., Euler equations). The heat loss can be significant when the leading shock and the reaction rate are slow. In this case the time scale of the heat transfer may have the same order of magnitude as

the time scale of chemical heat release. Therefore, when the blast decays to a very low velocity, which causes low reaction rate the chemical energy may be transferred to the surrounding media through heat transfer from boundaries, before the formation of pressure pulse. In reality, the combination of high temperature sensitivity in low temperatures and heat loss, causes a cut off for the value of the critical initiation energy.

3.3.2. Setting a criteria for the critical initiation energy

Strictly speaking, there is no critical initiation energy in the framework of our analytical model. However, still it is possible to define a critical initiation energy based on our observation of the initiation processes for different initiation energies.

An important factor regarding the initiation process is the relation between the run up distance and the initiation energy. For example, in Fig. 3.15 it is seen that the difference between the run up distances of Curves 7 and 8 is about 106 length units, while the difference between their initiation energy is about 8 units. On the other hand, for Curves 4 and 5, it is observed that a very higher difference in initiation energy (i.e., about 77) caused a difference in run up distance of only about 25. Therefore, the run up distance is very sensitive to the initiation energy for low initiation energies. In order to better demonstrate the initiation energy-run up distance correlation, the variation of the run up distance with initiation energy is plotted in Fig. 3.19 for $E_a/RT_o=24$. In this figure point A corresponds to Curve 5 of Fig. 3.15. Points B and C are due to Curves 7 and 8 of that figure, while E and F correspond to Curves 3 and 2 respectively. Now, it is clearly seen that a small decrease in the initiation energy causes large increase in run up distance for initiation energies less than point A. This means a much later formation of a detonation wave for small reduction in initiation energy. It is also interesting to note that, Fig. 3.19 suggests an asymptotic value for the minimum pos-

sible initiation energy. On the other hand for initiation energies higher than point A, the run up distance is rather in-sensitive to the initiation energy. For example, comparing the initiations correspond to points E and F of Fig. 3.19, it is found that for $\Delta(E_O/p_O) \cong 300$ the reduction in run up distance is about only 14. Therefore, the abrupt increase in the run up distance when the initiation energy reaches some critical range can be used to define the critical initiation energy.

While with the above definition we could define a critical initiation energy for $E_a/RT_O=24$, for lower activation energy, no sharp cut-off in initiation energy is observed, because the run-up distance increases more gradually. This is due to less temperature sensitivity for low activation energies. As an example the initiation energy-run up distance curve is plotted for $E_a/RT_O=15$ in Fig. 3.20. Nevertheless, a more sophisticated model which utilizes a better kinetics model and also considers the effect of heat loss can overcome this contradiction with reality.

3.4. Discussions and concluding remarks

In order to acquire more insight about the initiation problem, the transition process, from the energy deposition up to the formation of a self-sustained detonation, was studied in this chapter. The main conclusion from this study can be summarized as follows:

1- It was shown that the quasi-steady assumption, which has been utilized in several initiation models in past twenty years, is divorced from the dynamic nature of the initiation process. Although the leading shock has an almost constant velocity for a quite long time in the transition process, the structure behind the shock involves a very unsteady evolution. The

unsteadiness stems from the inherent instability of a shock induced reaction complex, which naturally seeks its stable condition which is the CJ detonation. In the case of unstable detonations (which is the subject of the next chapter), it can be expected that the instability of shock-induced combustion will eventually result in a self-sustained detonation with an average about CJ velocity. This gasdynamic instability of shock-induced reaction is manifested by the formation of a pressure pulse between the shock and reaction fronts. The in-phase propagation of the pressure pulse with the reaction front causes the fast amplification of the pressure pulse and the onset of a detonation. This chemical-gasdynamics interaction has not been considered in any of the current initiation models based on the Zeldovich initiation theory. Therefore, it cannot be expected that those models can predict anything more than the correct order of magnitude of the critical initiation energy. This is why such models have only a limited range of applicability.

2- It was observed that, specially when the shock has decayed to a very weak wave, the acceleration to detonation may occur far behind the shock front. This observation has the important implication that initiation phenomenon is not occurring in the vicinity of the reaction front. It is indeed due to pressure pulse generation and amplification process in the vicinity of the reaction front, no matter how far from the shock it may be.

3- To support a detonation at such high speed, the rate of transformation of energy in the reaction zone must be very high. The combustible gas immediately ahead of the reaction front should be heated to such a high temperature as to permit a high reaction rate in the reaction front. In the critical regime of initiation, when the blast decays to a low velocity, due to a long induction length and the relatively low speed of sound, the compression waves generated by chemical reaction cannot immediately catch up the front. This causes the formation of a pressure pulse ahead of the reaction front. Hence, the formation of the pressure pulse is

attributed to competition between generation and dispersion of the pressure waves.

4- When the leading shock is very slow the onset for low activation energies occurs far from the leading shock. Due to very fast reaction rate at the reaction front, a second shock forms between the reaction front and the leading shock. This second shock causes a lower importance for the role of the leading shock. On the other hand, for high activation energies, at low shock velocities, the onset is due to a multi-step shock merging mechanism. Nevertheless, in both cases the onset stems from the formation of pressure pulses at the reaction front.

5- The present results based on the assumption of a single-step Arrhenius rate law and no losses are in contradiction with the experimental observation that there is always a cut off value for the critical initiation energy, below which no detonation occurs. The reason of this contradiction is the analytical model used in the present work, i.e. a single-step Arrhenius rate law and the assumption of "no heat loss". Heat loss can be significant when the leading shock and the reaction rate are slow. In this case the time scale of the heat transfer may have the same order of magnitude as the time scale of chemical heat release. Therefore, when the blast decays to a very low velocity, which causes low reaction rate, the chemical energy may be transferred to the surrounding media through heat transfer from boundaries. It also should be noted that, the instability mechanism which proposed in section 3.2.3, is effective when some energy is added to the system. This does not always happen in the presence of heat loss. Indeed, the combination of high temperature sensitivity in low temperatures and heat loss, causes a cut off for the value of the critical initiation energy in reality.

6- The problem of the shock ignition of a gaseous mixture and its evolution to form a self-sustained detonation has been studied by many researchers. Among them the most systematic works are due to Clarke. In a series of numerical studies Clarke and his coworkers [Clarke *et al.* 1986, 1989, 1990 and Singh and Clarke 1992, Sileem an Kassoy 1990] investi-

gated the detonation initiation process by different means for generating the precursor shock. The initiation shocks in their works were generated via a heat source from a wall [Clarke *et al.* 1986, 1990], the generation of a strong shock by a piston [Clarke and Singh 1989, Singh and Clarke 1992], and heat addition from a thin layer adjacent to the wall for a finite period of time [Sileem and Kassoy 1990]. Due to their initiation condition, they, in fact, have investigated the "slow" mode of the formation of detonation which is commonly referred to as the deflagration to detonation transition (DDT) in literature (e.g., Lee 1977, Sichel 1992)[3]. They observed that [Singh and Clarke 1992], despite different approaches to the formation of the precursor shock, the subsequent events to onset a detonation wave is common for different initial conditions. Comparing their simulations with the present work, it is seen that the transition processes in their works, after the formation of the leading shock, are very similar to the shock amplification process in the so-called quasi-steady period in direct initiation. It appears that the transition process in the final stage of DDT (at least those cases studied by Clarke et al.) and blast initiation follow almost the same mechanism. The elements of this mechanism are a precursor shock wave, the unsteady reaction domain behind the shock, and the quasi-steady reaction front. The onset is due to the generation and amplification of a pressure pulse between the reaction front and the shock front. Therefor, as proposed in Chapter one, DDT and direct initiation differ only in the initial state.

7- Comparing the speed of the fast deflagration in different processes which end to detonation, Chue [1993] concluded that the quasi-steady fast deflagration prior to the formation of the detonation depends on the energetic (i.e., CJ deflagration) rather than the details of the structure. The present numerical investigation shows that the averaged properties in the quasi-steady period is different for mixtures with the same heat release but different activation energies. For example for $E_a/RT_o = 15$, the average shock pressure in the quasi-steady

[3] The title of the first paper of this series [Clark *et al.* 1986] is "On the direct initiation of the planar detonation waves", while Sileem *et al.* used the correct term "DDT" in their paper.

period, $p_{sh}/(\gamma p_o)$, is about 8, while for $E_a/RT_o = 29$ the average shock pressure is about 27. On the other hand, it was observed that the dynamic parameters of detonation such as the critical initiation energy or the run up distance are strongly depend on the wave structure.

8- The direct initiation process consists of the blast decaying to a minimum strength followed by its amplification to an overdriven wave. This procedure is similar to a cycle of a pulsating detonation. Studying the details of the profiles of pulsating detonations shows a very similar behavior as the initiation process in the critical regime. Indeed the transition process in the quasi-steady period is the same as the unsteady process in the amplification phase of the pulsating detonations in a profound form. It can be concluded that when the detonation front decays to a minimum state in pulsating detonation, the "shock-reaction zone instability" causes its amplification to an overdriven state. This similarity suggests that the more difficult instability problem of the pulsating detonation can be analyzed via direct initiation.

All investigations in this chapter was limited to "stable detonations", where the reduced activation energy is less than 25.5 [Lee and Stewart 1990]. In next chapter the results of direct initiation of one-dimensional "unstable detonations" will be presented.

Chapter 4

The Effect of "Detonation Instability" on Direct Initiation

4.1. Introduction

Unlike the classical steady ZND model, most gaseous detonations are inherently unstable. For self-sustained CJ detonations, the activation energy of the mixture controls the stability of one-dimensional detonations [Chue, 1993]. The linear stability analysis [Lee and Stewart, 1990] indicates that for a mixture with $Q/RT_o = 50$ and $\gamma=1.2$, the ZND structure is unstable for E_a /RT_o higher than 25. By increasing the activation energy beyond the stability limit, the detonation front becomes unstable and begins to exhibit oscillatory behavior. Figure 4.1 demonstrates the behavior of the shock front propagation for activation energies higher than the stability boundary. In this figure the shock front pressure (p_{sh})is plotted versus the shock radius (x_{sh}). For activation energy $E_a /RT_o = 25.5$ (Fig. 4.1-a) the shock pressure oscillation is quite linear. The period of the oscillation is very close to the period calculated by linear theory. Increasing the activation energy further causes a nonlinear oscillation on the shock front pressure (Fig. 4.1-b and c). For non-dimensional activation energy $E_a/RT_o = 29.5$, a chaotic oscillation appears in the leading shock motion (Fig. 4.1-d).

As explained in the Introduction, recent research [Moen *et al.* 1986, Shepherd 1986, and Lee 1991] all indicate the important role of detonation instability on the dynamic parameters of detonation. Particularly, the correlation $d_c = 13\ \lambda$, which was thought to be universal, is now believed to depend on the degree of cell regularity. The degree of cell regularity is an indication of detonation instability. Therefore, it is suspected that the detonation instability may affect the direct initiation phenomenon. This problem will be studied in this chapter. The only similar study was performed by Longting He [1996]. He, using numerical simulation, showed that the He-Clavin initiation criterion [He *et al.* 1994] is not valid for highly unstable detonations. The He-Clavin criterion is based on the quasi-steady assumption for a curved detonation wave. In Chapter 3, it was concluded that the front curvature is not an adequate parameter to characterize the highly unsteady events in the quasi-steady regime.

The initiation process for stable detonations was thoroughly studied in the previous chapter. The results of similar calculations are presented here for unstable detonations. Then, they are compared with those of the stable cases to find the role of instability in the initiation process. The current study examines the effect of activation energy, which is the main parameter controlling the stability of one-dimensional pulsating detonations, on the initiation process. In this chapter the same analytical model and the same numerical schemes as in Chapter 3 have been used.

4.2. Initiation process for unstable detonations

In previous chapter, it was observed that the re-establishment of the front in the critical regime of initiation is due to the generation and amplification of a pressure pulse between the

shock front and the reaction front. To study the role of instability on the initiation process, the critical initiation regime simulated for reduced activation energies, E_a/RTo, higher than 25 will be studied in this chapter. Figure 4.2 shows the three regimes of initiation for a typical unstable detonation (i.e., a mixture with activation energy E_a/RT_o=26). In this figure the shock pressure during the initiation process has been plotted versus the shock radius. The three regimes have the same trend as observed for E_a/RTo = 24 in the previous chapter. The only difference is the unstable nature of the final self-sustained detonation, which is not a result of the initiation process. A complete explanation of these three regimes was given before. Indeed, this figure involves no new information regarding the mechanism of the initiation in the critical regime. The main goal in repeating these plots is to demonstrate the similarity between the initiation process for both stable and unstable detonations. The structure and the evolution process in the quasi-steady period also show the same mechanism of formation and amplification of a pressure pulse prior to the onset of a detonation. As an example, Fig. 4.3 shows the pressure profiles during the initiation process in the critical regime for E_a/RT_o=26. The arrows show the location of the reaction front.

Figure 4.4 compares the initiation process at the critical regime for different activation energies ranging from a stable detonation (i.e., E_a/RT_o = 24) to a very unstable case (i.e., E_a/RT_o =29). It is seen that the initiation process has qualitatively the same trend for all cases. The run up distance appears to be longer for mixtures with higher activation energy, while the overshoot retains almost the same value for all activation energies. This value (i.e., $E_o/p_o \cong 65$) is about twice the corresponding steady detonations. On the other hand, the minimum shock strength in the quasi-steady period is lower for smaller activation energies. The minimum shock pressure in the quasi-steady period has a value about 18.9, 22.0, and 24.4 for E_a/RT_o = 24, 27, and 29, respectively. For lower activation energies the reaction rate is still quite significant at low temperatures. Thus, the minimum shock strength is lower for

low activation energies.

The qualitative similarity in the quasi-steady period for both stable and unstable detonations was not unexpected. The generation of pressure pulse is due to inherent instability of any sub-CJ "shock-reaction zone" complex (Chapter 3) regardless of the stability of the final self-sustained detonation. A longer run up distance can be expected when E_a/RT_o is higher; due to a longer induction time and lower reaction rate. To further elucidate this fact, a quantitative comparison for some of the important parameters in the critical regime initiation process is given in Table 4.1 for activation energies ranging from E_a/RT_o=15 to 29. The critical regime has been determined based on the asymptotic value of the initiation energy in "initiation energy-run up distance" curve, which proposed in Chapter 3. As was already discussed, the run up distance (row 2 in Table 4.1) is longer for higher activation energies. It is interesting to compare this length with the induction length of the chemical reaction. Row 3 in Table 4.1 contains the ratio of the run up distance to the induction length of the steady ZND detonation for different activation energies. For activation energy $E_a/RT_o = 15$ the run up distance is 400 times greater than the corresponding induction length for the steady ZND wave, while this ratio is 266 for $E_a/RT_o = 29$. This means a higher ratio for lower activation energies. Now, if an average induction length in the quasi-steady period is utilized (next row in the table), a completely different trend is observed. For activation energy $E_a/RT_o = 15$, only 7 induction lengths have passed by the initiation blast to form a detonation, while almost twice number of induction lengths are needed for $E_a/RT_o = 29$. This comparison shows the vital importance of the correct length scale for modeling the quasi-steady period. The ZND induction length, not only misrepresents the length of the quasi-steady regime, but it may even mislead the qualitative variation of important parameters such as the run up distance with the activation energy.

In the previous chapter, the role of the temperature sensitivity of the induction time (i.e., $-d\tau/dT_{sh}$) was discussed. The value of this parameter at the minimum state of the quasi-steady period is shown in Table 4.1 for different activation energies. It is seen that despite a large difference in the shock temperature at the minimum state, this parameter is nearly constant for a wide range of activation energies. This fact suggests that this parameter can be taken as an intrinsic property of the critical regime of initiation. As the blast wave decays, the value of $-d\tau/dT_{sh}$ increases. But in the critical regime, this value cannot increase indefinitely, since when it reaches ~20, the sudden onset of detonation is observed to occur. Rather than an arbitrary autoignition Mach number, as was proposed in some initiation models for the critical condition (e.g., the kernel model), here a dynamic criterion is proposed to determine the critical condition. This criterion is to assume a constant value for the sensitivity parameter in the critical regime. According to the present calculation, which has been performed for a one-dimensional gasdynamics model with a one-step reaction rate model, this parameter has a value about 20. This value is also a function of the parameters selected here (i.e., $Q/RT_0 = 50$ and $\gamma = 1.2$).

In the framework of the analytical model which is used here, even when the blast decays to a very low velocity, where the sensitivity parameter is much higher than 20 the onset of detonation occurs. This can be seen in Fig. 4.5 which shows the initiation process for different initiation energies. The current numerical experience suggests that if the calculation for Curve 1 or Curve 2 of Fig. 4.5 is continued, a detonation will eventually form. Comparing Curves 3 and 4, which differ by less than 1% in the initiation energy, it is seen that a small decrease in shock strength (or shock temperature) causes a great increase in the run up distances. However, in a more realistic model, which considers energy loss due to heat transfer from the system, the temperature sensitivity will have a very crucial role. Indeed, losses will result in a cut-off in the value of the initiation energy which can initiate a detonation. This

effect will be more severe for higher activation energies.

Activation energy is the main parameter which controls the dynamic aspects of one-dimensional pulsating detonations. On the other hand, the chemical kinetics depend on both the activation energy and temperature. Therefore, to see the effect of activation energy on the quasi-steady period, it is better that instead of the reduced activation energy, E_a/RT_o, an effective activation energy, for example E_a/RT_{sh}, be used to analyze dynamic phenomenon such as onset in the quasi-steady period. The value of this parameter, calculated at the minimum shock velocity in the quasi-steady period, is also shown in Table 4.1. A very gentle variation of this parameter for different activation energies is another indication of the similarity of the initiation process in the critical regime for both stable and unstable detonations. This parameter also was introduced by Manzhalei [1981] as a measure of the cell regularity. Manzhalei [1981] found that if E_a/RT_{sh} is greater than 6.4 the cellular structure of gaseous detonations will be irregular. On the other hand, in Chapter 3, it was suggested that the shock trajectory in the critical regime is similar to a cycle of pulsating detonations. A high value of E_a/RT_{sh} indicates that the quasi-steady period of the critical regime behaves like a very unstable detonation.

So far, all studies have been performed for activation energies up to $E_a/RT_o = 29$, where the final structure has either a stable velocity or a regular oscillation (linear or nonlinear, Fig. 4.1). The present numerical experiments show that some new phenomena appear for higher activation energies, where the final self-sustained detonation propagates with a chaotically varying velocity. Therefore, initiation for activation energies higher than 29 will be studied in a separate section.

4.3. Direct initiation for mixtures with activation energies higher than 29

For activation energies higher than 29, it has been shown that the resulting self sustained detonation is highly unstable and characterized by a chaotic oscillation of the leading shock (Fig. 4.1-d). This fact casts some doubts on the reliability of numerical simulation of the initiation process for very unstable detonations. In general, chaotic phenomena are usually very sensitive to the initial conditions as well as the details of the numerical simulation, such as the mesh sizes. Therefore, it is necessary to have some serious concerns about numerical simulations when the phenomenon is very unstable. Most of the calculations of the present work were performed with very fine mesh sizes (up to 50 grid points per half reaction zone length of the steady ZND detonation, see Chapter 2). However, due to the present uncertainty about the result of numerical simulations of highly unstable detonations [Zhang 1996], this thesis shall be restricted to mixtures with E_a/RT_o not more than 30.

As a typical simulation for a highly unstable case, Fig. 4.6 represents the initiation processes (i.e., p_{sh}-x_{sh} relation) for $E_a/RT_o = 29.5$. The initiation process for different values of the initiation energy are demonstrated in this figure. Curve 1 in this figure shows the subcritical initiation. Curve 2 in Fig. 4.6 corresponds to the minimum initiation energy (E_{o2}) which can generate a self-sustained detonation wave for this activation energy. In general, increasing the initiation energy to a higher value with respect to the critical initiation energy causes a reduction in run up distance, and thus an earlier formation of a self-sustained detonation wave. However, for E_{o3} which is higher than E_{o2} a different trend is observed (Curve 3, same figure). For initiation energy E_{o3}, the initiation blast first decays to a strength slightly lower than the corresponding CJ value. Then, after a short distance, the leading shock

accelerates to a slightly overdriven wave. In contrast to the previous cases, after this primary amplification, the shock fails to generate a detonation (during the time of this calculation) and decays to a low strength. If the initiation energy increases further to $E_{o4}>E_{o3}$ (Curve 4), it is seen that after the primary amplification, the shock front decays to the so-called quasi-steady period. At the end of this period, the shock front accelerates rapidly to a highly over-driven wave. The run up distance and the overshoot of Curve 2 of Fig. 4.6 have the same trend as the critical initiation regime for mixtures with activation energies up to $E_a/RT_o = 29$ (compare Curve 2 of Fig. 4.6 with Fig. 4.4). The overshoot has almost the same value, and the run up distance has increased with the same trend with respect to the case of $E_a/RT_o = 29$. However, the run up distance and the overshoot of initiation energy E_{o4} (Curve 4 of Fig. 4.6) are much higher than the corresponding value of $E_a/RT_o = 29$. The overshoot for Curve 4 is about (40%) higher than the corresponding value of Curve 2. The higher overshoot is due to a longer distance that the pressure pulse must travel before capturing the shock front. In this process the shock compressed reactants crosses the high pressure region, thus intensifies the reaction rate and amplifies the pressure pulse.

In Chapter 3, it was suggested that in the quasi-steady period, a pressure pulse develops between the reaction front and the shock front. The generation of this pressure pulse is due to fast reaction rate and long induction time in the quasi-steady period. In supercritical initiation the blast asymptotically decays to a CJ velocity. For low activation energies the pressure waves generated by chemical heat release meat each other right at the shock front (since the induction length is small). However, both Curves 3 and 4 in Fig. 4.6 correspond to supercritical initiations when activation energy is very high, which causes a long induction length. Therefore, a pressure pulse again has originated between the reaction front and the shock front, causing the primary amplification of the leading shock. This primary amplification can

also be attributed to "detonation instability," which started very soon after the decaying of the blast to a CJ detonation. This instability causes the formation of a pressure pulse and the primary amplification of shock pressure to about P_{sh}=42. The decaying of this overdriven wave is governed by a competition between the adiabatic cooling due to rapid expansion behind the shock and the heat release due to chemical reaction. A relatively long induction time and low reaction rate causes the dominant effect of the adiabatic cooling in the decaying phase, and hence the failure of initiation. To prevent the initiation from failure, the rate of expansion after the primary amplification should be slower. Increasing the initiation energy to E_{04} causes the suppression of the instability before the primary amplification, hence, a weaker overshoot results. Therefore, the expansion will be so slow that the chemical heat release can compensate it. The decaying for E_{03} may also be attributed to the chaotic nature of the propagation of this detonation. Thus, it can be assumed as a cycle of the chaotic-oscillatory propagation with a very long period.

Therefore, the current study shows that besides the effect of the instability on initiation process, when the detonation is highly unstable, it is even difficult to single out a unique value for the critical initiation energy. It should be noted that Curve 2 of Fig. 4.6 was not captured with mesh sizes larger than 30 grid points per half reaction zone length (hrl). Other three cases of Fig. 4.6 may be obtained with as few as 10 grid points per hrl. The calculations were repeated for 40 and 50 grid points per hrl, too. The same results as Fig. 4.6 were observed. A similar calculation was also repeated for activation energy E_a/RT_o=30, to see any possible difference with the above case. Figure 4.7 demonstrates the different regimes of initiation for this case, which shows very similar behavior as Fig. 4.6. It seems very unlikely that the presence of this new phase of initiation is a numerical artifact.[4]

---

[4]The numerical simulation for activation energies E/RT_0 = 30.5, and 31 were also performed during the current research. The general trend was the same as E/RT_0 = 29.5 and 30 for both cases.

As pointed out in Chapter 3, due to the inherent instability of any sub-CJ "shock-reaction zone" complex both cases 1 and 3 in Fig. 4.6 may eventually result in initiation after a very long time in the framework of the present analytical model. In reality, due to heat loss effects, when shock decays to a slow velocity, a sharp cut-off in the value of the initiation energy which can initiate a detonation wave is observed. Therefore, it is expected that even in reality, when activation energy is very high no unique value can be found as the critical initiation energy. Furthermore, the asymptotic value of the initiation energy as the run up distance goes to infinity can be taken as a criterion to determine the critical initiation energy, as was proposed in Chapter 3. Figure 4.8 represents these two limiting value of the initiation energies. In this figure it is seen that the minimum source energy, E_{O1}/p_O, which can initiate a detonation is about 6500, which can initiate a detonation at about 870. Increasing the initiation energy causes formation of detonation in a distance shorter than 870. For source energy E_O/p_O about 7800, the run up distance is about 210. However, increasing the source energy to 8000, the initiation fails to onset a detonation during the time of the present calculation. Moreover, initiation energy about 8240 can initiate a detonation at about 1400. Higher initiation energy than 8240, causes a decrease in the value of run up distance. Therefore, it appears that for very high activation energy it is not possible to specify a unique value of the source energy below that a detonation cannot be generated.

In Chapter 1 and Section 3.1 some of the drawbacks of the current initiation models were discussed. Most of the current models are based on the Zeldovich criterion (i.e., $E_O \sim \Delta j^{+1}$). The results of present calculations can be used to evaluate the validity of this criterion in a quantitative way. This is the subject of the next section.

4.4. On the Zeldovich initiation criterion

In the past forty years several models have been proposed to estimate the critical initiation energy from a point source. The first criterion is the pioneering work of Zeldovich *et al.* [1956]. The main idea behind the Zeldovich criterion is to recognize the role of the induction delay which necessitates a finite value for the initiation energy. According to Zeldovich [1956]: "in order to achieve a spherical gas detonation, it is necessary that the energy of the external source which causes the shock wave in the mixture should be proportional to the cube of the detonation wave thickness," i.e. $E_0 \sim \Delta^3$. Later, Lee [1977] extended the Zeldovich criterion to other geometries in form: $E_0 \sim \Delta^{j+1}$ where j=0, 1, and 2 for planar, cylindrical and spherical geometries, respectively. It is clear that the Zeldovich criterion is not directly applicable, since the quantitative link in this criterion is missing. Several models in the past forty years have been proposed to bring the Zeldovich criterion in a quantitative form. Among these works are the Kernel model of Lee [1976], the Sichel model [1977], and etc. The basic idea of these models is a balance between the initiation energy and the chemical heat energy release in the decaying phase of initiation. On the other hand the knowledge of an experimental length scale is necessary for these models. The second phase of initiation has not been considered in any of these models. To examine the validity of the Zeldovich criterion, which is the base of many of these models, the results of numerical simulation will be compared with one of them (i.e., the blast model of initiation of Lee 1977).

Using strong blast theory and choosing the cell size as the overall length scale, Lee [1977] recast the Zeldovich criterion to the following expression for the critical initiation energy:

$$E_0 / p_0 = k_j (j+3)^{j+1} I M_{CJ}^2 \gamma \lambda^{j+1} \qquad (4.1)$$

where λ is the cell size, (k_j , j) are (1 , 0), (2π , 1), and (4π , 2) for planar, cylindrical and spherical geometries, respectively. The different initiation models have been thoroughly reviewed by Lee [1977 and 1984] and Benedick *et al.* [1986]. In those reviews it is seen that not only Eq. 4.1, but none of the other initiation models consider the role of the pressure pulse and its amplification in the quasi-steady period of the initiation process. Most of the initiation models involve almost the same correlation as the Zeldovich criterion between a characteristic chemical length and the critical initiation energy. Since the numerical simulation reproduces all the unsteady processes of direct initiation, it is a good way to test the validity of the Zeldovich criterion. Therefore, in this section the critical initiation energy, determined via numerical simulation, is compared with Eq. 4.1, as a representative of the Zeldovich criterion.

To calculate the critical initiation energy by Eq. 4.1, the value of the cell size, λ, is needed. The ZND reaction zone thickness can be used to estimate the cell size, λ. Many researchers [e.g., Westbrooke 1982] have reverted to the simplest approach first suggested by Shchelkin and Troshin [1965]. This method suggests that the cell size is simply proportional to the chemical induction length, i.e.:

$$\lambda = A\Delta \tag{4.2}$$

Then, A is calculated by matching Δ and λ with a single experimental point [Shepherd 1986, Lee 1984]. In order to have a qualitative comparison between the results of the present numerical simulations and Eq. 4.1, this method has been used here. Substituting the critical initiation energy determined by numerical simulation and the ZND induction length of the mixture with $E_a/RT_0 = 25$ in Eq. 4.1, the constant A will be 12.75. Thus:

$$\lambda = 12.75\Delta \tag{4.3}$$

The critical initiation energies calculated by numerical simulation are plotted versus the in-

duction length of the steady ZND detonation in Fig. 4.9. Increasing induction length, Δ, corresponds to increasing activation energy. The hollow squares show the critical initiation energies determined by the numerical simulation. The initiation energy calculated based on Eqs. 4.1 and 4.3 is shown as a solid line in Fig. 4.9. This figure shows that for an induction length less than about 0.5, which corresponds to the stability boundary E_a/RT_o =25, the critical initiation energy correlates well with the induction length (as indicated by Eq. 4.1). However, for unstable detonations (i.e., E_a/RT_o >25) the slope of the E_c-Δ plot increases. Hence, the linear correlation between the critical initiation energy and the ZND induction length, appears to be invalid over the full range of activation energies. This deviation from the linear dependency on the induction length of the steady ZND detonation has two reasons. First, it was shown in Section 4.2 that the ZND induction length is not an appropriate chemical length scale for the very unsteady events in the quasi-steady period. Second, the highly dynamic events of generating and amplifying of the pressure wave in the quasi-steady period cannot be modeled by an energy balance (Section 3.1). Furthermore, in Section 4.3, it was observed that for highly unstable detonations it was not possible to specify a unique value for the critical initiation energy. Indeed, we can specify a second critical energy, shown as solid squares in Fig. 4.9, corresponding to this limit. The presence of this new mode of initiation was attributed to the "detonation instability" in Section 4.3. Deviation of "E_c-Δ" relation after E_a/RT_o = 25 and the appearance of the second limit for initiation energy are indications of the breakdown of the Zeldovich initiation criterion. In other words, the steady induction zone thickness, at least alone, cannot characterize the dynamic parameters of detonation such as the critical initiation energy, which has been linked to a very unsteady process. Besides a chemical length scale, another parameter which characterizes the dynamics of the second phase of the initiation process should be considered in initiation models.

Due to the importance of the numerical scheme, the developed code has been exam-

ined with several test problems. Most of the calculations were repeated for different fine sizes between 10 to 50 grid points per half-reaction-length. Although the results never converged to a single value (or single curve), the main trend remained the same. It seems very unlikely that the main conclusions are contaminated by a lack of numerical resolution. To illustrate this fact, the variation of the initiation energy with the ZND induction length are compared in Fig. 4.10, for three different mesh sizes. Indeed, this figure shows that the present results appear to be independent of mesh resolution.

4.5. Discussions and concluding remarks

Following the studies of Moen *et al.* [1986], Shepherd [1986], and Lee [1991, 1993], regarding the dependence of some dynamic parameters of detonation on the "detonation instability," the present work has been performed to investigate the role of "detonations instability" on the direct initiation problem. The instability effect has never been explicitly considered in any of the current initiation models. From the studies carried out in this chapter some conclusions may be made as follows:

1- The extensive numerical simulations carried out in the present research have shown that the process of onset in the quasi-steady period of the critical regime is the same for both stable and unstable detonations. This process consists of the formation and amplification of a pressure pulse between the two fronts in the quasi-steady period. As shown in Chapter 3, this process stems from the reaction front and strongly depends on the chemical kinetics. The reaction rate at low temperature strongly depends on the temperature sensitivity of the induction time. Despite the large difference in the shock strength in the quasi-steady period for different activation energies, it was demonstrated that the sensitivity parameter($-d\tau/dT_{sh}$) is

nearly constant at the minimum shock strength for different activation energies.. The same feature can also be observed from the very weak variation of the effective activation energy (i.e., E_a/RT_{sh}) for a wide range of the reduced activation energy (E_a/RT_o). These observations suggest that the mechanism of detonation onset in the quasi-steady period is the same for both stable and unstable detonations.

For highly unstable detonations, it is observed that for some supercritical initiation, detonation failure may occur. This is due to a long induction length and a low rate of reaction for high activation energies. Therefore, for high activation energies, even when shock is strong, it is possible that some event from the rear boundary of the reaction zone dominates the wave propagation. Therefore, for highly unstable detonations, no unique value can be specified as the critical initiation energy.

2- The numerical simulation of a pulsating detonation shows that the mechanism of decay and amplification in a period of oscillation is the same as initiation process in the critical regime. After a pulsating detonation decays to a minimum strength, the amplification of the shock front is also the result of the generation of a pressure pulse from the reaction front. The preceding discussions regarding the decay and re-establishment of the detonation front can be extended to the propagation mechanism for pulsating detonations. Therefore, the oscillatory propagation of unstable detonations can be interpreted as follow:

a)- Due to long induction time and low rate of reaction, a pressure pulse is formed ahead of the reaction front. The amplification of this pressure pulse causes the formation of overdriven wave (i.e., the peaks of oscillation).

b)- When shock is overdriven, due to fast expansion behind it, low reaction rates, and high temperature sensitivity of reaction rate at low temperatures, the front decays to a sub-CJ

velocity (the minimum states of oscillation). When the temperature sensitivity is very high, the oscillation becomes chaotic.

3- It was demonstrated that those models based on the Zeldovich criterion cannot predict the initiation energy over the full range of activation energies. The failure of the Zeldovich criterion was attributed to the unsteady effects in the second phase of the initiation process which is not considered in this initiation model. The possibility of two different modes for the critical initiation regime, when the detonation structure is highly unstable, is another indication of the role of the unsteadiness in the initiation process. These results indicate the necessity of including a dynamic parameter in initiation modeling.

4- Describing the mechanism of an unstable detonation front, Dremin [1992] concluded that the stability is settled during the transition process. According to Dremin, if the reaction front decouples from the leading shock[5] during the transition process, the self-sustained detonation will have an unstable front. Otherwise, it propagates with a steady velocity. In other words, according to Dremin, the decoupling in the transition process occurs only for unstable detonations. The present numerical simulations clearly show that the decoupling takes place in the critical initiation regime regardless of the degree of the instability of the final self-sustained detonation. In fact, instability is an intrinsic characteristics of a detonation regardless of the history of its initiation.

5- That the transition process from blast to detonation is due to the unsteadiness in wave structure has also been pointed out by Sichel [1992]. Sichel suggested that the transition process does not occur smoothly and requires an explosion within the structure when E_0 is near the critical value. Sichel also stated that an explosion is probably also involved in the supercritical case. Unfortunately, the explosive nature of the transition process could not be captured with the present one-dimensional analysis. However, the role of unsteadiness was

[5] This is called the break down phenomenon by Dremin [1992].

clearly demonstrated in the present numerical simulations. For highly unstable detonations, multidimensional effects may become important. For example, recently Oran and coworkers [William, Bauwens, and Oran 1996] showed that in two dimensions, the initiation occurs much earlier than the corresponding one-dimensional case. Their numerical simulation was carried out for the generation of piston supported detonations when the degree of overdrive was very low. A multidimensional numerical simulation of the blast initiation process is needed to clarify this effect

6- Temperature sensitivity of the induction time was introduced first by Oppenheim et al. [1971] as a demarcation parameter to distinguish between two modes of autoignition. According to Oppenheim, strong ignition is manifested by a instantaneous appearance of a relatively planar pressure front across the whole cross section of the tube. Strong ignition corresponds to low temperature sensitivity. On the other hand, mild ignition, which occurs when the sensitivity parameter is high, starts in the form of distinct reaction centers whose growth is comparatively slow. To study this effect, a multidimensional simulation is necessary. Therefore, these two modes of ignition cannot be analyzed in the framework of the present study.

Chapter 5

The Effect of Hot Spots on the Initiation of Detonations

5.1. Introduction

In the previous chapters it was observed that the initiation process in the critical regime is due to the generation and amplification of a pressure pulse inside the structure in the second phase of the initiation process (i.e., during the quasi-steady period). On the other hand, experimental observations of the direct initiation of detonations in a homogeneous explosive have revealed that the onset of detonation develops from discrete hot spots. The hot spots are formed from various hydrodynamic fluctuations such as turbulence and shock-boundary layer interactions. Due to the random nature of the hot spots, the detailed process of the development of the detonation from a hot spot cannot be readily studied. In a numerical simulation, hot spot formation can be controlled by introducing temperature (density) perturbation in the media. This permits a detailed observation of the subsequent development process of the detonation from the hot spots. Periodic perturbations, introduced in the quasi-steady regime of the initiation process, were first studied by Chue [1993]. Chue demonstrated that periodic perturbations of about the same period as the induction period of the mixture are the most effective in inducing the formation of a detonation wave. However, no detailed study of

the acceleration process from the hot spots, nor the effect of the hot spot on the direct initiation parameters were carried out.

The present study is an extension of the previous work by Chue, aiming at elucidating the mechanism of the onset of detonation from the hot spots. This study has been performed by the numerical simulation of the governing hydrodynamic-chemical kinetics equation in a one dimensional planar geometry.

5.2. The method of study

The results of blast initiation of detonations in a homogeneous gaseous explosive in the presence of a single hot-spot will be presented in this chapter. A density perturbation having the form of a half sinusoidal profile is introduced in the front of the leading shock in the initiation process to generate a hot spot. Figure 5.1 shows the size and location of the perturbation just ahead of the leading shock. In this figure, the spatial density profile is plotted versus the distance from the center of initiation. The perturbation is located in the unburnt mixture just ahead of the shock at x=100. The density perturbation is characterized by its amplitude "H", and its half-wavelength, "W", where $H = (\rho-\rho_o)/\rho_o$, and $W = 0.5*(D_{CJ}/2)*\tau$. Here τ is a time scale of the order of the chemical induction time. D_{CJ} is the CJ velocity. The pressure in the unburnt mixture is kept constant, hence, since the mixture obeys the ideal gas equation of state (i.e. $p = \rho RT$), the negative density perturbation is equivalent to a positive temperature perturbation. The interaction of the leading shock with this perturbation, which results in the formation of a hot spot[1] and eventually the onset of detonation, has then been simulated computationally. The details of the governing equations and numerical methods have already been discussed in Chapter 2.

[1] or a hot layer in one-dimensional analysis.

5.3. Results

5.3.1. The effect of the hot-spot on the initiation process

Figure 5.2 shows the detonation formation process in the critical regime of initiation for a mixture with $E_a/RT_o=27$, $Q/RT_o=50$, and $\gamma=1.2$[2]. In Fig. 5.2, the shock pressure is plotted versus the shock radius. Curve a shows the transition process in the critical regime where a strong blast wave decays to the sub-CJ quasi-steady regime followed by a rapid acceleration to form a self-sustained detonation wave. The details of this process was thoroughly studied in the previous chapters. Curve b in Fig. 5.2 corresponds to the same initiation energy. However, a small density perturbation is put in the front of the leading shock at x=100. The length of the perturbation is about W = 6 and its amplitude, H = 0.4. It is observed that after the interaction with the density perturbation, the shock pressure has dropped first. This is because the shock was passed through a low density region. However, the shock pressure starts to increase when the shock passes the second half of the perturbation (where the density increases to its unperturbed value). It is observed that the shock trajectory is very different from the unperturbed initiation. In contrast to the unperturbed initiation, the second phase now involves a small peak at x=120 before a primary shock pressure acceleration to $P_{sh}=30$ at x=140. Then, after a short period, the shock front abruptly accelerates at about x=165 and forms an overdriven wave at x=175. A decrease of about 12% in the run up distance and the overshoot are observed in Curve b with respect to the initiation in the unperturbed mixture (i.e. Curve a of Fig. 5.2). Therefore, as it was expected, the density perturbation hastens the onset of detonation.

[2] The following analysis in this chapter correspond to this mixture. Otherwise it will be referred.

5.3.2. Mechanism of the shock amplification in the presence of a hot spot

The process of onset of a detonation in the "critical regime" of normal direct initiation (without hot spot) has already been investigated. The main feature of the quasi-steady period was the formation of a pressure pulse between two fronts. The pressure pulse gently grows for a while in the quasi-steady period. At the end of this period, the pressure pulse rapidly accelerates to form a detonation wave, which finally catches up with the leading shock. Therefore, the onset of detonation can be interpreted as the natural development of a pressure pulse inside the structure during the quasi-steady period. Figure 5.2 shows that introducing the density perturbation has promoted the process of the development of the pressure pulse. This effect is indeed due to an external mean (i.e., the prescribed perturbation). To have a clear picture of the events, the effect of a single hot spot on the "subcritical regime" of initiation will be studied in this section.

The shock pressure history for a "subcritical initiation" is shown in Fig. 5.3. Curve a in this figure corresponds to a subcritical initiation with the initiation energy about 5% less than the critical initiation energy. It is seen that, the initiation energy is not enough to create the proper condition for the formation of a pressure pulse. The blast thus decays to a weak shock. However, when the density perturbation is introduced at x=100 ahead of the shock (Curve b in Fig. 5.3), it can act as a trigger to generate a pressure wave within the structure. The propagation of the shock front after interaction with the density perturbation does not have a quasi-steady form anymore. The unstable propagation of the leading shock involves three periods in this case, where every period is decreased with respect to the previous one. In Curve b in Fig. 5.3, it is observed that after the amplifications at x=120, and 160, the shock has slightly decayed. On the other hand, the average shock strength is increased in each pe-

riod with respect to the previous period. However, after its amplification at x=210, it has not decayed anymore. Therefore, the presence of the density perturbation has caused the onset of a self-sustained detonation with the same initiation energy as the subcritical regime of Fig. 5.3-a. More insight about this process can be obtained by studying different profiles.

After hitting the density perturbation (a small region with lower density and higher temperature with respect to other unburned mixture), the shock velocity increases. The sudden increase in shock velocity and its passage through a higher temperature region causes a sudden increase in shock temperature and the formation of a hot layer behind the leading shock. The passage of the shock over the perturbed region and the formation of the hot layer can be seen in pressure, temperature, and reaction rate profiles in Fig. 5.4. The profiles correspond to the period between the moment of the interaction of the shock with the perturbation to the time of the formation of a strong hot-spot. These profiles will be referred according to their numbers which are shown in Fig. 5.4-a (i.e., in pressure profiles). Profile 1 corresponds to the moment when the shock front is at the edge of the perturbation but has not touched it yet. The decrease in pressure behind the shock, which is accompanied with a temperature increase behind the shock is observed in profile 2. As the structure moves forward, a highly excited region is developed behind the shock (i.e., a hot-spot). When the shock is located at x=114 (i.e., profile 11), the hot layer has the maximum temperature in the reaction zone. It is important to note that no significant temperature rise outside this hot-region is observed. Indeed, this hot spot acts very locally. The reaction rate profiles are shown in Fig. 5.4-c. It is observed that the reaction rate in the hot-layer is higher than the surrounding compressed reactant. This is due to higher temperature at the hot-layer. When the shock reaches around x=115, the reaction rate at the hot spot is almost twice the reaction rate at the reaction front (profile 11, Fig. 5.4-c). In fact, the structure involves two reaction fronts at this moment. The fast reaction rate in the hot region acts as a trigger of the instability by generating a pressure

pulse ahead of the hot layer. The formation of the pressure pulse can be seen in pressure profiles. The merging of the pressure pulse with the shock front causes the formation of a temperature wave.

Due to the complexity of the reaction rate profiles, it is preferred to study the next events with only temperature and pressure profiles. Figure 5.5 (a-f) shows temperature and pressure profiles after the merging of the pressure pulse with the shock front up to the onset a self-sustained detonation. Figure 5.5-a and b show the formation of a contact surface (or a temperature wave) after the merging of the pressure pulse with the shock front. The development of the temperature wave as it moves away from the shock can be clearly seen in Fig. 5.5-b. The temperature wave increases the temperature of the reaction zone and hence causes a higher rate of reaction. This causes the formation of another pressure pulse (at x=142). The propagation of this pressure pulse in a motivated region causes that it amplifies very fast. The merging of this pressure pulse with the shock front at x=168 causes the formation of another temperature wave (Fig. 5.5-d). It is seen that, as temperature waves move back with respect to the shock, the region behind them is heated, which induces temperature increase in the compressed reactant. This behavior is different from the propagation of the hot layer which had formed due to the presence of the temperature perturbation. The temperature waves cause the evolution behind the shock and the preconditioning of the reaction zone for the pressure pulse amplification, while the hot spots cause the temperature rise in a narrow layer in the structure. This cycle of formation of a temperature wave, the subsequent evolution of the reaction zone and the formation of the pressure pulse and its merging with the shock, repeats itself several times. Eventually, when the condition behind the shock is prepared, the fast amplification of the pressure pulse causes the formation of an overdriven wave.

To further study the wave interactions and follow the path of different waves, a "t-x"

plot (i.e., a wave diagram) is very helpful. The "t-x" diagram of the initiation process in the presence of the density perturbation is shown in Fig. 5.6. In this figure the path of the shock wave, contact surface, the pressure pulse, and also the path of the some selected particles which cross the shock at the moment of merging of the pressure pulse with the shock, are shown. The wave diagram starts from the moment of the hitting of the density perturbation by the shock and continues to the point of the formation of an overdriven wave. After hitting the density perturbation, a hot-spot (or a hot layer) is formed behind the shock. Due to the high reaction rate at this layer, a pressure pulse is created around x=113. If we follow the pressure wave corresponding to this pressure pulse, it will hit the front around x=120. Figure 5.6 (as well as Fig. 5.5) shows that at the point of the merging of the pressure pulse with the leading shock, a temperature wave has been formed. The trajectory of this temperature wave coincides with the path of the particle hit by the leading shock at x=120. The temperature wave increases the temperature and reaction rate behind the shock and generates a stronger pressure pulse around x=148. This pressure pulse merges with the leading shock at x=169. Next contact discontinuity is formed at this point. When the increase in the rate of energy release can be coupled with the traveling compression pulse, a positive feedback mechanism is formed. Thus, a multi-shock merging mechanism causes the formation of a proper condition for the positive feedback cycle. Each step involves the development of a temperature wave, which is generated at the shock, and a pressure pulse, which originates ahead of the reaction front. The temperature wave moves from the shock towards the reaction front, while the pressure pulse moves in a region which is heated by the temperature wave, towards the shock. The duration of each step is reduced with respect to the previous ones. Or, in other words, the frequency of these waves propagation increases as the structure moves forward. This is similar to a resonance mechanism. When the shock becomes overdriven (i.e., after x=232) two fronts are coupled and move together. Examining temperature profiles

shows that at the first merging (i.e., x=120) the shock temperature is about 2. At the next merging the shock temperature is about 3 and at the 3rd. one, about 4. On the other hand, it is observed that the induction time of each particle after merging is reduced with respect to the previous one. While for the particle which passed the shock at x=120 the induction time is about 12 time units, this time interval is about one unit of time for the particle that crosses the shock at x=232. This is due to the preconditioning of the region behind the leading shock in the previous steps. When a proper condition is built behind the shock, a detonation wave is formed.

In summary, it can be concluded that the role of the hot spot is to generate a local strong reaction center which creates a pressure pulse and triggers a multi-step shock merging mechanism in the complex. Then, the interaction of the pressure pulse with the shock and the formation of temperature waves cause the proper coupling between the chemical heat release and gasdynamics flow. Here, the unburnt mixture is assumed to be homogeneous, thus no hot spot can be expected to form without an external assistance. The shock merging mechanism also has been observed in Chapter 3 when the initiation energy was much lower than the critical value (Fig. 3.15). In chapter 3, it was concluded that the generation of the first pressure pulse is due to a long distance between two fronts and the low temperature of the reaction zone. In reality, due to the presence of discrete inhomogenities in mixtures, or gasdynamics fluctuations such as shock-boundary layer interaction, hot spots are formed.

After understanding the role of hot spots on initiation, some of the questions regarding Fig. 5.2 can be answered now. In the simulation of the critical initiation regime with the presence of a density perturbation (i.e., Fig. 5.2-b), it was observed that the run up distance and the overshoot were both decreased by about 12%. On the other hand, in the previous chapter, it was observed that a smaller induction length causes a shorter run up distance. By

introducing a density perturbation, the temperature behind the shock increases, which causes a shorter induction length, or a smaller distance between the shock and the pressure pulse. Therefore, a smaller run up distance is expected. On the other hand, when the pressure pulse travels in a shorter distance in the compressed mixture, before capturing the front, it has shorter time for amplification. That is the reason for the reduction of the overshoot.

So far, the effect of a special (i.e., H=0.4 and τ=4 or W=6) density perturbation on the initiation has been investigated. However, it is still not clear how the properties of the perturbation, such as its size or its location, may influence the initiation process. In the next section, the effect of hot spot parameters on the initiation process will be studied.

5.4. The effect of the hot spot parameters

5.4.1. Effect of the hot spot size

The single density perturbation was characterized by its amplitude, H, and its wavelength, W, in Fig. 5.1. The amplitude has been measured relative to the density of the unburnt mixture. Thus H=0.4 means a 40% decrease of density with respect to the unburnt mixture. Moreover, the wave length was chosen to be proportional to a length scale of the order of the chemical induction length in the quasi-steady period. In all the calculations, so far, "W" was chosen about 6 (corresponds to τ=4) and "H" was 0.4. Figure 5.7 shows the result of the simulations for different perturbation widths, while the perturbation amplitude is kept constant. It is observed that increasing the length of the perturbation reduces the run up distance. In the previous section, it was shown that when the shock travels over the perturbation, a hot layer is formed behind the shock. A longer perturbation causes a thicker hot layer behind the shock. Therefore, in a thicker layer, the reaction rate is very high, which causes a stronger

pressure pulse to be formed. The stronger pressure pulse captures the shock faster and hastens the onset of detonation. The initiation energies for all cases in Fig. 5.7 are equal and about 5% less than the critical initiation energy.

Figure 5.8 represents the result of the numerical simulation when the amplitude of the perturbation is varied for a given wavelength. On the top of this figure, the variation of the run up distance with the perturbation amplitude is plotted. It is observed that there is an optimum value for the amplitude of the perturbation which causes the minimum run up distance. This optimum case corresponds to a 50% perturbation in density of the unburned mixture. The amplitude of the perturbation has two effects. In general, moving over a low density region (i.e., a high temperature region), causes an increase in shock velocity and temperature. This effect in general causes a higher rate of the chemical reaction behind the shock for a higher amplitude. On the other hand, when the shock passes a low density region, its pressure drops sharply. This can be seen in all cases in Fig. 5.8 around x=100. The drop in shock pressure, which is stronger for higher amplitude, causes a drop of the pressure of the reaction zone. This can be seen in pressure profiles (e.g., Fig. 5.4). Therefore, although a pressure pulse is generated due to the high reaction rate, its strength may be lower for higher perturbation amplitude. Figure 5.8 shows that a 50% perturbation can trigger the instability inside the structure faster than both weaker and stronger perturbations.

5.4.2. Effect of the hot spot location

In previous chapters it was observed that the initiation process involves two phases prior to the final abrupt amplification of the shock front. Two different physical effects were responsible for these two phases. The decaying phase was governed by the blast energy to modifying the flow structure. The second phase (i.e., the quasi-steady period), was character-

ized by the formation and development of a pressure pulse. In this section, the effect of the perturbation in the two phases will be studied. Figure 5.9 shows the results of some simulations for a given perturbation (i.e., size is fixed) which is located at different locations ahead of the leading shock. It is seen that when the perturbation is located before x=50 it cannot promote the initiation and the blast continues to decay, even faster than the unperturbed case. On the other hand, when it is located ahead of the shock in the quasi-steady region, the same perturbation can help to onset a detonation. The different profiles corresponding to the perturbation located at x=100 has already been studied (i.e., Fig. 5.4, and 5.5). Pressure, temperature, and reaction rate profiles during the initiation process corresponding to a perturbation at x=30, are shown in Fig. 5.10 (a-c). These profiles show that a hot layer with a very high reaction rate is formed in this case too. However, due to the high shock strength, the reaction front is coupled with the shock. In Chapter 3 it was shown that a "sub-CJ shock-reaction zone" complex is inherently unstable and always undergoes a transition to detonation. The mechanism of this transition is the development of a pressure pulse in a long induction length. Hot spots generate a local reaction center which hastens the formation of the pressure pulse. When the wave is overdriven, no pressure pulse or temperature wave may be developed between two fronts, since the induction length is too small. This observation can also be interpreted from another point of view. If we consider the role of the perturbation as the trigger of the instability, it can be amplified only in an unstable medium. According to the linear stability analysis of one-dimensional detonation [Lee and Stewart 1988], the detonation wave becomes unstable for $E_a/RT_o>25$ or $E_a/RT_{sh}>6.2$. When the shock is arrived at x=30, it is very strong and $E_a/RT_{sh}<6.2$, while at x=100 we have $E_a/RT_{sh}=7.6$. Therefore, the perturbation cannot trigger the instability when the shock hits it at x=30. This observation confirms the necessary condition of the amplification in the quasi-steady period, as proposed in previous chapters (for both stable and unstable detonations).

5.5. Effect of the hot spot on initiation process for different activation energies

It has already been shown that in general the initiation process is governed by the same mechanism for both stable and unstable detonations (i.e., different activation energies). To study the effect of the hot spots for different activation energies, some of the previous calculations were repeated for a very stable detonation (i.e., $E_a/RT_o=21$). The results of two typical calculations are presented in Figs. 5.11 and 5.12. Figure 5.11 shows the calculation for the critical regime of initiation. Figure 5.11-a corresponds to the initiation process without perturbation, and Fig. 5.11-b shows the shock pressure evolution in the presence of a single density perturbation. The general trend is the same as Fig. 5.2 which corresponds to $E_a/RT_o=27$. The reduction in run up distance and the overshoot are 10% and 12% respectively, which are very close to the corresponding values for the unstable case. Figure 5.12 represents the initiation process for initiation energy which is about 5% less than the critical value. It is observed that the formation of hot spots triggers the development of a pressure wave and causes the onset of a detonation for this subcritical initiation energy. Therefore, as it was expected, no significant difference is observed with respect to the initiation of $E_a/RT_o=27$. To have a more comprehensive comparison, the run up distance and the overshoot calculated for the critical initiation regime, with and without the presence of hot spot, are given in Table 5.1 for different activation energies. By increasing the activation energy, a slightly higher reduction in run up distance is observed. However, the variation is not significant. Therefore, it can be concluded that a single hot spot has almost the same effect for both stable and unstable detonations. This confirms the results of the previous chapters regarding the similarity of the critical initiation process for both stable and unstable detonations.

5.6. Discussion and Concluding remarks

The present work demonstrates the salient feature of a simple model to illustrate many aspects of the hot spot mechanism. The main results of the present chapter may by summarized as follows:

1- It was shown that by putting a density perturbation in the front of the leading shock, a hot layer (i.e., the one-dimensional counterpart of a hot spot) is generated behind the leading shock. The generation of this hot layer is due to an external mean. This hot spot generates a local reaction center and generates a pressure pulse. The merging of the pressure pulse with the shock front causes the formation of a backward (with respect to the shock) temperature wave. A multi-step shock merging mechanism is responsible to prepare the condition for rapid acceleration of the leading shock to an overdriven wave.

2- It was also shown that the amplitude of the density perturbation has an optimal value which can onset a detonation faster. The existence of an optimal value is due to two different effects of the perturbation: decreasing the shock pressure and increasing the shock temperature.

3- By examining the effect of a single perturbation, located in different phases ahead of the shock, it was observed that the perturbation is effective when we have a "sub-CJ shock-reaction zone" complex. In Chapter 3, it was shown that this complex is inherently unstable and always undergoes a transition to detonation. The mechanism of this transition is the development of a pressure pulse within a long induction length. A hot spot generates a local reaction center which hastens the formation of the pressure pulse. Using the instability criterion $E_a/RT_{sh}>6.2$, it was shown that the hot spot can promote the initiation when this

condition is satisfied. On the other hand, in our previous calculations, it was observed that in the quasi-steady period, the effective activation energy, E_a/RT_{sh}, is usually much higher than 6.2, regardless of the value of the reduced activation energy, E_a/RT_o.

4- Comparing the processes before the rapid amplification for different activation energies, no significant difference was observed. Therefore, it may be concluded that this phase is mainly dominated by gasdynamics effects such as wave interaction. This observation is in agreement with the experimental observation of Campbell et al [1961]. Investigating the effect of gas bubbles on the initiation of nitromethane by strong plane shocks, they observed that the major effect of the bubbles was to produce a shock-interaction mechanism. They used bubbles of gases with different γ such as Argon (γ=1.67) and Butane (γ=1.1). To show conclusively that the pressure interaction is the effective cause, they even used small pieces of plastic and tungsten. For all cases, the perturbation caused initiation in a smaller time with respect to a homogeneous mixture. The reduction in the time of initiation was very close for all cases. Then, they concluded that the heating role of the perturbation does not have an important effect on the initiation process. The main role of a perturbation is to produce a hot spot and to generate a pressure pulse to trigger the instability.

5- The hot spot mechanism observed here is similar to the McVey-Toong mechanism [McVey and Toong 1972], which was proposed to describe the instability observed in the hypersonic reacting flow around blunt bodies. According to this mechanism, the reason of the instability is the sensitivity of the location of the reaction front or reaction rate to change in shock strength. The wave interaction observed in their experiments and the formation of contact discontinuity are the same as what is observed in Figs. 5.5 and 5.6. The shock merging mechanism has also been observed in Chapter 3 when the initiation energy was much

lower than the critical value (Fig. 3.15). In chapter 3, it was concluded that the generation of the first pressure pulse was due to a long distance between two fronts and the fast chemical reaction at the reaction front.

Chapter 6

Conclusion

6.1. Introduction

The objective of the present study was to elucidate the physical processes underlying the onset of detonations in the critical regime of blast initiation. The effect of "detonation instability" and the role of "hot spots" on direct initiation were also investigated in the present study. Due to the different complexities of the real problem, a simplified analytical model was used during this research. This model consists of the one-dimensional reactive Euler equations in a planar geometry and a single-step Arrhenius rate law to represent the chemical kinetics. The mixture under study was assumed to obey the ideal gas equation of state. The phenomenon of direct initiation was then simulated by numerical integration of the governing gasdynamics-chemical kinetics equations. It is very important to note that the results obtained in the present work should be interpreted within the frame work of the above mentioned gasdynamics and chemical kinetics models. Before concluding this investigation, some important results from previous chapters will first be summarized.

6.2. Summary

- The quasi-steady assumption, which has been utilized in several initiation models in the past twenty years, fails to express the dynamic nature of the initiation process. Although the leading shock has an almost constant velocity for a long time in the quasi-steady period, the flow behind the shock is unsteady.

- The unsteadiness stems from the inherent instability of a shock induced reaction complex, which naturally seeks the stable condition which is CJ detonation.

- It was observed that, especially when the blast has decayed to a very weak shock, the acceleration to detonation may occur far behind the shock front. This observation has the important implication that the initiation phenomenon may not occur in the vicinity of the shock front. Indeed, initiation is due to the development of a pressure pulse in the vicinity of the reaction front, no matter how far from the shock it may be.

-The present results contradict with the experimental observation that there is always a distinct value for the critical initiation energy, below that no detonation occurs. The reason for this contradiction is the analytical model used in the present work, i.e. a single-step Arrhenius rate law and the assumption of no heat loss. Heat loss can be significant when the leading shock and the reaction rate are slow. In this case, the time scale of the heat transfer has the same order of magnitude as the time scale of chemical heat release. However, the asymptotic value of E_o/p_o in the "initiation energy vs. run up distance" curve was suggested as the representative of the critical initiation energy. When the activation energy is low, the change in this curve is gradual and no asymptotic value exists.

- The transition process in the final stage of "DDT" and "blast initiation" follows es-

sentially the same mechanism. The elements of this mechanism are a precursor shock wave, the unsteady reaction domain behind the shock, and the quasi-steady reaction front. The onset is due to the generation and amplification of a pressure pulse between the reaction front and the shock front. Therefore, as proposed in Chapter 1, DDT and direct initiation differ only in the initial state.

- Comparing the speed of the fast deflagration in different processes which result in a detonation, Chue [1993] concluded that the quasi-steady fast deflagration prior to the formation of detonation depends on the energetics (i.e., CJ deflagration) rather than the details of the structure. The present numerical investigation shows that the averaged properties in the quasi-steady period are different for mixtures with the same CJ detonation velocity but different activation energies.

- Studying the details of one cycle of a pulsating detonation shows a very similar behavior to the initiation process in the critical regime. This consists of the decoupling of the reaction front from the leading shock and the shock amplification due to the instability of the wave structure. This similarity suggests that the more difficult instability problem of a pulsating detonation can be analyzed via the direct initiation phenomenon.

-No qualitative difference was observed during the quasi-steady period for different activation energies. In other words, considering the key role of the activation energy on the "detonation instability," it seems that the onset in the quasi-steady period of the critical regime follows the same mechanism for both stable and unstable detonations.

- Despite the large difference in the shock strength in the quasi-steady period for different activation energies, it was observed that the sensitivity parameter (i.e., the derivative of the induction time with respect to shock temperature) for the minimum shock strength in

the quasi-steady period varies within a narrow range.

- For highly unstable detonations, no unique value can be specified as the critical initiation energy. Indeed, there are two asymptotic values in the "initiation energy vs. run up distance" curve. Failure may occur below both values.

- It was demonstrated that those models based on the Zeldovich criterion cannot predict the initiation energy for all ranges of activation energies. The invalidity of the Zeldovich criterion was attributed to the unsteady effects in the second phase of the initiation process which is not considered in the Zeldovich initiation theory.

- The local and explosive nature of the initiation process, as well as two different modes of ignition, introduced by Oppenheim, could not be studied by the present one-dimensional simulation.

- The present work demonstrated the salient features of a simple model to illustrate many aspects of the hot spot mechanism. This model consists of a single sinusoidal density perturbation prescribed ahead of the shock front.

- It was shown that by prescribing a density perturbation in the front of the leading shock, a hot layer (i.e., the one-dimensional counterpart of hot spot) is generated behind the leading shock. This hot layer generates a local reaction center and generates a pressure pulse. The merging of the pressure pulse with the shock front causes the formation of a backward running (with respect to the shock) temperature wave. A multi-step shock merging mechanism is responsible to prepare the condition for a rapid acceleration of the leading shock to an overdriven wave.

- The amplitude of the density perturbation has an optimal value which can initiate a

detonation most rapidly. The existence of an optimal value is due to two different effects of the perturbation: decreasing the shock pressure and increasing the strength of a hot reaction layer generated by the perturbation.

- Examining the effect of a single perturbation, located in different phases ahead of the shock, it was observed that the perturbation is most effective when we have a "sub-CJ shock-reaction zone" complex.

- Comparing the initiation process in the presence of a hot spot for different activation energies, no significance difference was observed. Therefore, it may be concluded that this phase is mainly dominated by gasdynamics effects such as wave interactions.

6.3. Concluding remarks

Extensive numerical simulations has been carried out in the present research show that the onset of detonation in the critical regime is predominately due to the generation and development of a pressure pulse in the quasi-steady period. This pressure pulse may be interpreted as the counterpart of the "detonation bubble" of Lee [1977] within the framework of the present analytical model. The role of the leading shock is essentially the conditioning of the unburned reactant. The simulation of initiation at low initiation energies can show the role of the leading shock in a profound way. As shown in Chapter 3, when the leading shock is very weak the onset of detonation may occur far from the leading shock. When activation energy is low, due to a fast reaction rate at the reaction front, a second shock may even form between the reaction front and the leading shock, which means the leading shock plays only a passive role.

The above conclusion helps to understand the drawbacks of current initiation models. Most of the current models are based on energetics (i.e., a simple energy balance). Furthermore, these models prescribe some properties to the leading shock to determine the critical initiation energy. The present study suggests that the onset in the quasi-steady period is a rather dynamic phenomenon which cannot be expressed by a simple energy balance. On the other hand, the properties of the leading shock is not as important as proposed by some theories. The dynamic processes in the quasi-steady period strongly depend on the rate of chemical heat release and the induction length. It seems that the dependence of the initiation on dynamic properties such as the temperature sensitivity of the induction time in the quasi-steady period is much more important than the leading shock properties.

During the present research, the essential role of the reaction rate as well as the induction length were observed. In particular, the generation of the pressure pulse is due to competition between the generation and dispersion of compression waves. The abrupt amplification of the pressure pulse depends on the synchronization between the traveling pressure pulse and the chemical heat release (i.e., SWACER mechanism). The essential elements of this process are the induction length and the reaction rate. Due to the special kinetics model was used in the present work, the role of these two parameters cannot be studied independently. Besides the amplification process, the existence of a critical initiation energy may also depend on the reaction model. In fact, if no heat is transferred from the system, within the framework of a single-step exothermic reaction model, a detonation always is formed regardless of the value of the initiation energy (Chapter 3). Therefore, to predict a critical initiation energy in a lossless model, chemical kinetics should involve some endothermic steps. The above facts would justify the use of a more complicated kinetic model in future research of the initiation problem.

Another conclusion which can be made from the present study is the universality in the second phase of the initiation. Comparing the results of the present work for "direct initiation" and the studies of Clarke and coworkers for three other initial conditions in the category of "DDT," it is seen that a detonation is formed by abrupt amplification of a pressure pulse at the end of a quasi-steady period. The mechanism of this onset is independent of the first phase of initiation which is determined by the initial and boundary conditions. As stated in Chapter 3, from a purely gasdynamics point of view, it can be shown that any sub-CJ "shock induced reaction complex" is unstable and seeks the stable condition which is a Chapman-Jouguet detonation. It appears that the mechanism of transition, when the "shock-reaction zone" complex has been formed, is universal regardless of the history of the complex.[3]

The propagation of a self-sustained pulsating detonation is believed to be a process of continuous failure and re-initiation. If we consider a single cycle of a pulsating detonation, it resembles the decay of a blast wave which is followed by the re-establishment of an overdriven detonation. Comparing different profiles in a cycle of a pulsating detonation with the corresponding profiles of a blast initiation, we can observe more similarity between the two phenomena. Therefore, the mechanism of the onset of detonation in blast initiation may be used to interpret the oscillatory propagation of pulsating detonations. Investigating the initiation of highly unstable detonations in Chapter 4 it was observed that, even in supercritical initiation, the leading shock may accelerate to an overdriven wave. This problem was attributed to the formation of a pressure pulse inside the induction zone. This fact can be generalized to all pulsating detonations. When the distance between the leading shock and the

[3] The above fact regarding the instability of a shock induced reaction, may be generalized to all combustion waves. In general, a given explosive can support a spectrum of flame speeds from about 0.5 m/s to about 2000 m/s depending on the initial and boundary conditions. If boundary conditions permit, a laminar flame always tends to accelerate to a turbulent flame which can further accelerate to a detonation. Hence, we may say that all combustion waves are unstable and always tend toward a maximum burning rate compatible with the boundary conditions. The upper limit of a stable combustion wave is a CJ detonation.

reaction front (i.e., the induction length) is high and the rate of generation of pressure waves is higher than the rate of dispersion, a pressure pulse is formed between the reaction front and the leading shock. The amplification of this pressure pulse causes the instability of the detonation front. In the case of stable detonations, the pressure waves generated by the chemical reaction meet each other right at the leading shock and no pressure pulse is formed behind the shock.

One of the major objectives of the present study was to examine the role of "detonation instability" on the initiation process. The above discussions suggest that the mechanism of detonation instability is the same as for the establishment of a detonation in the quasi-steady period. In the critical regime of initiation, the leading shock decays to a minimum velocity. The value of this minimum velocity depends on the activation energy. Due to the inherent instability of a sub-CJ "shock-reaction zone" complex, it transits to an overdriven detonation. Extensive numerical simulations performed during the present work suggest that the initiation process is similar for both stable and unstable detonations. In other words, the structure during the quasi-steady period is very unstable for all activation energies. Further investigation has revealed that for highly unstable detonations, after decaying to a strength close to the CJ velocity in supercritical initiation, the structure is inherently unstable. This instability causes the occurrence of a second initiation limit for highly unstable detonations. A better kinetics model as well as the inclusion of heat losses lead to a cut off value for the critical initiation energy. Therefore, it seems very unlikely that the presence of the second limit depends on the hydrodynamics or chemical kinetics model used in the present work.

It is well-known that hot spots correspond to the generation of a local high temperature region which promotes the reaction rate. However, the detailed processes leading to the for-

mation of detonations from hot spots have not been studied. The reason for this is the complexity of the detailed gasdynamics processes such as shock-boundary layer interactions and also the random nature of the formation of hot spots. In the present study, the salient feature of a simple model to illustrate many aspects of the hot spot mechanism was demonstrated. It was observed that the hot spot mechanism is mainly a gasdynamics process rather than one of chemical kinetics. In particular, it was observed that a hot spot promotes the initiation process by a multi-step shock merging mechanism.

6.4. Contribution to knowledge

The numerical studies carried out in the present research have contributed to the understanding of the blast initiation of gaseous detonations. The main contributions are summarized below.

1- The onset of detonations in the second phase of initiation (i.e., in the quasi-steady period) is due to the generation and amplification of a pressure pulse ahead of the reaction front in the induction region. This is a rather dynamic phenomenon which strongly depends on the heat release mechanism. Furthermore, according to the present observations the initiation stems far from the leading shock, at the reaction front.

2- The mechanism of initiation in the second phase of initiation is universal. The mechanism of onset is independent of the first phase of initiation which is determined by the initial and boundary conditions. Therefore, the onset in the quasi-steady period has the same mechanism for both "DDT" and "blast initiation".

3- In the framework of the analytical model used in the present study, no unique value

exists for the critical initiation energy. However, the asymptotic value of the initiation energy in the "initiation energy vs. run up distance" curve was proposed as the critical initiation energy for the current analytical model.

4- The mechanism of detonation onset in the quasi-steady period is the same for both stable and unstable detonations. However, for very high activation energies (characterized by chaotic oscillation of the final self-sustained detonation), no unique value can be defined as the critical initiation energy. There are two asymptotic values in the "initiation energy vs. run up distance" curve. Below these values failure may occur.

5- In contrast to what was suggested by Chue [1993], the properties (e.g., the velocity) of high speed deflagrations prior to the onset of self-sustained detonations depend on the chemical kinetic properties of the mixture . In other words, fast deflagrations in the quasi-steady period are not necessarily Chapman-Jouguet deflagrations. Chue [1993] suggested that the quasi-steady fast deflagration prior to the formation of a detonation depends on the energetics (i.e., CJ properties) rather than the chemical kinetics.

6- Hot spots promote initiation through a multi-step shock merging mechanism. This mechanism is mainly a gasdynamics process rather than a chemical kinetics one.

7- The presence of a single hot spot reduces the critical initiation energy as well as the run up distance. There is an optimum value for the amplitude of the hot spot which can promote initiation faster.

6.5. Recommendation for future research

In the present research, all studies have been restricted to a simplified analytical model.

This was a necessary step in understanding the basic mechanisms underlying the onset of detonation in the quasi-steady period. During analysis of the results, some drawbacks of the assumptions regarding the gasdynamics model as well as the chemical rate law were referred to. Now, to further clarify the initiation problem, the following modifications with respect to the present research are recommended.

1- As shown in Chapter 3, the amplification process as well as the existence of a critical initiation energy depend on the chemical kinetics model. The generation and amplification of the pressure pulse depend on both the reaction rate and the induction length. In a single-step model, the effect of these two parameters cannot be investigated independently. It seems that using a multi-step chemical kinetic model, which would allow the independent variation of the induction length and the reaction rate, is a logical continuation of the present work.

2- During the analysis of some results, the important role of the heat loss was pointed out. This effect is important when the chemical reaction time scale is of the same order as the time scale of heat transfer to boundaries. To address some important questions such as the existence and the value of the critical initiation energy, the effect of heat loss should be included in the analytical model. It should be noted that this effect can be achieved through endothermic reaction steps as well.

3- Experimental observations of the initiation problem all indicate some very local phenomena such as local reaction centers and local explosions prior to the formation of a self-sustained detonation. It is not clear whether this is another mechanism or still some kind of wave amplification process. A multidimensional analysis may shed light on this question.

4- The main challenge in this field is to develop a quantitative model that predicts ini-

tiation parameters (such as the critical initiation energy) based on the dynamic aspects in the quasi-steady period. It seems that some concepts such as the temperature sensitivity of the induction time or the effective activation energy can assists this modeling.

References

1) Abouseif, G.E., and Toong, T.Y., (1982), "Theory of Unstable One-Dimensional Detonations," *Combust. Flame*, Vol. 45, pp. 67-94.
2) Bach, G.G., and Lee, J.H., (1970-a), "An Analytical Solution for Blast Waves," *AIAA J.*, Vol. 8, pp. 271-275.
3) Bach, G.G., and Lee, J.H., (1970-b), "On the Propagation of Spherical Detonation Waves," Paper presented at the twenty-third Annual Meeting of the APS Division of Fluid Dynamics, Virginia.
4) Bach, G.G., Knystautas, k., and Lee, J.H., (1969), "Direct Initiation of Spherical Detonations in Gaseous Explosives,", *12th. Symposium (International) on. Combustion*, pp. 853-864.
5) Benedick, W.B., (1982), "Review of large scale Fuel-Air Explosion tests and Techniques," *Proceeding of the First International Specialist Meeting on Fuel-Air Explosion*, SM Study No. 16, pp. 507-552. University of Waterloo Press, Waterloo, Ontario, Canada.
6) Benedick, W.B., Guirao, C.M., Knystautas, R., and Lee, J.H., (1986), "Critical Charge for the Direct Initiation of Detonation in Gaseous Fuel-Air Mixtures," *Prog. Astronautics and Aeronautics*, Vol. 106, pp. 181-202.
7) Berger, M.J., and Colella, P., (1989), "Local Adaptive Mesh Refinement for Shock Hydrodynamics," *J. Comput. Phys.*, Vol. 82, pp. 64-84.
8) Bourlioux, A., (1991), *Numerical studies of Unstable Detonations*, Ph.D. Thesis, Department of Applied and Computational Mathematics, Princeton University.
9) Bourlioux, A., Majda, A., and Roytburd, V., (1990), "Non-Linear Development of Low Frequency One-Dimensional Instabilities For Reacting Shock Waves," *Dynamical Issues in Combustion Theory*, I.M.A. Vol. 35, pp. 1-29.
10) Campbell, A.W., Davis, W. C., Ramsay, J. B., and Travis, J. R., (1961), "Shock Initiation of Detonation in Liquid Explosives", *Phys. Fluids*, Vol. 4, pp. 498-510.
11) Chern, I.L., and Colella, P., (1987), "A Conservative Front Tracking Method for Hyperbolic Conservation Laws," Lawrence Livermore National Laboratory, UCRL-97200.
12) Chue, R.H.S., (1993), *High Speed Deflagration and Its Transition to Detonation*, Ph.D. Thesis, Department of Mechanical Engineering, McGill University, Canada.
13) Clarke, J. F., (1989), "Fast Flames, Waves, and Detonations," *Prog. Energy Combust. Sci.*, Vol. 15, pp. 241-271.
14) Clarke, J. F., and Singh, G., (1989), "A numerical Simulation of Shock Generated Ignition Using the Random Choice Method", *Lecture Notes In physics*, Vol. 351, pp. 22-35.
15) Clarke, J.F., Kassoy, D. R., and Riley, N., (1986), "On the Direct Initiation of a Plane Detonation Wave," *Proc. R. Soc. Lond. A*, Vol. 408, pp. 129-148.
16) Clarke, J.F., Kassoy, D. R., Meharzi, N. E., Riley, N., and Vasantha, R., (1990), "On

the Evolution of Plane Detonations," *Proc. R. Soc. Lond. A*, Vol. 429, pp. 259-283.
17)Colella, P., and Woodward, P.R. (1984), "The Piecewise Parabolic Method (PPM) for Gas-Dynamical Simulations," *J. Comput. Phys.*, Vol. 54, pp. 174-201.
18)Desbordes, D., (1986), "Correlation Between Shock Flame Predetonation Zone and Cell Spacing in Critically Initiated Spherical Detonations," *Prog. Astronautics and Aeronautics*, Vol. 106, pp. 166-180
19)Dremin, A.N., (1993), "Mechanism of Unstable Detonation Front Origin," *Prog. Astronautics and Aeronautics*, Vol. 153, pp. 105-111.
20)Edwards, D.H., Hooper, G., and Morgan, J.M., (1976), "An Experimental Investigation of the Direct Initiation of Spherical Detonation," *Acta Astronaut*, Vol. 3, pp. 117-130.
21)Fickett, W., and Davis, W.C., (1979), *Detonation*, University of California Press.
22)Fickett, W., and wood, W.W. (1966), "Flow Calculation for Pulsating One-Dimensional Detonations," *Phys. Fluids.*, Vol. 9, pp. 903-916.
23)Fry, R.S., and Nicholls, J.A., (1969), "Blast Wave Initiation of Gaseous and Heterogeneous Cylindrical Detonation Waves," *12th Symposium (International) on Combustion*, pp. 43-52.
24)He, L., and Clavin, P., (1994), "On the Direct Initiation of Gaseous Detonation by an Energy Source," *J. Fluid Mech.*, Vol. 277, pp. 227-248.
25)He, L., and Larrouturou, B., (1993), "Moving Grid Numerical Simulations of Planar Time-Dependent Detonations," CERMICS , No. 93-23.
26)He, Longting, (1996), "Theoretical Determination of the Critical Conditions for Direct Initiation of Detonations in Hydrogen-Oxygen Mixtures," *Combust. Flame*, Vol. 104, pp. 401-418.
27)He, Longting, and Lee, J.H.S., (1995), "The dynamical limit of one-dimensional detonations," *Phys. Fluids*, Vol. 7, pp. 1151-1158.
28)Hirsch, C., (1988), *Numerical Computation of Internal and External Flows*, Wiley
29)Knystautas, R., (1968), *An Experimental Study of Spherical Gaseous Detonation Waves*, Ph.D. Thesis, Department of Mechanical Engineering, McGill University, Canada.
30)Knystautas, R., Lee, J.H., and Guirao, C.M. (1982), "The Critical Tube Diameter for Detonation Failure in Hydrogen-Air Mixtures," *Combust. Flame*, Vol. 48, pp. 63-83.
31)Knystautas, R., Lee, J.H., and Moen, I., (1979), "Direct Initiation of Spherical Detonation by a Hot Turbulent Gas Jet," 17th Symposium (International) on Combustion, pp. 1235-1245.
32)Kyong, W.H., (1972), *A Theoretical Study of Spherical Gaseous Detonation Waves*, Ph.D. Thesis, Department of Mechanical Engineering, McGill University, Montreal, Canada.
33)Lee, H.I., and Stewart, D.S., (1990). "Calculation of Linear Detonation Instability: One-Dimensional Instability of Plane Detonation," *J. Fluid Mech.*, Vol. 216, pp. 103-132.
34)Lee, J.H. (1984), "Dynamic Parameters of Gaseous Detonations," *Ann. Rev. Fluid.*

Mech., Vol. 16, pp. 311-336.

35)Lee, J.H. (1991), "Dynamic Structure of Gaseous Detonation, *Dynamic Structure of Detonation in Gaseous and Dispersed Media*, A. A. Borissov (ed.), Kluwer Academic Publishers, pp. 1-25.

36)Lee, J.H., and Ramamurthi, K., (1976), "On the Concept of the Critical Size of a Detonation Kernel, ", *Combust. and Flame*, Vol. 27, pp. 331-340.

37)Lee, J.H., Knystautas, R., and Guirao, C., (1982), "The Link Between Cell Size, Critical Tube Diameter, Initiation Energy, and Detonability Limits," *Proceedings of the First Specialist Meeting on Fuel-Air Explosions*, SM Study No.16, pp. 157-187. University of Waterloo Press, Waterloo, Canada.

38)Lee, J.H., Knystautas, R., and Yoshikawa, N., (1978), "Photochemical Initiation of Gaseous Detonations," *Acta Astronautica*, Vol. 5, pp. 971-982.

39)Lee, J.H.S. (1977), "Initiation of Gaseous Detonation," *Ann. Rev. Phys. Chem.*, Vol. 28, pp. 75-104.

40)Lee, J.H.S., (1965), *The Propagation of Shocks and Blast Waves in a Detonating Gas*, Ph.D. Thesis, Department of Mechanical Engineering, McGill University, Montreal, Canada.

41)Lee, J.H.S., (1972), "Gasdynamics of Detonations," *Astraunica Acta.*, Vol. 17, pp. 455-466.

42)Lee, J.H.S., and Moen, I.O., (1980), "The Mechanism of Transition From Deflagration to Detonation in Vapor Cloud Explosions," *Prog. Energy Combust. Soc.*, Vol. 6, pp. 359-389.

43)Lee, J.H.S., Lee, B.H.K., and Knystautas, R., (1966), *Phys. Fluids*, Vol. 9, pp. 221-222.

44)Lundstrom, E.A., and Oppenheim, A.K., (1969), "On the Influence of Non-Steadiness on the Thickness of the Detonation Wave," *Proc. Roy. Soc. A.*, Vol. 310, p. 463-478.

45)Manzhalei, V. I., (1977), *Fizika Goreniya Vzryva*, Vol. 13, pp. 47-72.

46)Matsui, H., and Lee, J.H., (1979), "On the Measure of the Relative Detonation Hazards of Gaseous Fuel-Oxygen and Air Mixtures", *17th Symposium (International) on Combustion*, pp. 1269-1280.

47)Meyer, J. W., and Oppenheim, A. K., (1971), "On the Shock-Induced Ignition of Explosive Gases", *13th Symposium (International) on. Combustion.*, pp. 1153-1164.

48)Moen, I.O., Funk, J.W., Ward, S.A., and Thibault, P.A., (1984), "Detonation Length Scales for Fuel-Air Explosives," *Prog. Astronautics and Aeronautics*, Vol. 94, pp. 55-79.

49)Moen, I.O., Sulmistras, A., Thomas, G.O., Bjerketvedt, D., and Thibault, P.A., (1986), "Influence of Cellular Regularity on the Behavior of Gaseous Detonations," *Prog. Astronautics and Aeronautics*, Vol. 106, pp. 220-243.

50)Oran, E. S., and Boris, J. P., (1987), *Numerical Simulation of Reactive Flow*, Elsevier Science Publicating Co., Inc.

51)Shchelkin, K. L., and Troshin, YA. K., (1965), *Gasdynamics of Combustion*, Mono Book Corp., Baltimore, Md.

52)Shepherd, J.E., and Lee, J.H.S., (1992), "On the Transition From Deflagration to Detonation," *Major Research Topics in Combustion*, pp. 439-490.

53)Shepherd, J.E., Moen, I.O., Murray, S.B., and Thibault, P.A. (1986), "Analysis of the Cellular Structure of Detonations," *21st Symposium (International) on Combustion*, pp. 1649-1658.

54)Sichel, M., (1977), "A Simple Analysis of the Blast Initiation of Detonations," *Acta Astronaut*, Vol. 4, pp. 409-424

55)Sichel, M., (1992), "Transition to Detonation, Role of Explosion within an Explosion," *Major Topics in Combustion*, pp. 491-528.

56)Sileem, A.A., Kassoy, D.R., and Hayashi, A.K., (1991), "Thermally Initiated Detonation through Deflagration to Detonation Transition," *Proc. R. Soc. Lond. A*, Vol. 435, pp. 459-482.

57)Singh, G., and Clarke, J. F., (1992), "Transient Phenomena in the Initiation of a Mechanically Driven Plane Detonation," *Proc. R. Soc. Lond. A*, Vol. 438, pp. 23-46.

58)Sod, G.A., (1977), "A Numerical Study of Converging Cylindrical Shock," *J. Fluid Mech.*, Vol. 83, pp. 785-794.

59)Soloukhin, R.I. (1968), "Nonstationary Phenomena in Gaseous Detonation," *12th Symposium (international) on Combustion*, pp. 799-807.

60)Taki, S., and Fujiwara, T. (1984), "Numerical Simulation on the Establishment of Gaseous Detonation ," *Prog. Astronautics and Aeronautics*, Vol. 94, pp. 186-200.

61)Taylor, S.G., (1950), "The Formation of Blast Wave by a very Intense Explosion, I-Theoretical Discussion," *Proc. Roy. Soc. A.*, Vol. 201, pp. 159-174.

62)Toong, T. Y., (1983), *Combustion Dynamics*, McGraw-Hill Book Company.

63)Ul'yanitskii, V. Yu., (1981), "Role of Flashing and Transverse-Wave Collisions in the Evolution of a Multifrontal Detonation Wave Structure in Gases," *Fiz. Georeniya Vzrya*, Vol. 17, pp. 127-133.

64)Westbrook, C. K., (1982), "Chemical Kinetic Prediction of Critical Parameters in Gaseous detonations," *19th. Symposium (International) on Combustion*, pp. 615-623.

65)Williams, D. N., Bauwens, L., and Oran, E. S., (1996), "A Numerical Study of the Mechanism of Self-Reignition in Low-Overdrive Detonations," *Shock Waves*, Vol. 6, pp. 93-110.

66)Yang, H.Q., and Przekwas, A.J., (1992), "A Comparative Study of Advanced Shock-Capturing Schemes Applied to Burger's Equation," *J Comput. Phys.*, Vol. 102, pp. 39-159.

67)Zel'dovich, B., Kograko, S.M., and Simonov, N.N., (1956), "An Experimental Investigation of Spherical detonation of Gases," *Translation of J. Tech. Phys.*, Vol. 1, pp. 1689-1713.

68)Zhang, F. (1996), "Private Communication".

Appendix A. Numerical Methods

A.1. The piecewise parabolic method (PPM)

The piecewise parabolic method (PPM) of Colella and Woodward [1984] is a higher-order extension of the Godunov method. To explain PPM we consider the numerical solution of an initial-boundary value problem for the hyperbolic equation:

$$u_t + \alpha f_x = 0 \tag{1}$$

here, u(x,t) is an unknown function of x and t, and f(u) is called the flux function. Figure A.1 illustrates space-time domain and indexing.

Equation 1 has the following discretized form:

$$u_j^{n+1} = u_j^n - \frac{\alpha \Delta t}{\Delta x}(f_{j+\frac{1}{2}} - f_{j-\frac{1}{2}}) \tag{2}$$

where $\Delta x = x_{j+1/2} - x_{j-1/2}$, and $\Delta t = t^{n+1} - t^n$. " f " is the flux at the interface between two cells. Knowing the value of u at a time level t^n, the key to finding the solution at a new time level t^{n+1} is to properly compute the interface fluxes $f_{j+1/2}$, and $f_{j-1/2}$. Indeed, the difference between the different methods mentioned above is in the treatment of these fluxes [Hirsch 1988].

The main contribution of Godunov is the way in which the fluxes are computed. Instead of using some averaging between cells values, in Godunov method the fluxes are computed from an exact solution of Riemann problem at the interface between two adjacent cells. PPM is a higher-order Godunov method which, instead of using a constant value for the de-

pendent variable at each cell (as in the Godunov method), uses a parabolic profile in each cell of the form:

$$u(x) = u_{j-\frac{1}{2}} + \xi\,[\Delta u_j + u_{6,j}(1-\xi)], \tag{3}$$

where,

$$\xi = \frac{(x - x_j)}{\Delta x}, \qquad x_{j-\frac{1}{2}} \le x \le x_{j+\frac{1}{2}}, \tag{4}$$

$$\Delta u_j = u_{j+\frac{1}{2},L} - u_{j-\frac{1}{2},R}, \text{ and} \tag{5}$$

$$u_{6,j} = 6[u_j - \tfrac{1}{2}(u_{j+\frac{1}{2},L} + u_{j-\frac{1}{2},R})] \tag{6}$$

The left and right side state variables for the Riemann solver, $u_{j+1/2,L}$ and $u_{j+1/2,R}$, are calculated by first using an interpolation scheme to obtain u(x) and an approximation to the value of u at $x_{j+1/2}$, subject to the constraint that $u_{j+1/2}$ does not fall outside of the range of values given by u_j and u_{j+1}. The interface value is calculated as

$$u_{j+\frac{1}{2}} = \tfrac{1}{2}(u_{j+1} + u_j) + \tfrac{1}{6}(\delta_\ell u_j - \delta_\ell u_{j+1}), \tag{7}$$

where,

$$\delta_\ell u_j = \min(|\delta u_j|, 2|\Delta_{j+1/2}|, 2|\Delta_{j-1/2}|)\,\mathrm{sign}(\delta u_j), \text{ if: } \Delta_{j+1/2}.\Delta_{j-1/2} > 0 \tag{8}$$

$$\delta_\ell u_j = 0, \text{ otherwise.} \tag{9}$$

Here, $\delta u_j = \frac{1}{2}(u_{j+1} - u_{j-1})$, $\Delta_{j+1/2} = u^n_{j+1} - u^n_j$, and $\Delta_{j-1/2} = u^n_j - u^n_{j-1}$.

In smooth regions away from the high gradients, the left and right states can be computed directly as:

$$u_{j+\frac{1}{2},L} = u_{j+\frac{1}{2},R} = u_{j+\frac{1}{2}} \tag{10}$$

then, the interpolation function is continuous at the interface. If the interpolation function u(x) takes on the values which are not between $u_{j+1/2,L}$ and $u_{j+1/2,R}$ to satisfy the monotonocity condition, more limitations must be applied. The left and right states, $u_{j+1/2,L}$ and $u_{j+1/2,R}$, are modified so that u(x) is a monotone function on each cell. The new expressions for $u_{j+1/2,L}$ and $u_{j+1/2,R}$ are as follows:

$$\text{I. } u_{L,j} = u_{R,j} = u_j^n, \qquad \text{if: } (u_{R,j} - u_j^n)(u_j^n - u_{L,j}) \le 0,$$

$$\text{II. } u_{L,j} = 3u_j^n - 2u_{R,j}, \quad \text{if: } (u_{R,j} - u_{L,j})[u_j^n - \tfrac{1}{2}(u_{R,j} + u_{L,j})] > \frac{(u_{R,j} - u_{L,j})^2}{6}, \text{ and}$$

$$\text{III. } u_{R,j} = 3u_j^n - 2u_{L,j}, \quad \text{if: } -\frac{(u_{R,j} - u_{L,j})^2}{6} > (u_{R,j} - u_{L,j})[u_j^n - \tfrac{1}{2}(u_{R,j} + u_{L,j}). \tag{11}$$

Finally, the cells interface flux is computed as:

$$f_{j+\frac{1}{2},L}(y) = u_{R,j} - \frac{x}{2}[\Delta u_j - (1 - \tfrac{2}{3}x)u_{6,j}], \text{ where: } x = \frac{y}{\Delta\xi_j}$$

$$f_{j+\frac{1}{2},R}(y) = u_{L,j+1} + \frac{x}{2}[\Delta u_{j+1} + (1 - \tfrac{2}{3}x)u_{6,j+1}], \text{ where: } x = \frac{y}{\Delta\xi_{j+1}} \tag{12}$$

in equations 11, and 12, $y = \alpha\Delta t$ if $\alpha>0$, and $y = -\alpha\Delta t$ if $\alpha<0$.

With the left and right states at interface known, the next step is to solve the Riemann problem to compute the value of state variables at interface. Details of the PPM method for the system of Euler equations are described by Colella [1984].

A.2. The conservative shock front tracking

In analyzing the initiation and propagation of pulsating detonations, the tracking of the

front shock has an essential role. In the past twenty years several methods have been developed to track the front and other discontinuities in flow field. For present purposes, the simplest one is conservative front tracking of Chern and Colella [1987], which will be utilized here.

Suppose at time t^n, the solution u_i^n at all cells and the location of shock X_{sh}^n which is in cell j_{sh} are known. The cell which contains the shock front is shown by j_{sh}. The shock front divides this cell into two subintervals. The average value of the conservative variable U at the left subinterval $\overline{U}_L$, is defined as:

$$\overline{U}_L = U_L^n \frac{x_L^n}{\Delta x} + U_{jsh-1}^n (1 - \frac{x_L^n}{\Delta x}) \tag{13}$$

where, x_L is the length of left subinterval of the cell which contains the shock. The front speed S_f is computed from the Rankine-Hugoniot relations,

$$S_f = [\frac{\gamma p_R}{\rho_R}(1 + \frac{\gamma + 1}{2\gamma}(\frac{\overline{p}_L - p_R}{p_R}))]^{\frac{1}{2}} + u_R \tag{14}$$

The shock position is updated at time t^{n+1} by:

$$x_{sh}^{n+1} = x_{sh}^n + S_f \Delta t \tag{15}$$

While the state variables are updated in all cells for $j<j_{sh}$ with PPM algorithm, the cell containing the shock needs a special treatment. Considering two possible cases, the conservative variables for this cell are updated as follows;

Case a)- $j_{sh}^{n+1} = j_{sh}^n$

The flux across the shock is defined as:

$$F_s = F(U_0) - S_f U_0 \tag{16}$$

Considering Fig. A.2, the conservation of U for the left subinterval between t^n and t^{n+1} may be written in this form:

$$x_L^{n+1}U_L^{n+1} = x_L^nU_L^n + \Delta t(F_1 - F_s) \tag{17}$$

Although U_L^{n+1} can be computed from this equation, when $X_L^{n+1} << 1$ the CFL condition[1] may be violated. In order to overcome this problem, Chern [1987] suggested the following procedure

$$x_L^{n+1}U_L^{n+1} = x_L^nU_L^n + \Delta t(F_1 - F_s) + x_L^{n+1}U_L^n - x_L^{n+1}U_L^n \tag{18}$$

or:

$$x_L^{n+1}U_L^{n+1} = x_L^{n+1}U_L^n + (x_L^n - x_L^{n+1})U_L^n + \Delta t(F_1 - F_s) \tag{19}$$

he defined :

$$\delta M_L = (x_L^n - x_L^{n+1})U_L^n + \Delta t(F_1 - F_s) \tag{20}$$

thus,

$$x_L^{n+1}U_L^{n+1} = x_L^{n+1}U_L^n + \delta M_L \tag{21}$$

to avoid the above-mentioned trouble (i.e., the violation of CFL condition), δM_L is divided into two parts,

$$\delta M_L = \frac{x_L^{n+1}}{\Delta x}\delta M_L + (1 - \frac{x_L^{n+1}}{\Delta x})\delta M_L = \delta M_{L1} + \delta M_{L2} \tag{22}$$

we replace δM_L with δM_{L1} in Eq. (21), then:

$$U_L^{n+1} = U_L^n + \frac{\delta M_L}{\Delta x} \tag{23}$$

---

[1]The Courant-Friedrichs-Lewy (CFL) condition is a criterion which restricts the computational time step and the grid spacing according to:

$$CFL = \left|\frac{(u+c)\Delta t}{\Delta x}\right| \le 1$$

where c is the local speed of sound.

Now, the above difficulty is overcome. To avoid losing the conservation at the shock front, δM_{L2} is re-distributed between left subinterval of j_{sh} and its left cell (i.e. cell j_{sh}-1). This redistribution is performed according to their volume weight[2]. Thus,

$$x_L^{n+1}U_L^{n+1} = x_L^{n+1}U_L^{n+1} + \frac{x_L^{n+1}}{\Delta x + x_L^{n+1}}\delta M_{L2} \tag{24}$$

$$\Delta x U_{j_{sh}-1}^{n+1} = \Delta x U_{j_{sh}-1}^{n+1} + \frac{\Delta x}{\Delta x + x_L^{n+1}}\delta M_{L2} \tag{25}$$

and finally,

$$U_L^{n+1} = U_L^{n+1} + \frac{\delta M_{L2}}{\Delta x + x_L^{n+1}} \tag{26}$$

$$U_{j_{sh}-1}^{n+1} = U_{j_{sh}-1}^{n+1} + \frac{\delta M_{L2}}{\Delta x + x_L^{n+1}} \tag{27}$$

Case b)- $j_{sh}^{n+1} = j_{sh}^{n} + 1$

This case is slightly more complicated than case 'a'. Here, at first τ, the fraction of Δt which is elapsed in new shocked cell, is introduced as:

$$\tau \equiv \frac{x_L^{n+1}}{S_f} \tag{28}$$

Then, the conservation law will be applied in two steps (Fig. A.3). Once between t^n and $t^n+(\Delta t-\tau)$, and then between $t^n+(\Delta t-\tau)$ and t^{n+1}. The conservation is applied for both j_{sh}^n and j_{sh}^{n+1}.

$$\Delta x U_{j_{sh}^n}^{n+1} = x_L^n U_L^n + \Delta t F_1 - \tau\bar{F} - (\Delta t - \tau)F_s \tag{29}$$

$$x_L^{n+1}U_L^{n+1} = \tau(\bar{F} - F_s) \tag{30}$$

[2] Chern [1987], using characteristic method, performed this redistribution in a more general manner.

where, $\overline{F} = F(\overline{U}_L)$. With a manipulation similar to case a,

$$x_L^{n+1}U_L^{n+1} = x_L^{n+1}\overline{U}_L - x_L^{n+1}\overline{U}_L + \tau(\overline{F} - F_s) \tag{31}$$

δM_L is defined as,

$$\delta M_L = -x_L^{n+1}\overline{U}_L + \tau(\overline{F} - F_s) \tag{32}$$

and again we divide δM_L into two parts,

$$\delta M_L = \frac{x_L^{n+1}}{\Delta x}\delta M_L + (1 - \frac{x_L^{n+1}}{\Delta x})\delta M_L = \delta M_{L1} + \delta M_{L2} \tag{33}$$

then,

$$U_L^{n+1} = \overline{U}_L + \frac{\delta M_L}{\Delta x} \tag{34}$$

and finally the same redistribution,

$$U_L^{n+1} = U_L^{n+1} + \frac{\delta M_{L2}}{\Delta x + x_L^{n+1}} \tag{35}$$

$$U_{j_{sh}^n}^{n+1} = U_{j_{sh}^n}^{n+1} + \frac{\delta M_{L2}}{\Delta x + x_L^{n+1}} \tag{36}$$

A.3. The mesh refinement strategy

Here, two sets of uniform grids are used to discretize the computational domain. The entire domain is covered by a coarse grid, and a fine mesh is superimposed on the coarse grid in the vicinity of front. Fine grid boundaries always coincide with coarse grid faces. Usually fine grids are used in 20-40 coarse-grid cells behind the shock, and in a few coarse-grid cells ahead of the shock.

After introducing the initial condition to the code, the solution procedure is as follow:

1- The state variables are updated in coarse grids with time step Δt^c,

2- The fine grids are updated. If N_R is the refinement ratio, N_R successive integrations are performed with $\Delta t^f = \Delta t^c / N_R$.

3- Those coarse grids involving fine meshes updated again. The values of the state variables are replaced with the average of the corresponding values of the fine grid points within them.

4- The shock location on coarse grids is replaced with its value on fine grids.

5- The solution at the first cell on the left boundary of fine grids is corrected in order to preserve conservation according to [Bourlioux 1991]:

$$\Delta x U_{j_L-1}^{c,n+1} = \Delta x U_{j_L-1}^{c,n+1} + \Delta t F_L^c - \sum_{N_R} \frac{\Delta t}{N_R} F_L^f \tag{37}$$

where F_L^c is the flux at the interface between coarse and fine grids calculated at step 1, F_L^f is the flux at the same place calculated in step 2, and $U_{j_L-1}^{c,n+1}$ is the conservative variable on the first coarse cell at the left of the interface between coarse and fine meshes.

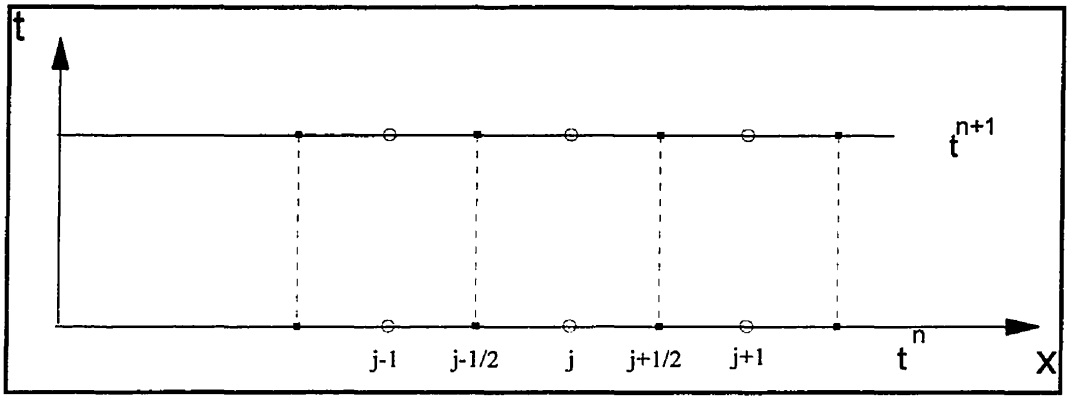

Figure A.1. Computational Domain, Indexing.

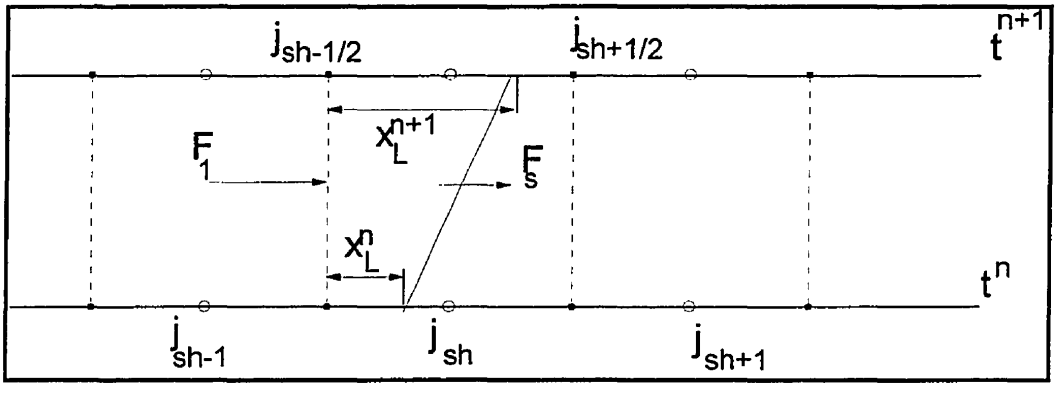

Figure A.2. Conservation law for the left subinterval when $j_{sh}^{n+1} = j_{sh}^{n}$.

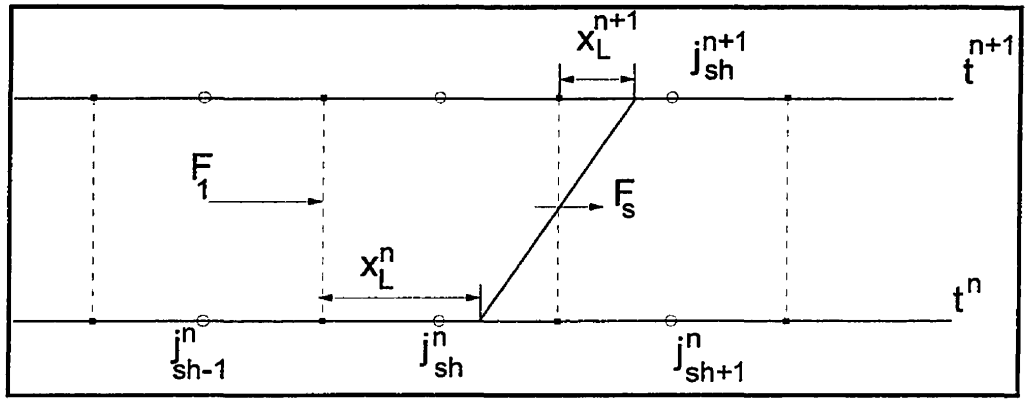

Figure A.3. Conservation law for the left subinterval when $j_{sh}^{n+1} = j_{sh}^n + 1$.

Tables

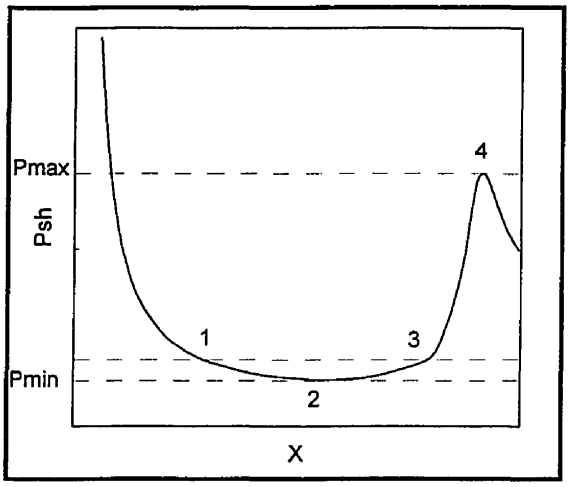

Ea/RTo	15	22	24	26	27	29
X_4 (run up distance)	31.7	98.9	129	180	193	253
X_4/Δ_{ZND}	400	341	314	310	311	266
$X_4/\Delta_{ave.}$	6.7	10.7	11	13.2	13.5	15.1
$(T_{sh})_2$	1.5	2.35	2.55	2.77	3.06	3.17
$(-d\tau / dT_{sh})_2$	22.13	20.36	22.94	23	22.79	20.4
$(E_a/RT_{sh})_2$	8.3	7.8	7.84	7.82	7.89	7.75

Table 4.1. Properties of the initiation process in the critical regime.
Note: Δ is induction length, and τ is induction time (Q/RT_o=50, γ=1.2).

E_a/RTo	RUD (up)	RUD (p)	Ratio (RUD's)	O.S. (up)	O.S. (p)	Ratio (O.S.'s)
21	97.34	90.37	0.928	64.7	56.7	0.876
27	197.14	176.67	0.896	64.2	57.5	0.896
28	232.48	203.12	0.875	64.2	58.7	0.914
29	258.56	221.368	0.86	68.1	57.9	0.863

Table 5.1. Comparison between run up distances (RUD) and overshoots in shock pressure (O.S.) for un-perturbed (un) and perturbed (p) simulations for different E_a/RT_o.

Figures

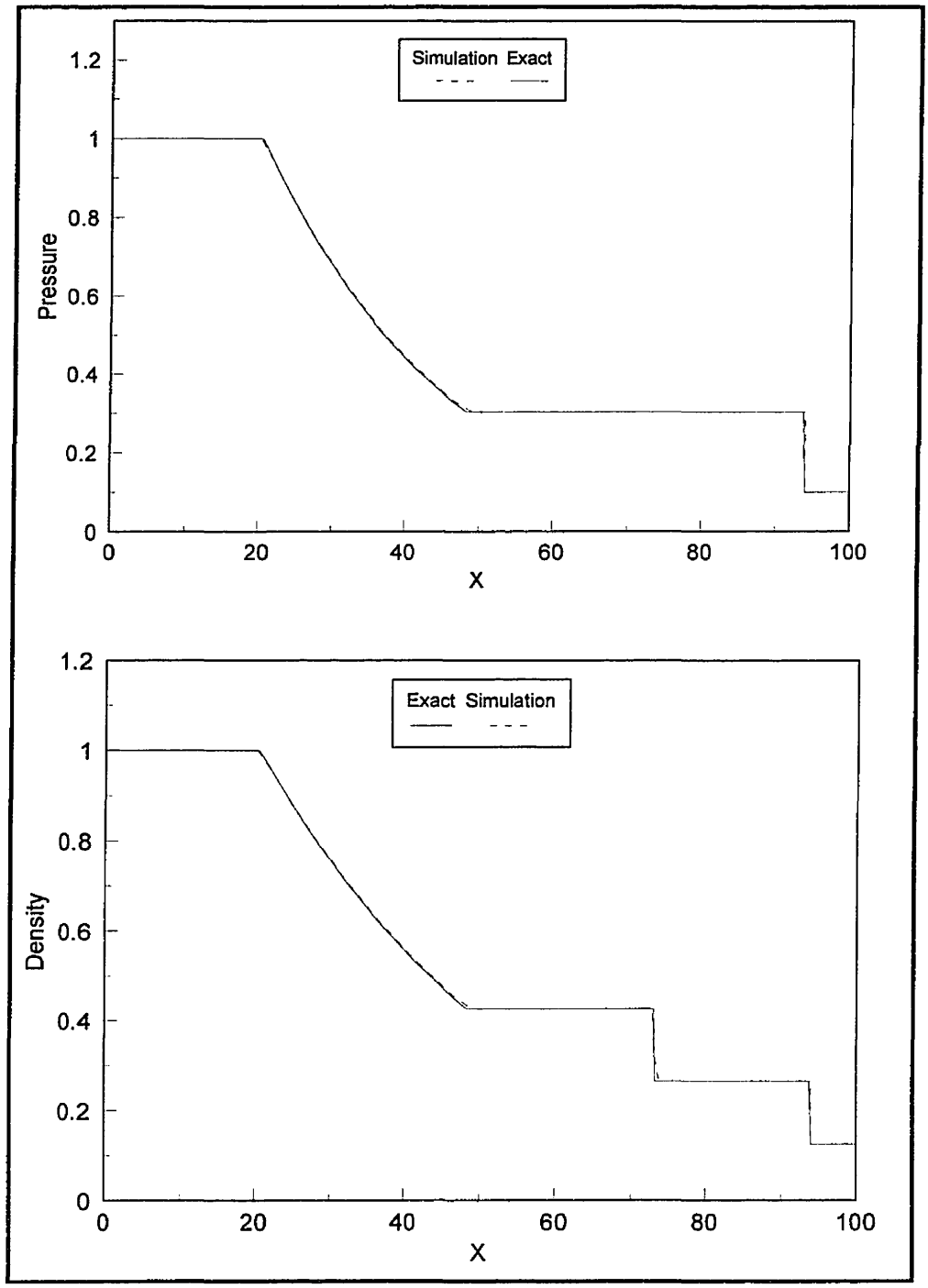

Figure 2.1. Comparison between the exact solution and numerical simulation for Sod's problem (t=25, Δx= 0.5).

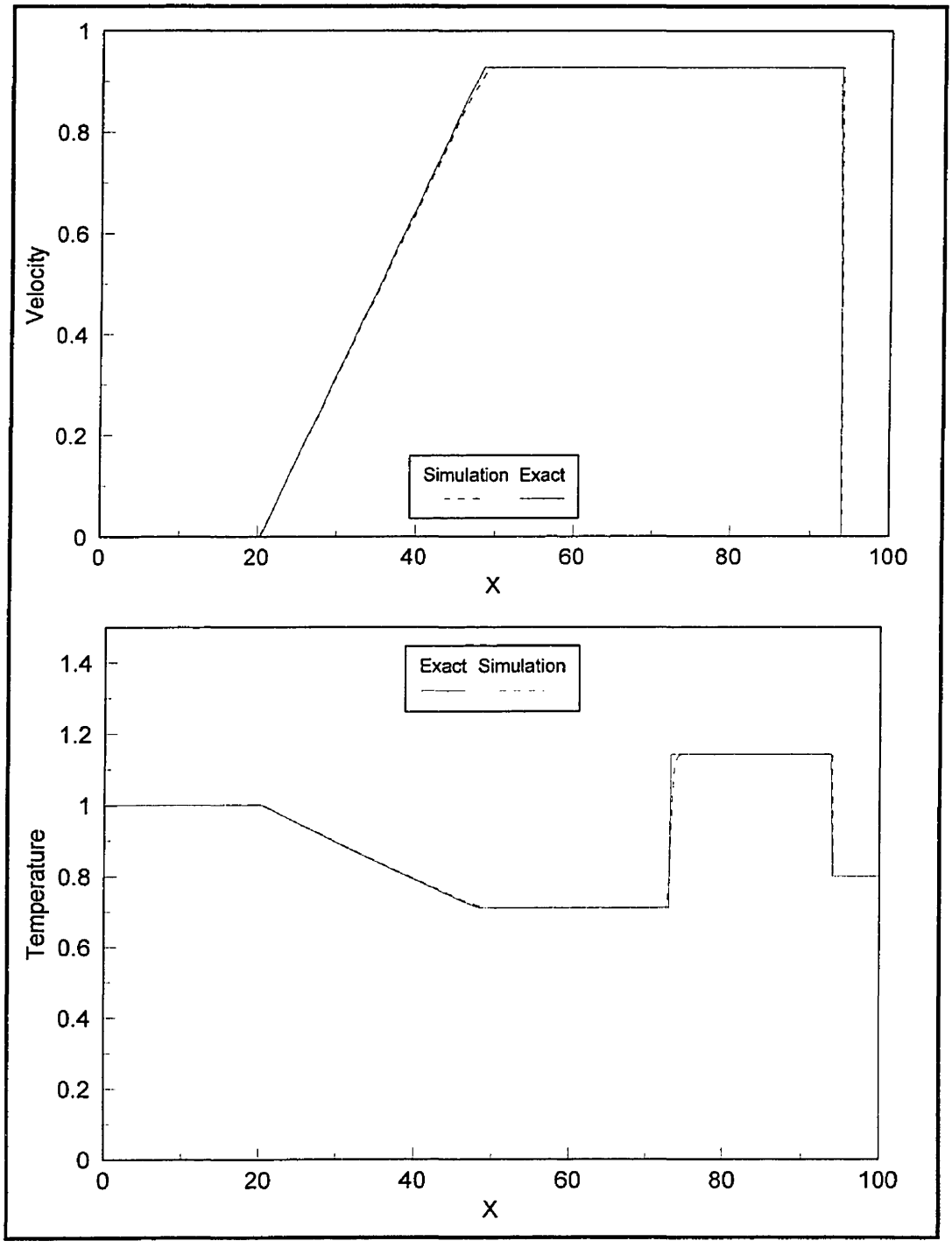

Figure 2.1. (Continued).

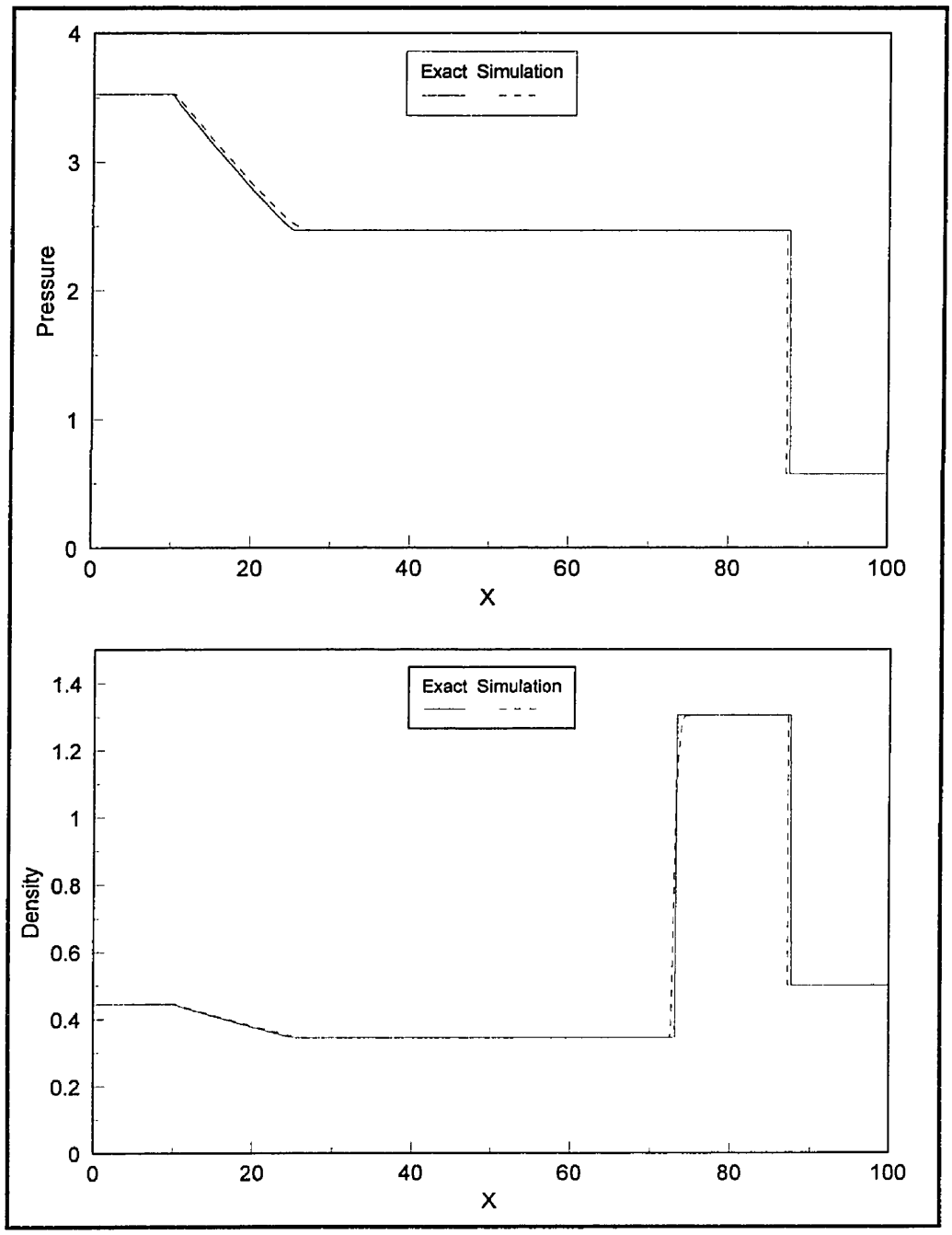

Figure2.2. Comparison between the exact solution and numerical simulation for Lax's problem ((t=15, Δx= 0.5).

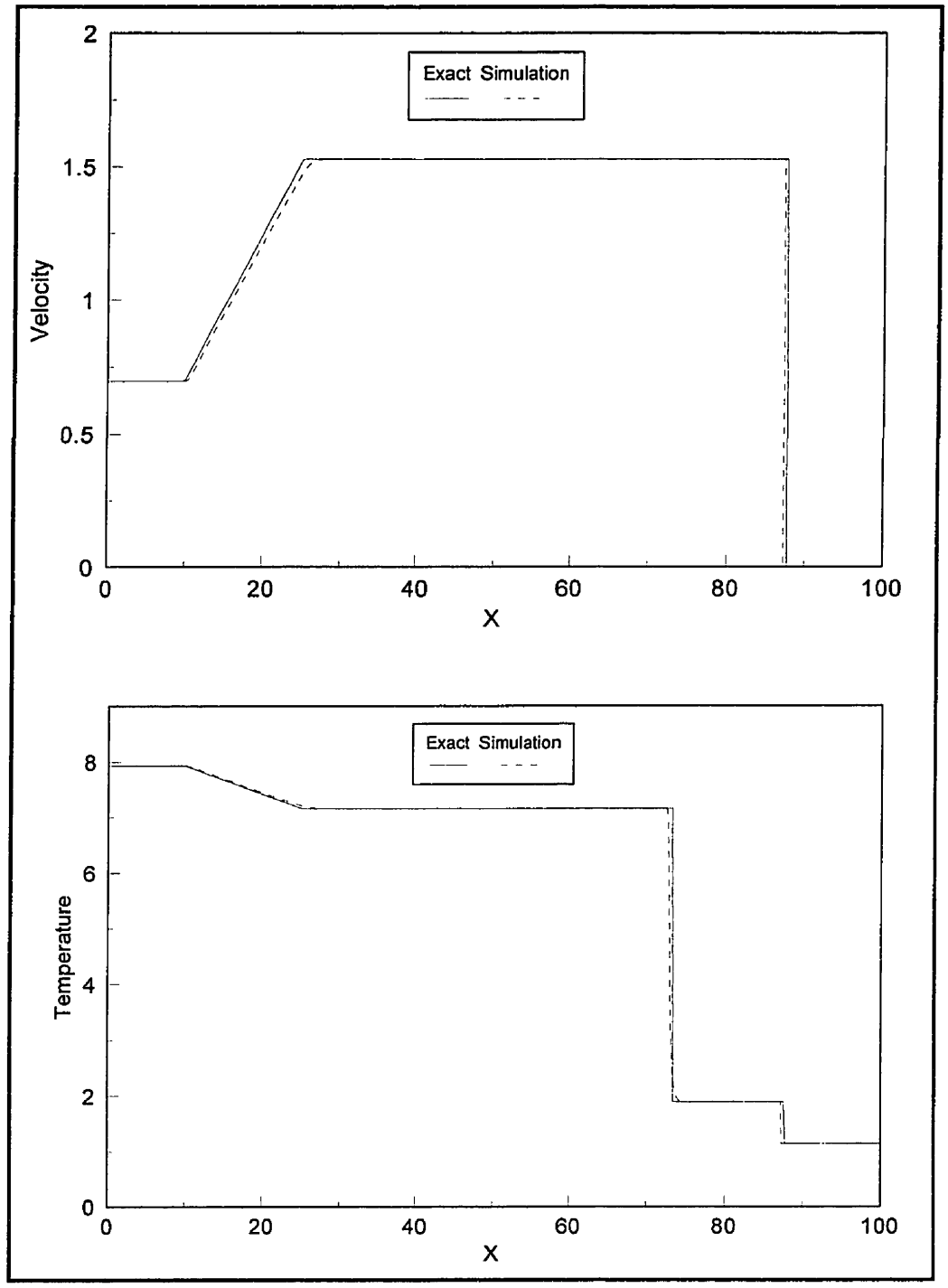

Figure 2.2. (Continued).

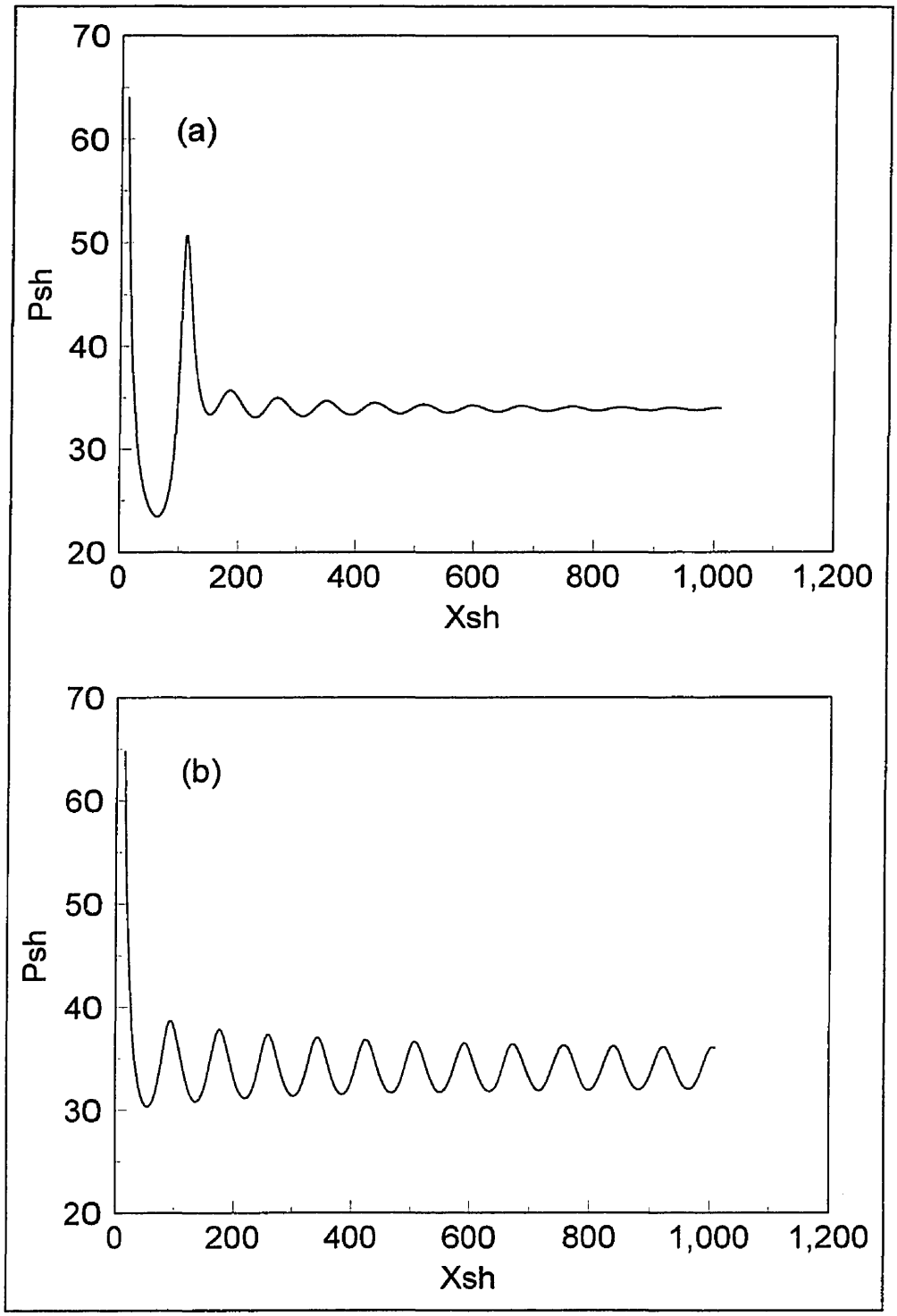

Figure 2.3. Shock history for stable propagation of planar detonations ($Q/RT_0 = 50$, $\gamma = 1.2$). a - $E_a/RT_0 = 24.5$, b - $E_a/RT_0 = 25$.

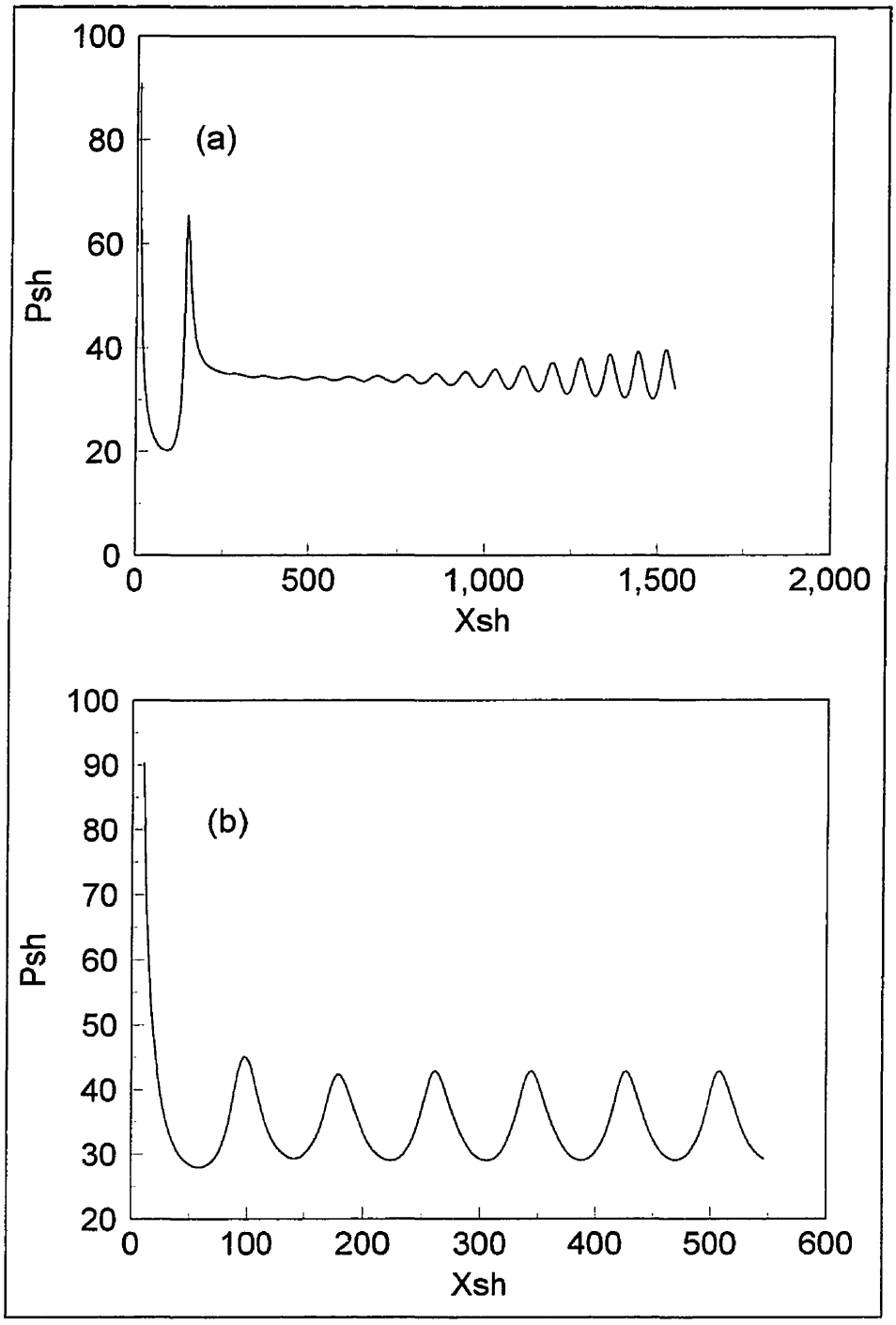

Figure 2.4. Shock history in detonation stability boundary ($Q/RT_0 = 50$, $\gamma = 1.2$, and $E_a/RT_0 = 25.5$).

Note: In (b) initiation energy is higher than (a).

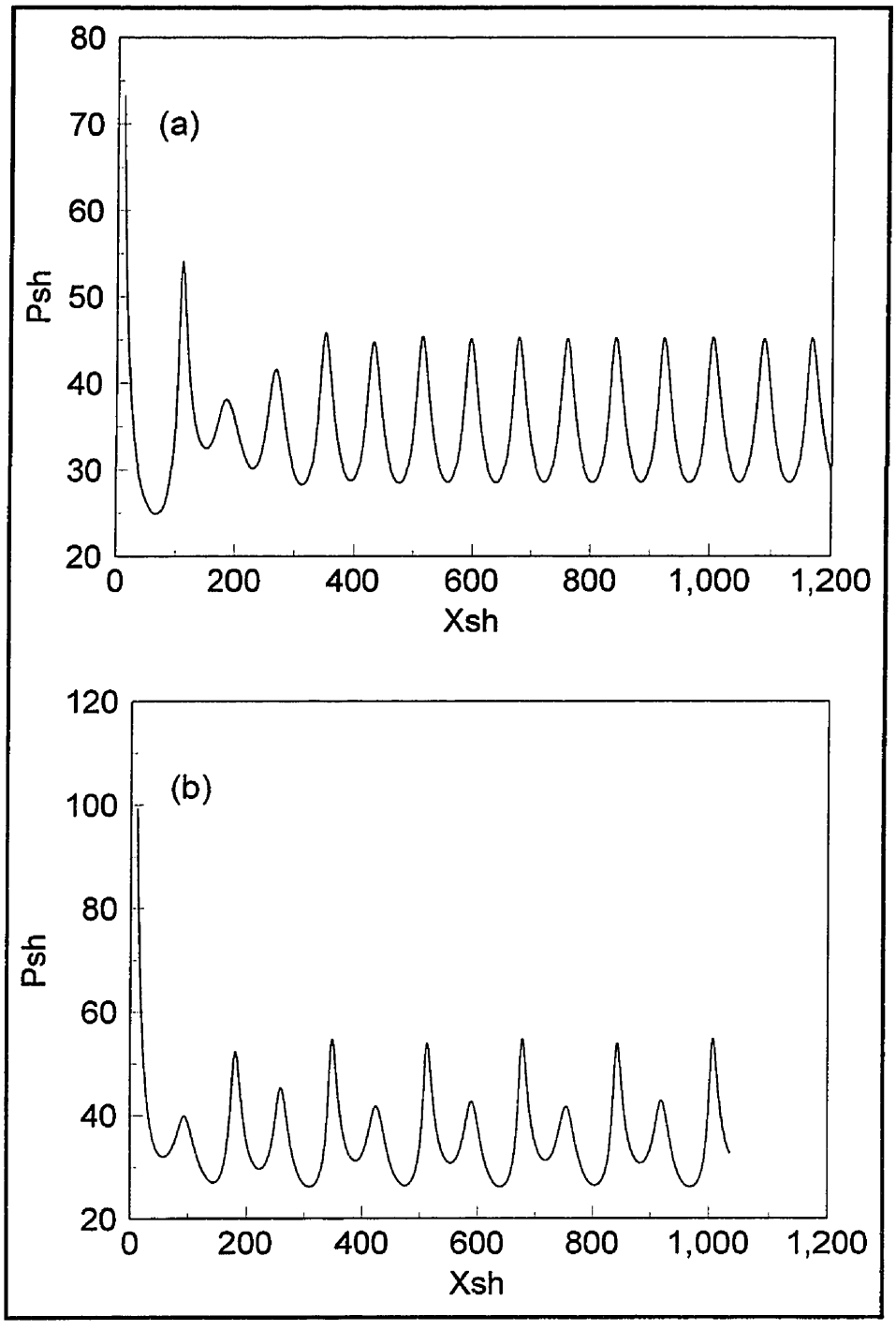

Figure 2.5. Shock history for unstable propagation of planar detonations ($Q/RT_o = 50$, $\gamma = 1.2$). a - $E_a/RT_o = 26$, b - $E_a/RT_o = 27.5$.

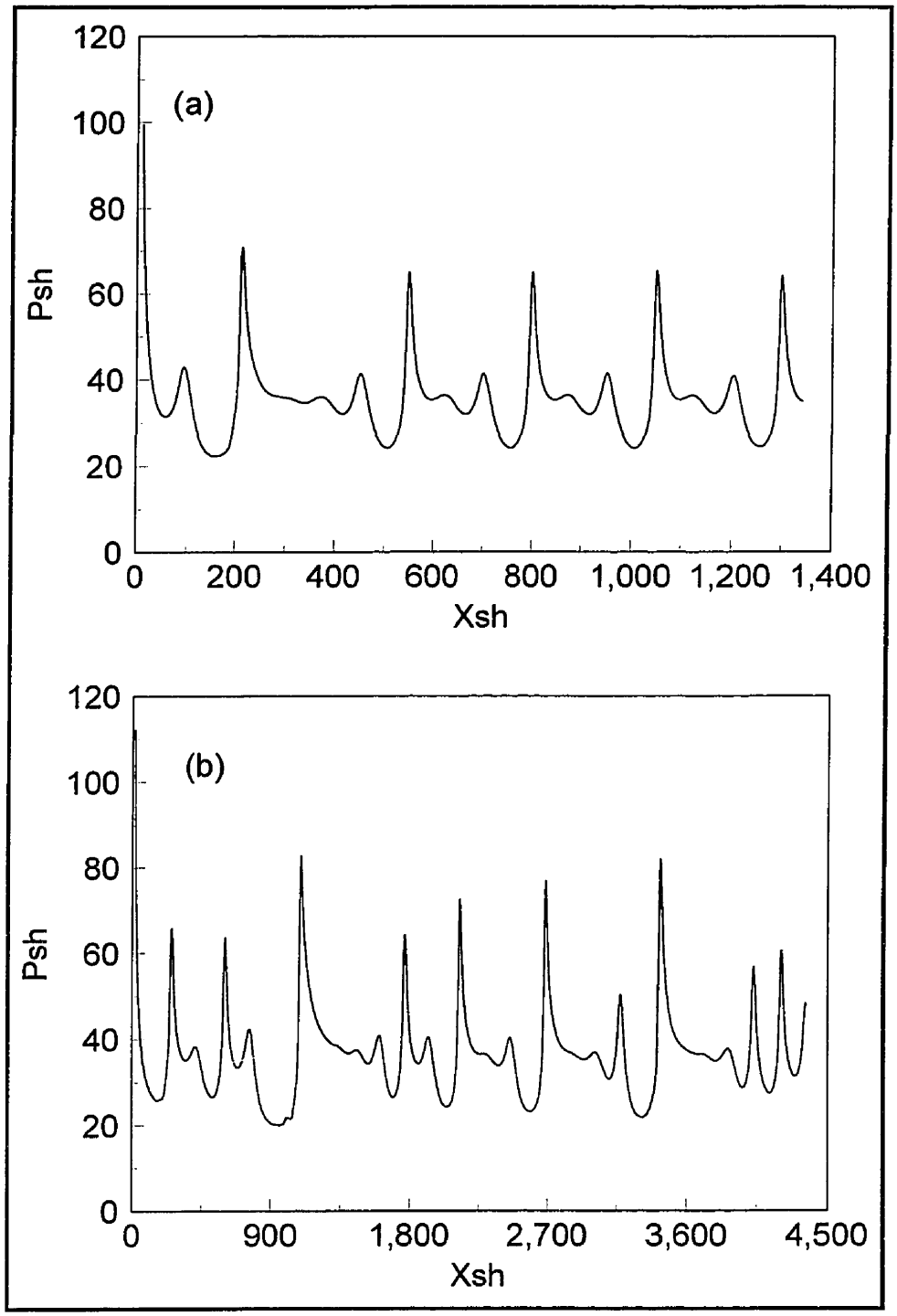

Figure 2.6. Shock history for unstable propagation of planar detonations ($Q/RT_o = 50$, $\gamma = 1.2$). a - $E_a/RT_o = 28.5$, b - $E_a/RT_o = 29.5$.

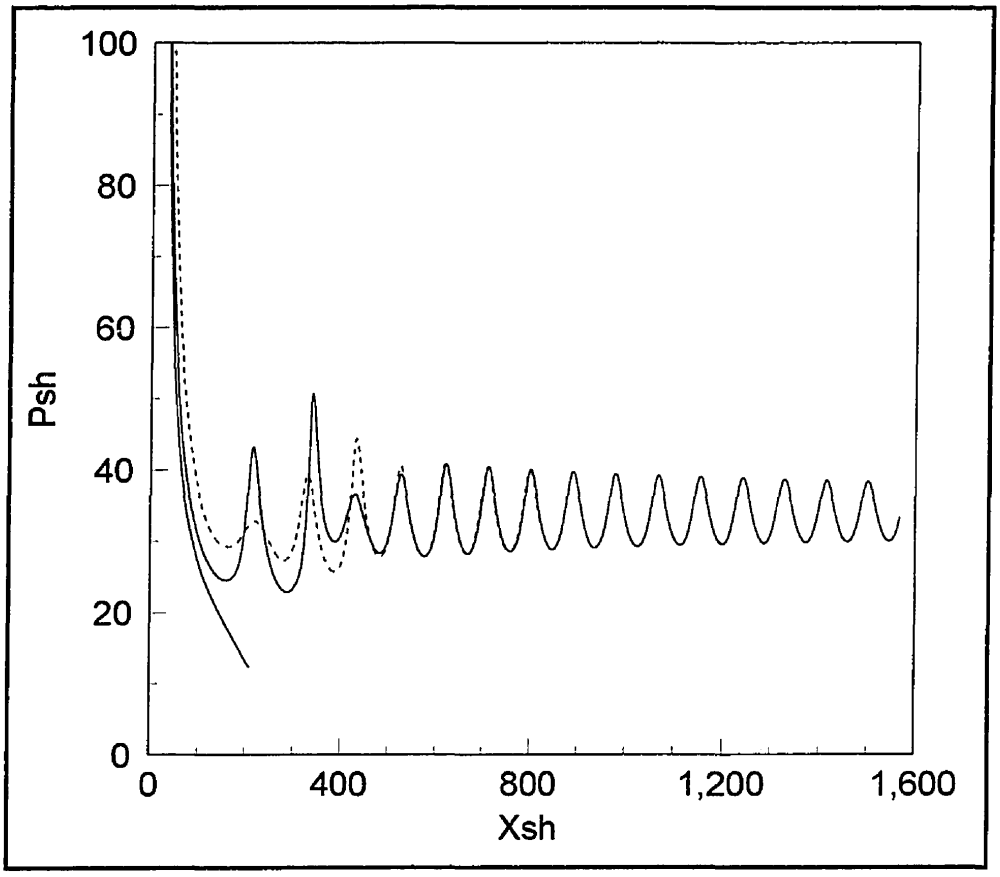

Figure 2.7. Shock history for different regimes of initiation in cylindrical geometry ($Q/RT_0 = 50$, $\gamma = 1.2$, and $E_a/RT_0 = 25$).

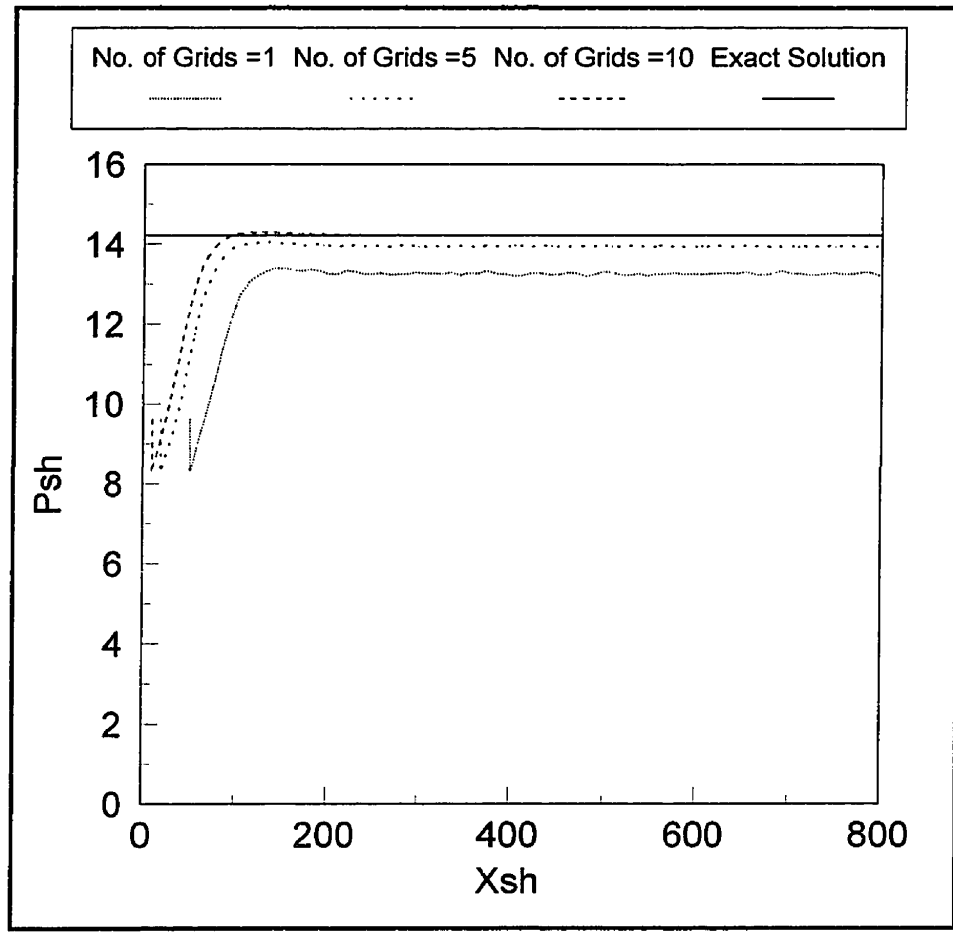

Figure 2.8. The propagation of a steady ZND detonation for three different mesh sizes calculated with the numerical code, compared with the exact solution ($Q/RT_0 = 10$, $\gamma = 1.4$, $E_a/RT_0 = 10$, and f (the degree of overdrive) = 1.1).

Note: "No. of Grids" refers to the number of grid points per half reaction length of the corresponding ZND detonation.

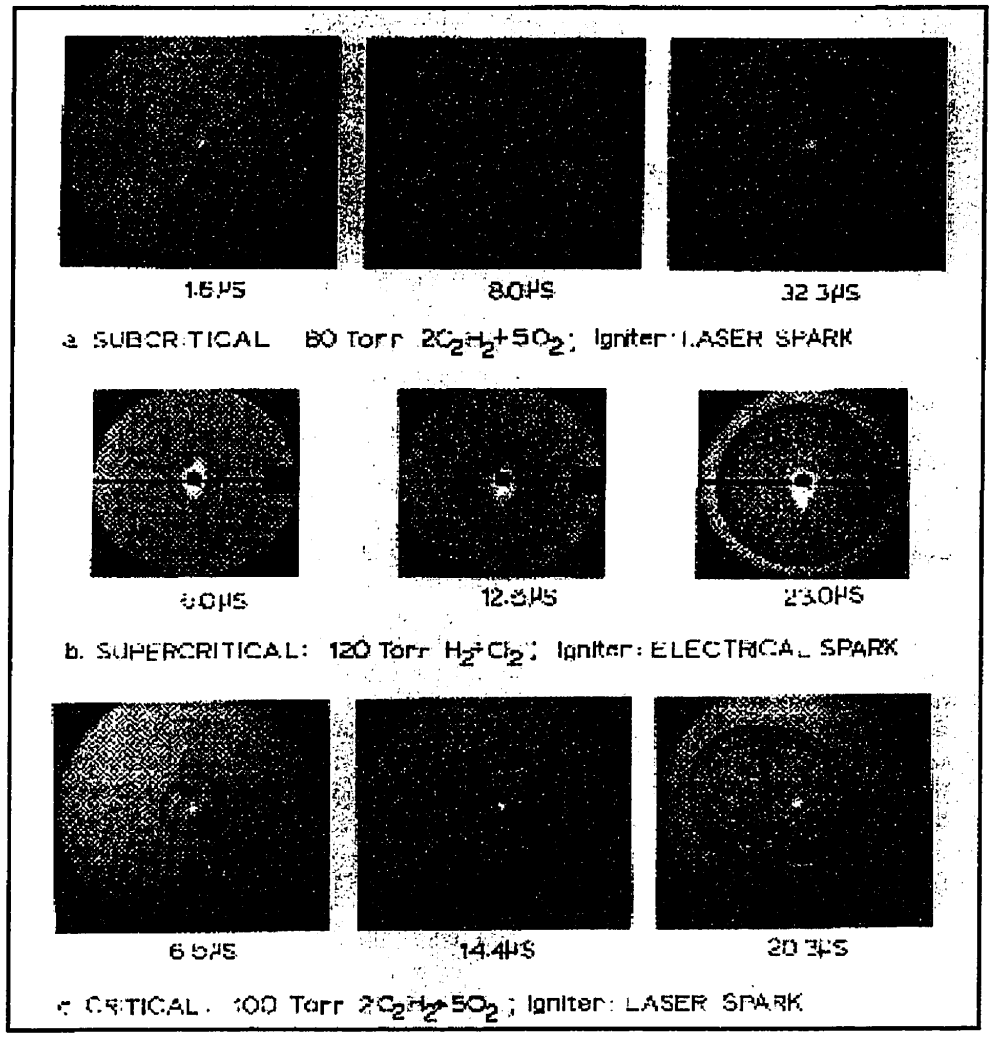

Figure 3.1. Spark schlieren photograph of a spherical detonation illustrating the subcritical, supercritical, and critical regimes of initiation (Knystautas 1968).

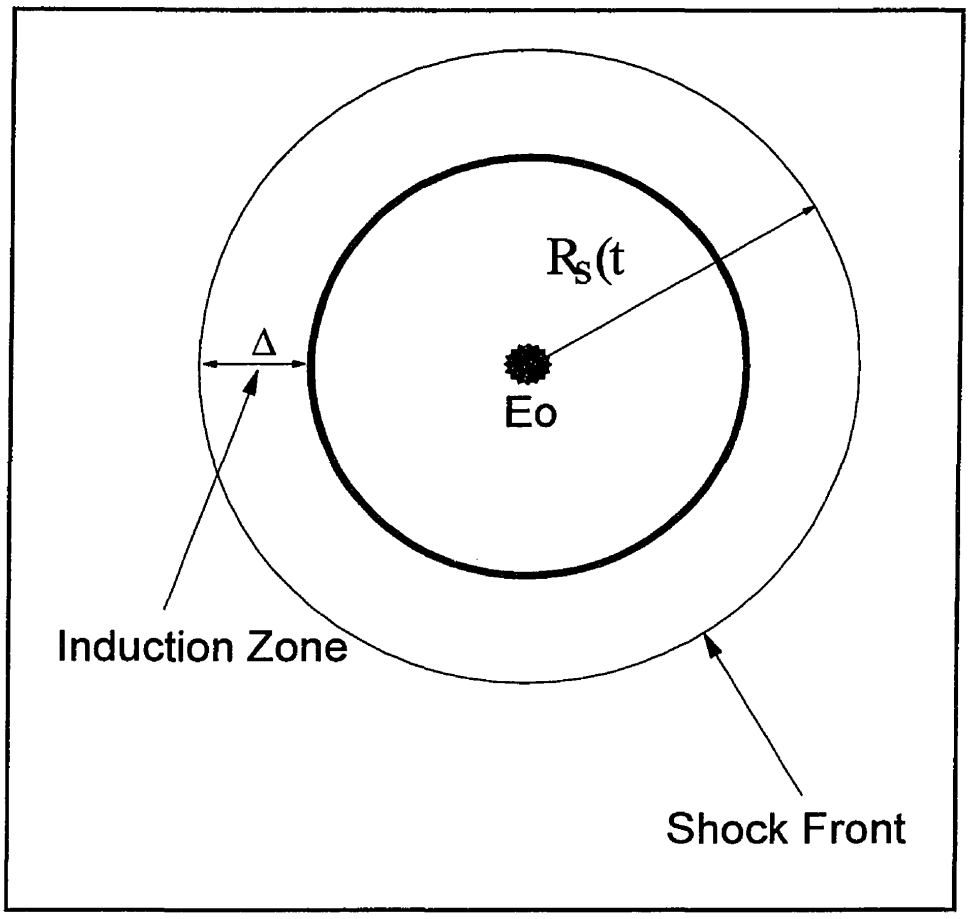

Figure 3.2. The blast-reaction zone complex in direct initiation. Δ shows the induction length and Rs is the shock radius.

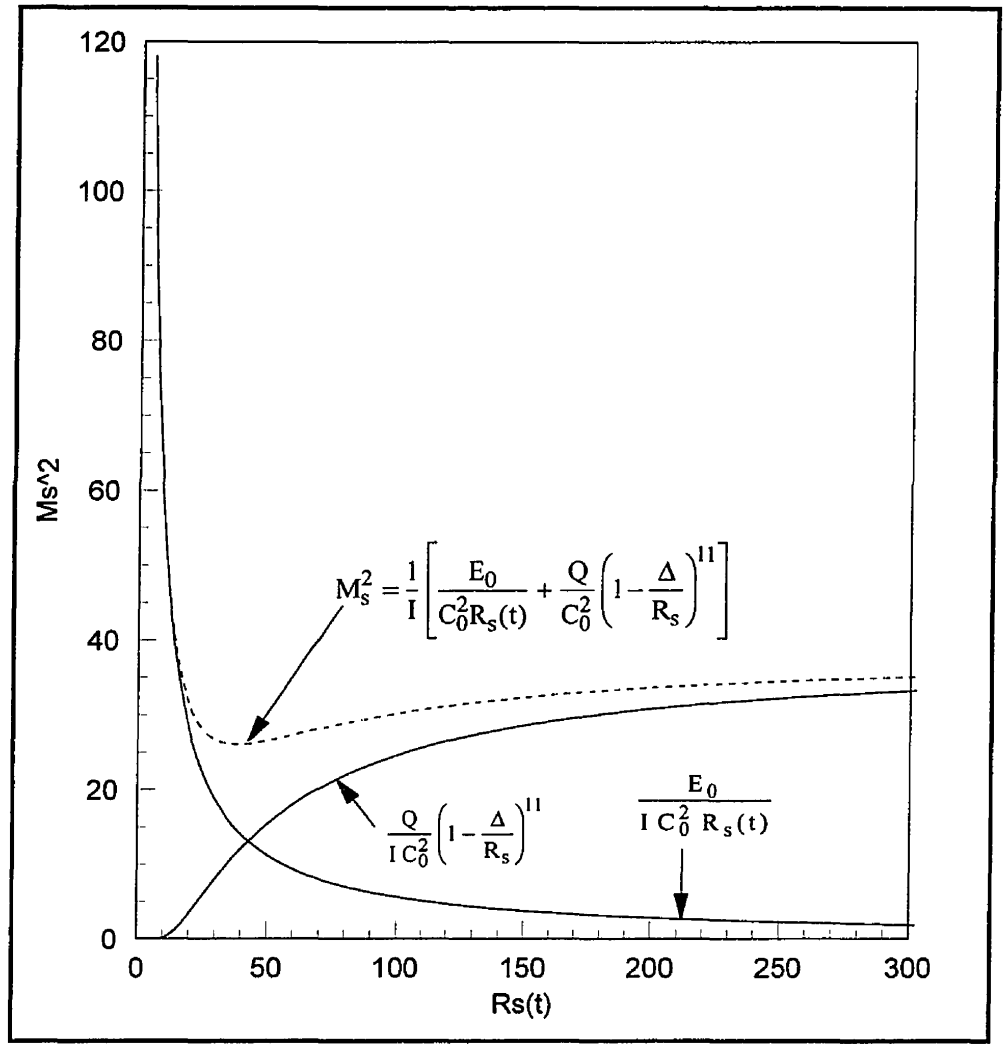

Figure 3.3. The variation of shock strength, calculated by two terms of Equation 3.1, with shock radius. The dashed line shows the sum of two terms ($E_a/RT_o = 24$, $Q/RT_o = 50$, $\gamma = 1.2$, $E_o/p_o = 1765$, and $\Delta = 4$).

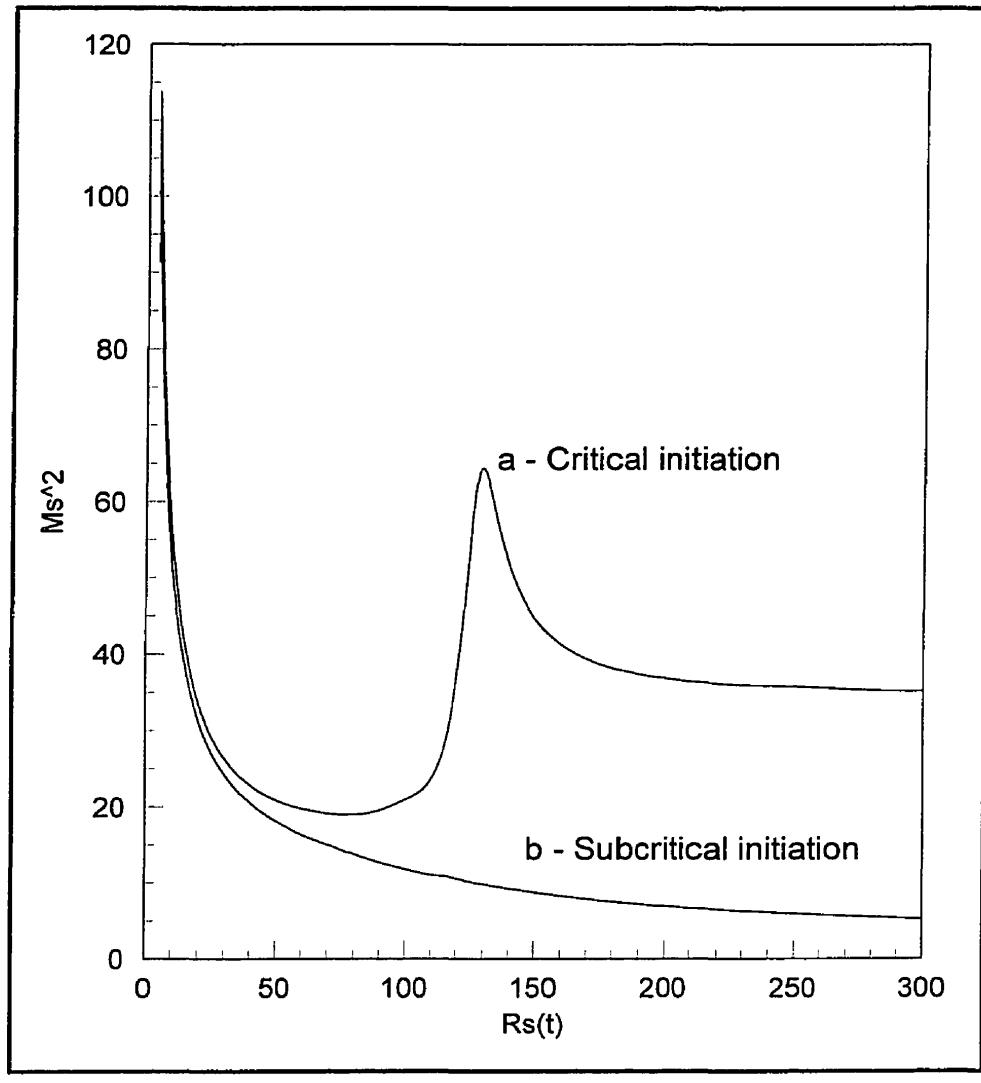

Figure 3.4. The initiation process for two different initiation energies calculated by numerical simulation. Corresponding initiation energies are 1765 for critical and 1614 for subcritical initiation ($Q/RT_0 = 50$, $\gamma = 1.2$, and $E_a/RT_0 = 24$).

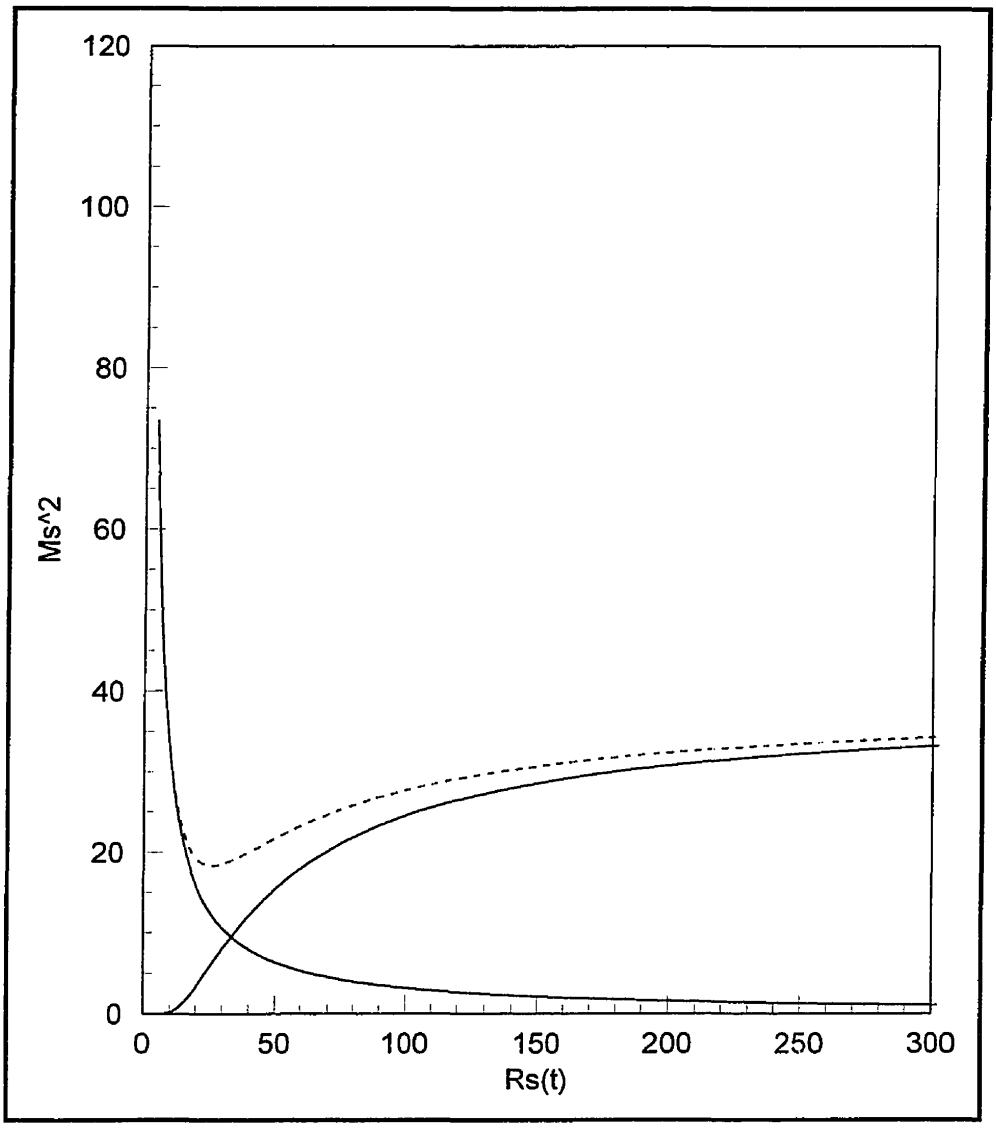

Figure 3.5. The variation of shock strength, calculated by two terms of Equation 3.1, with shock radius for a very low initiation energy. The dashed line shows the sum of two terms (E_a/RT_o=24, Q/RT_o=50, γ= 1.2, E_o/p_o=1000, and Δ = 4).

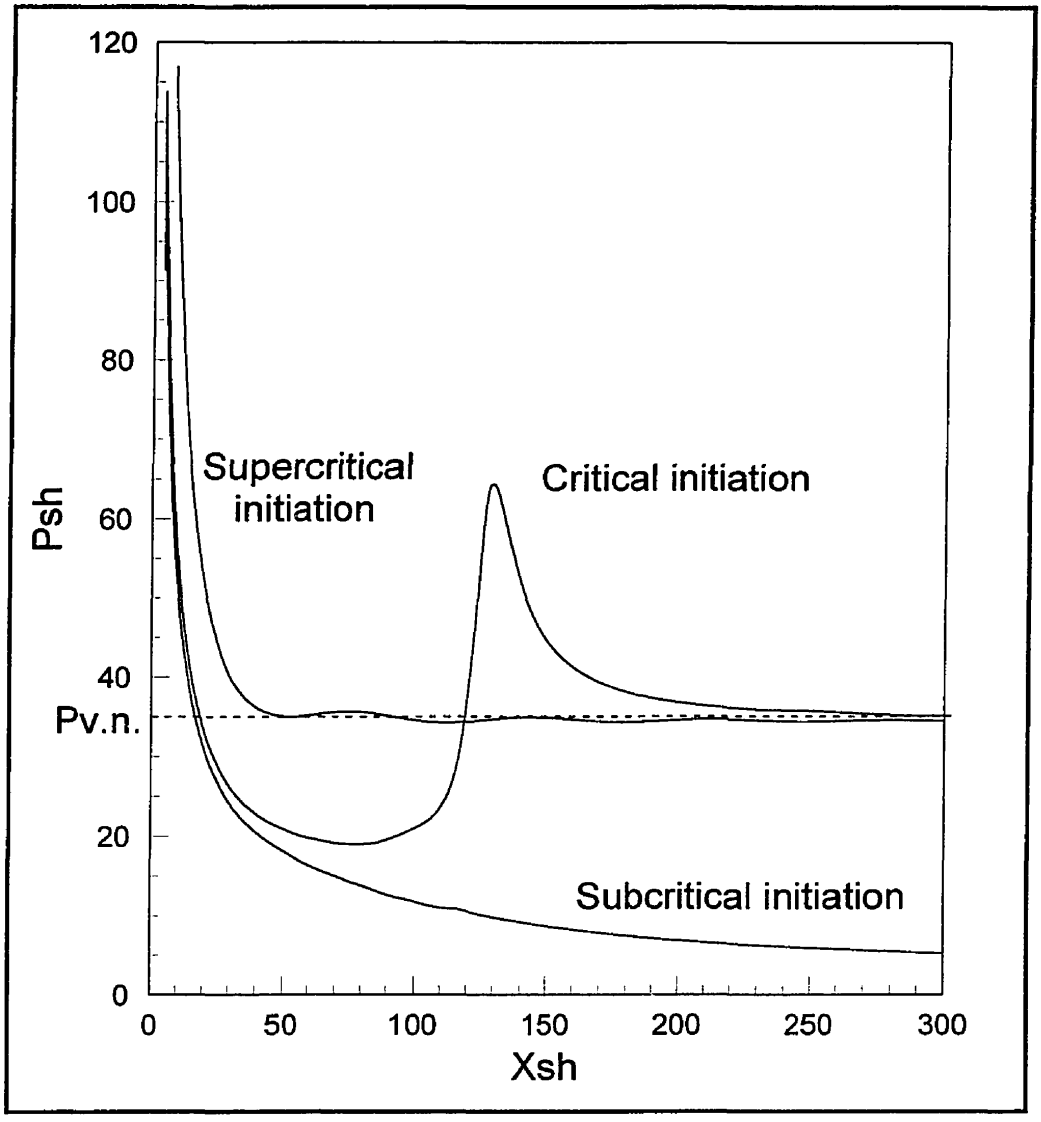

Figure 3.6. The three regimes of initiation. The corresponding initiation energies are 3415 for supercritical, 1765 for critical, and 1614 for the subcritical initiation (Q/RT_0=50, γ = 1.2, and E_a/RT_0=24).

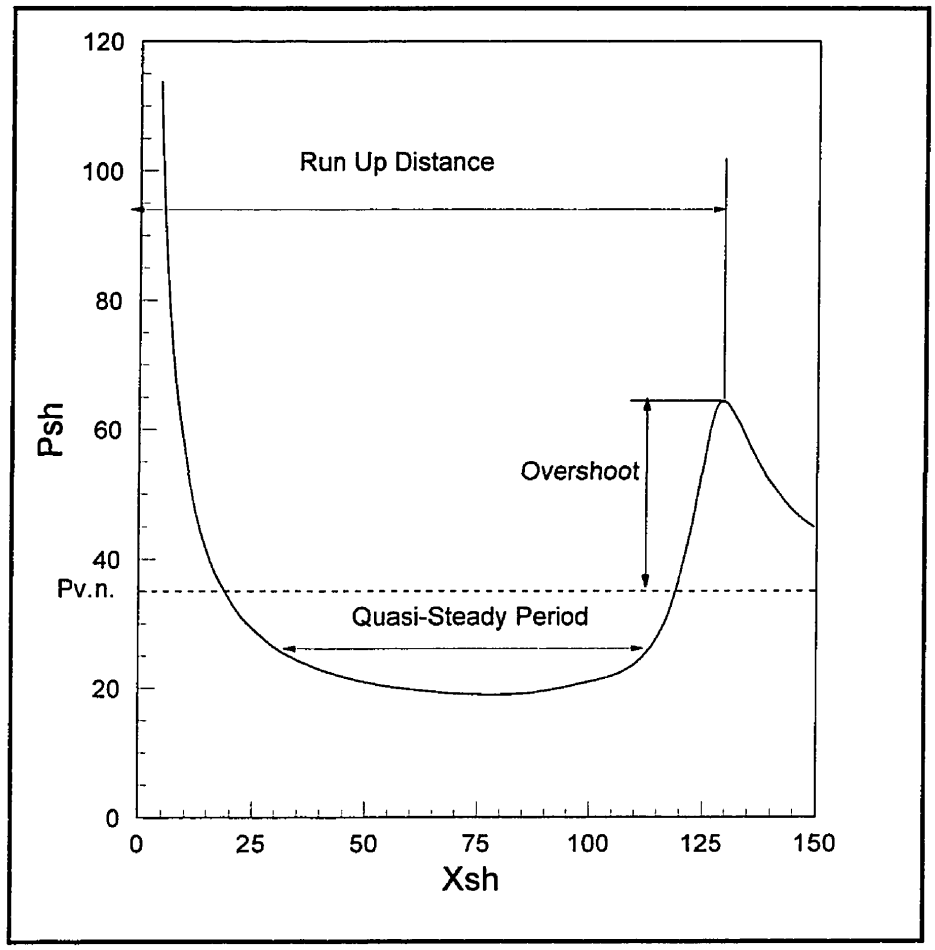

Figure 3.7. The definition of the important parameters in the initiation process.

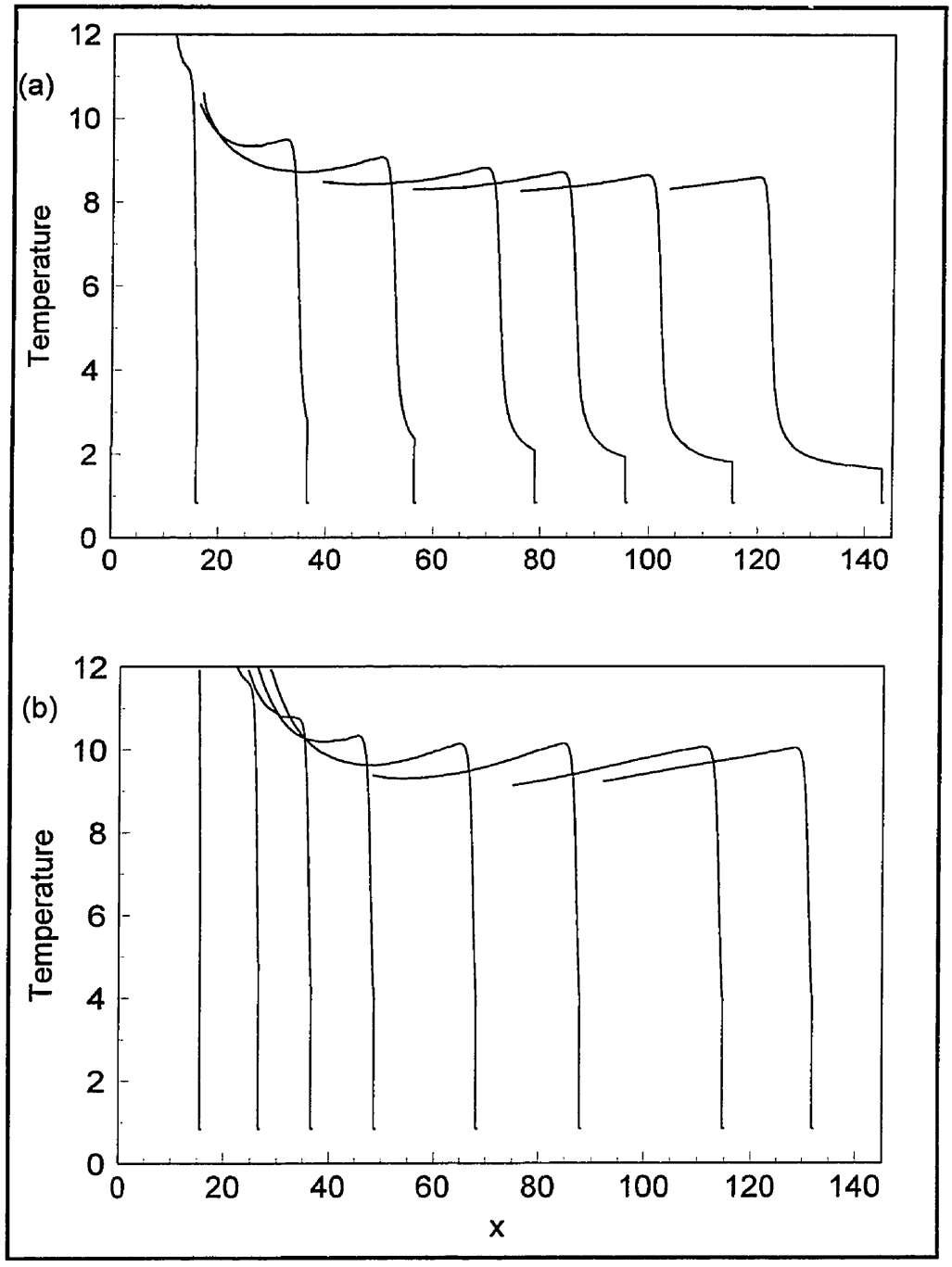

Figure 3.8. The temperature profiles for direct initiation ($Q/RT_O = 50$, $\gamma = 1.2$, and $E_a/RT_O = 24$). a - Subcritical regime ($E_O/p_O = 1614$). b - Supercritical regime ($E_O/p_O = 3415$).

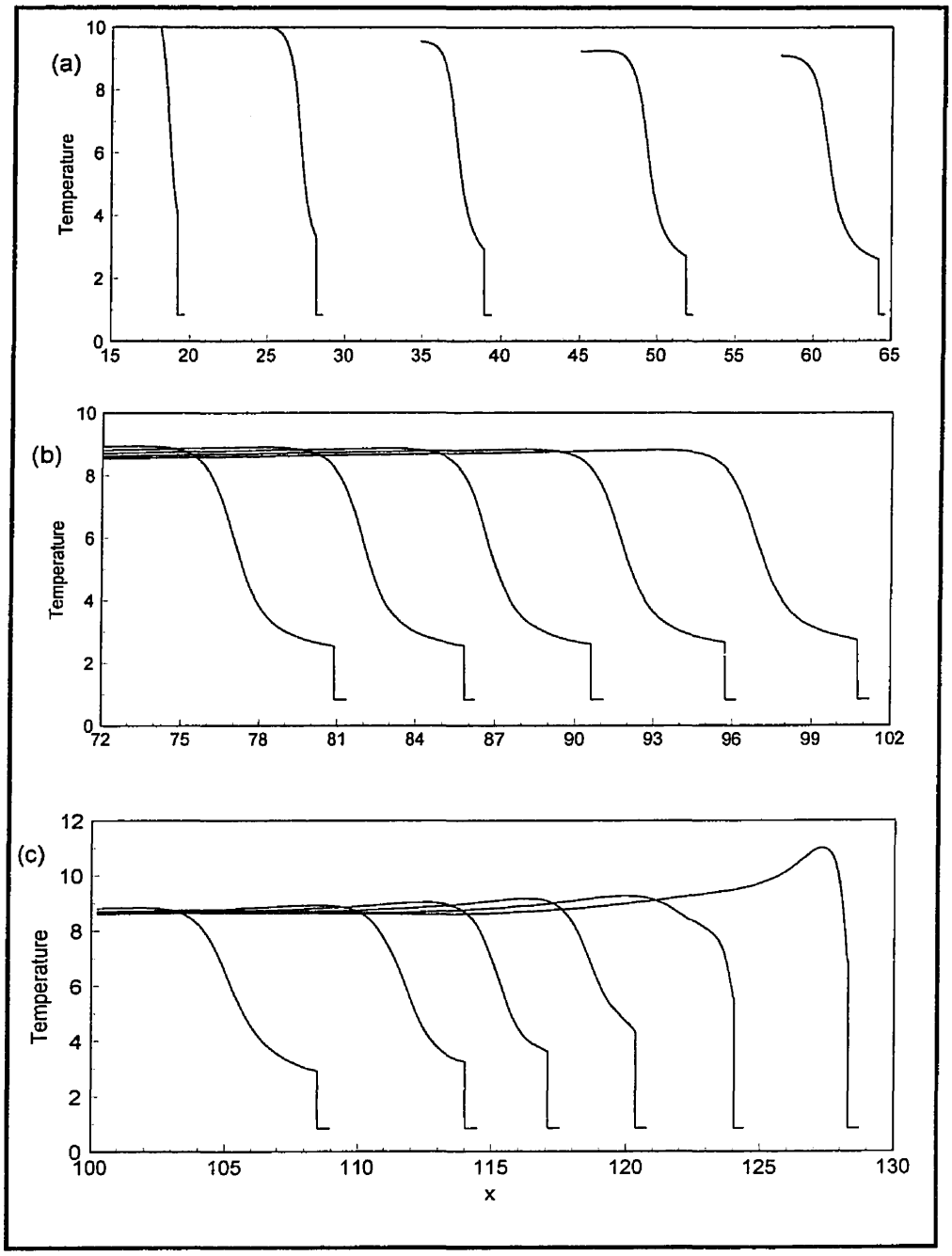

Figure 3.9. The temperature profiles for the critical initiation regime (Q/RT_O = 50, γ = 1.2, E_a/RT_O = 24, and E_O/p_O = 1765).

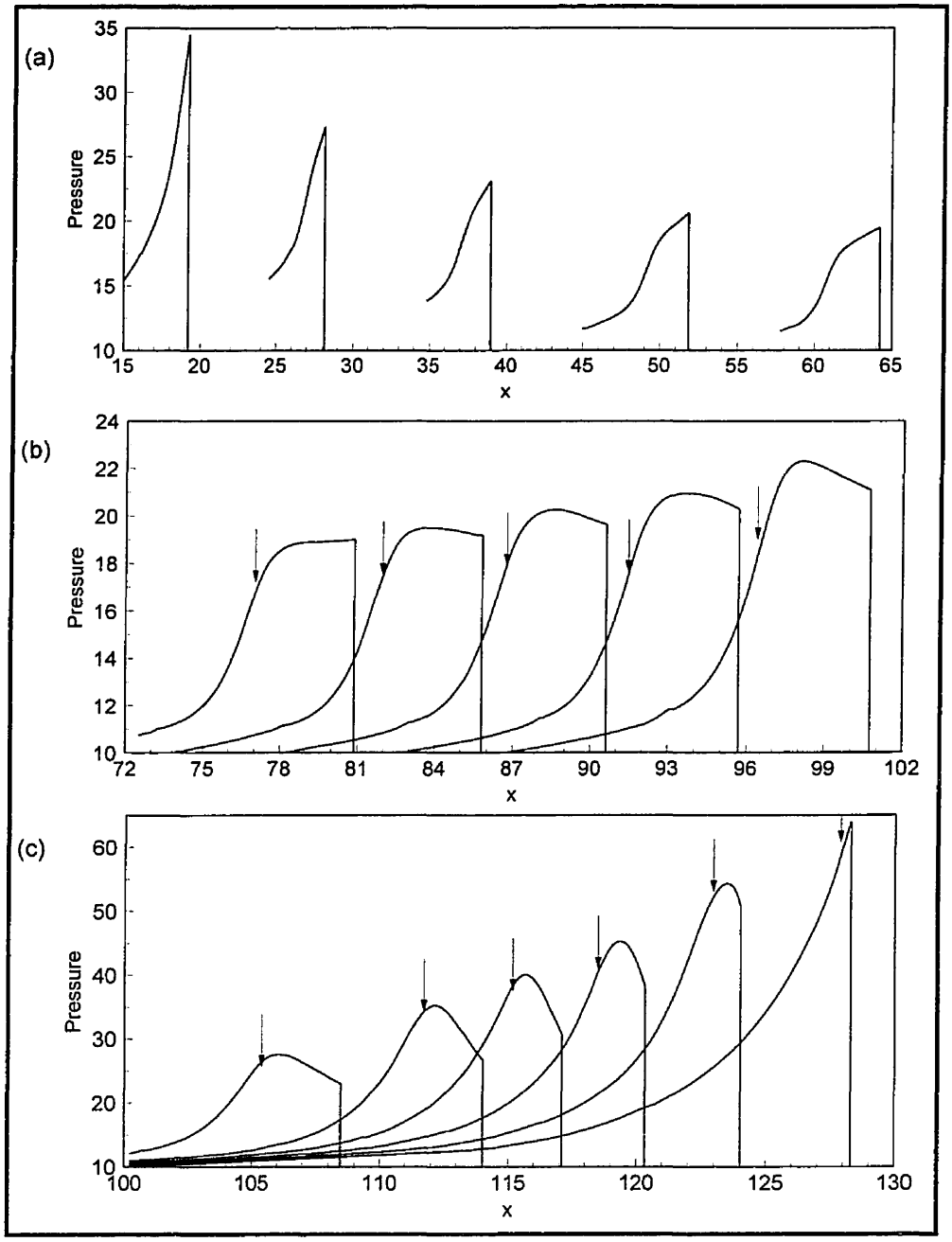

Figure 3.10. The pressure profiles in the initiation process for the critical regime. Arrows show the location of the reaction fronts ($Q/RT_0 = 50$, $\gamma = 1.2$, and $E_a/RT_0 = 24$).

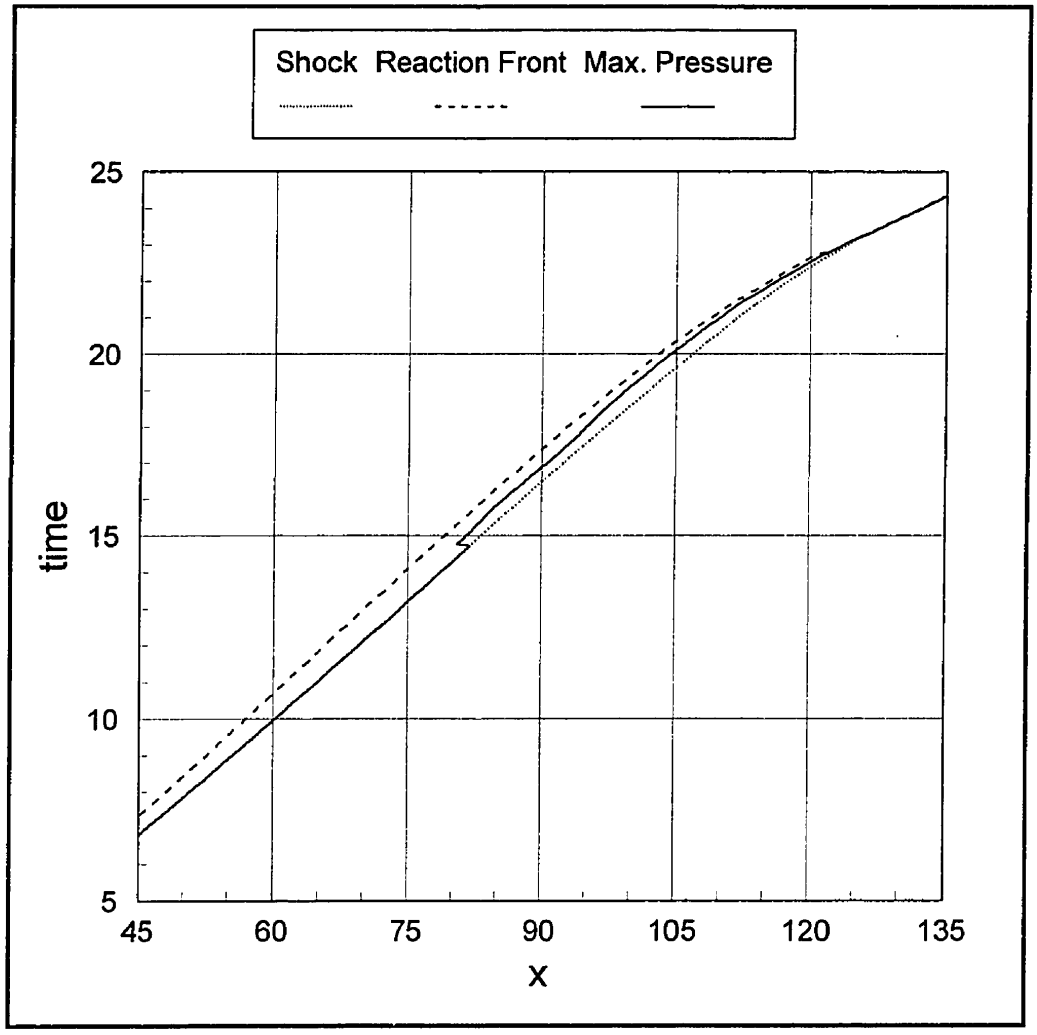

Figure 3.11. The relative propagation of the shock front, the reaction front, and the location of maximum pressure ($Q/RT_o = 50$, $\gamma = 1.2$, $E_a/RT_o = 24$, and $E_o/p_o = 1764$).

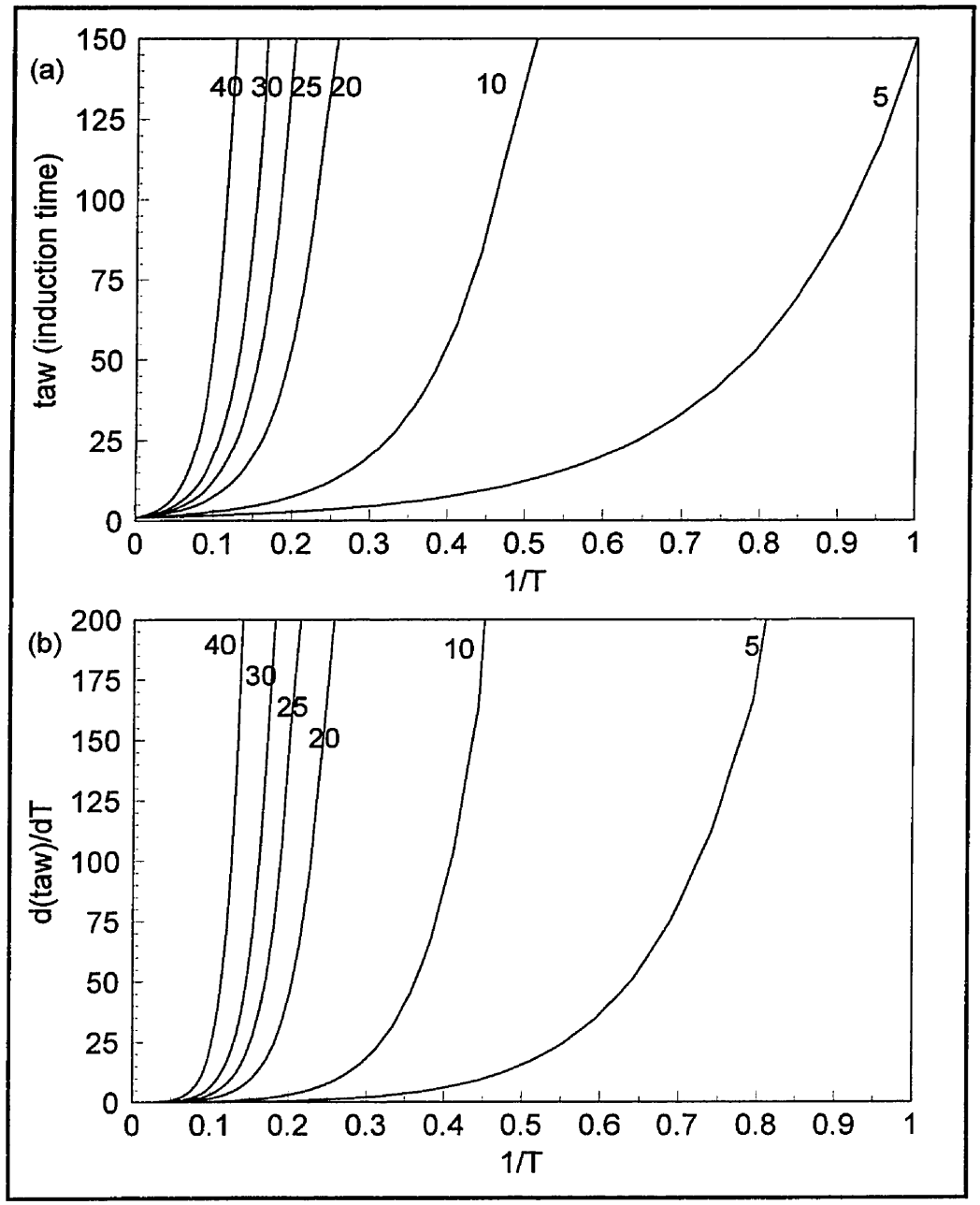

Figure 3.12. a - The variation of induction time (τ) with temperature. b - The variation of the temperature sensitivity of the induction time with temperature.

Note: The number on each curve shows the corresponding activation energy, E_a/RT_o.

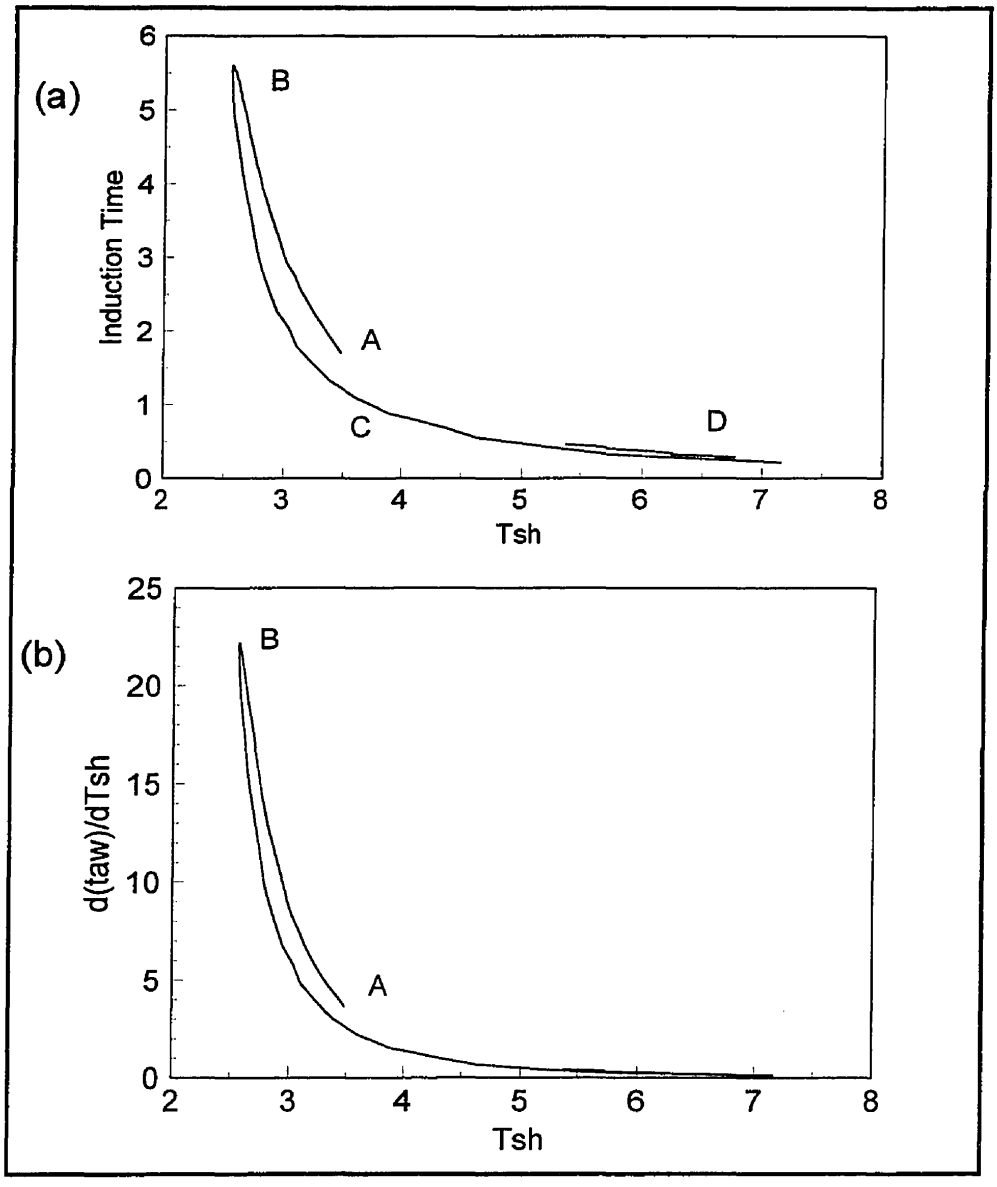

Figure 3.13. The variation of: a - the induction time, and b - the temperature sensitivity of the induction time with the shock temperature during the initiation process. ($Q/RT_o = 50$, $\gamma = 1.2$, $E_a/RT_o=24$, and $E_o/p_o=1764$).

A: Beginning of the quasi-steady period.
B: The minimum state in the quasi steady period.
C: The end of the quasi-steady period.
D: The overdriven wave.

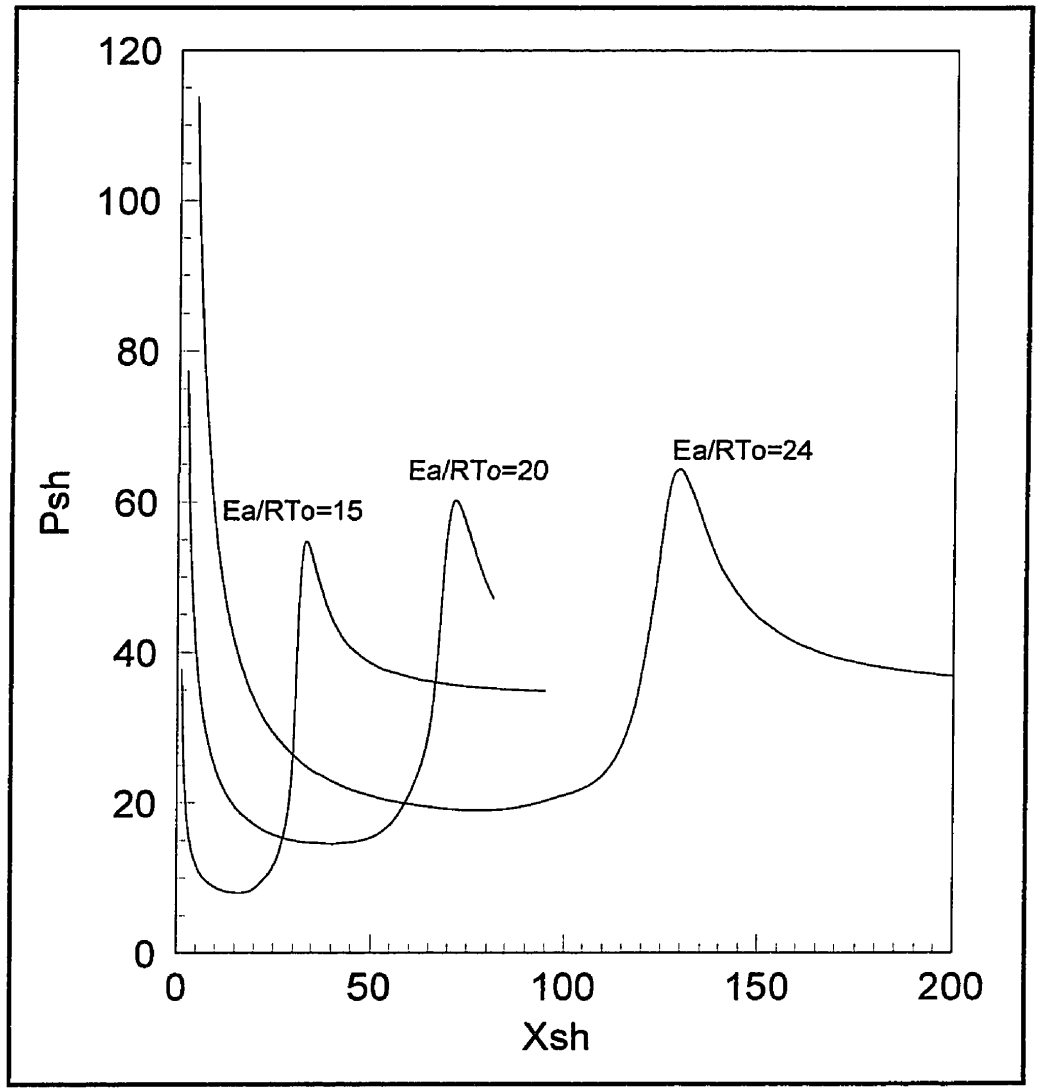

Figure 3.14. The shock evolution process in critical regime for different activation energies ($Q/RT_0 = 50, \gamma = 1.2$).

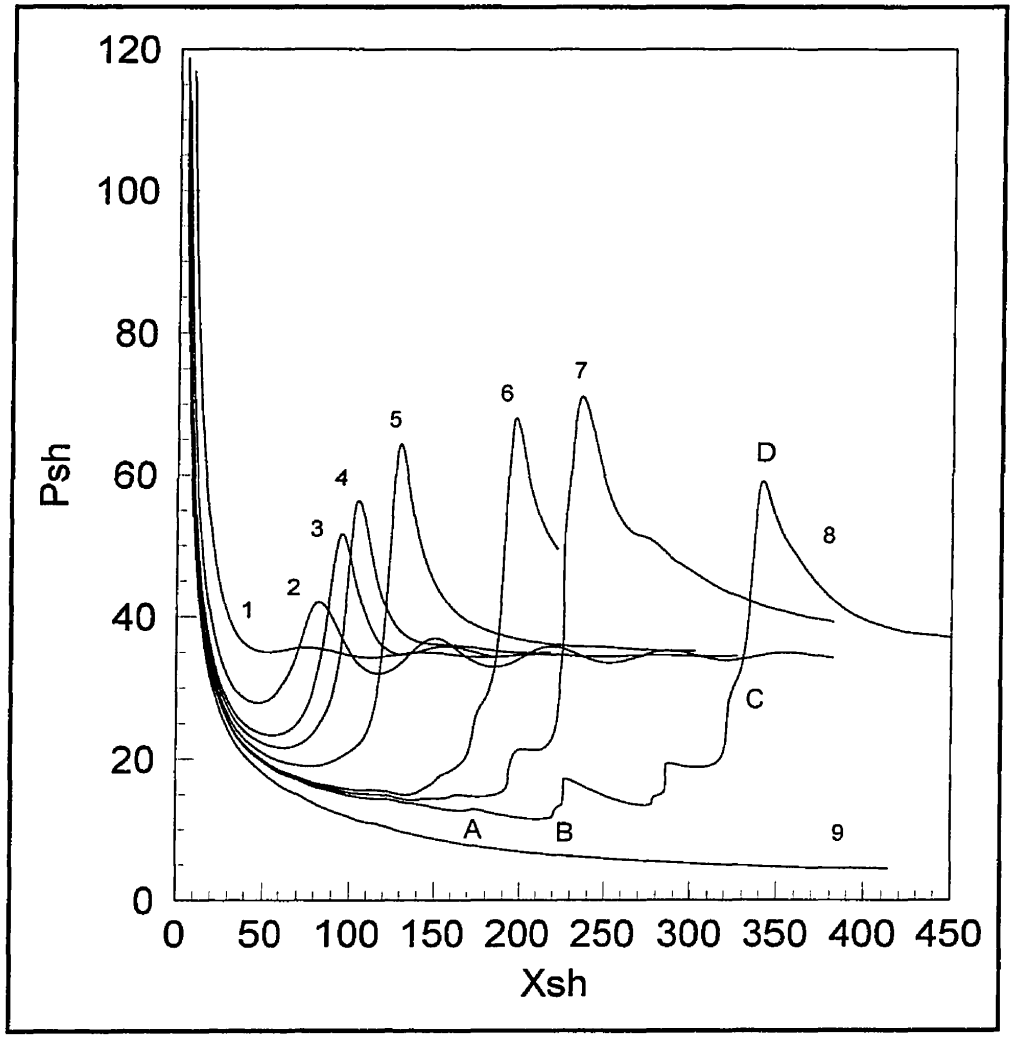

Figure 3.15. The shock evolution process for different initiation energies ($Q/RT_o = 50$, $\gamma = 1.2$, and $E_a/RT_o = 24$). The initiation energies are: E_{o1}=3415, E_{o2}=2254, E_{o3}=1921, E_{o4}=1841, E_{o5}=1764, E_{o6}=1711, E_{o7}=1703, E_{o8}=1695, and E_{o9}=1614.

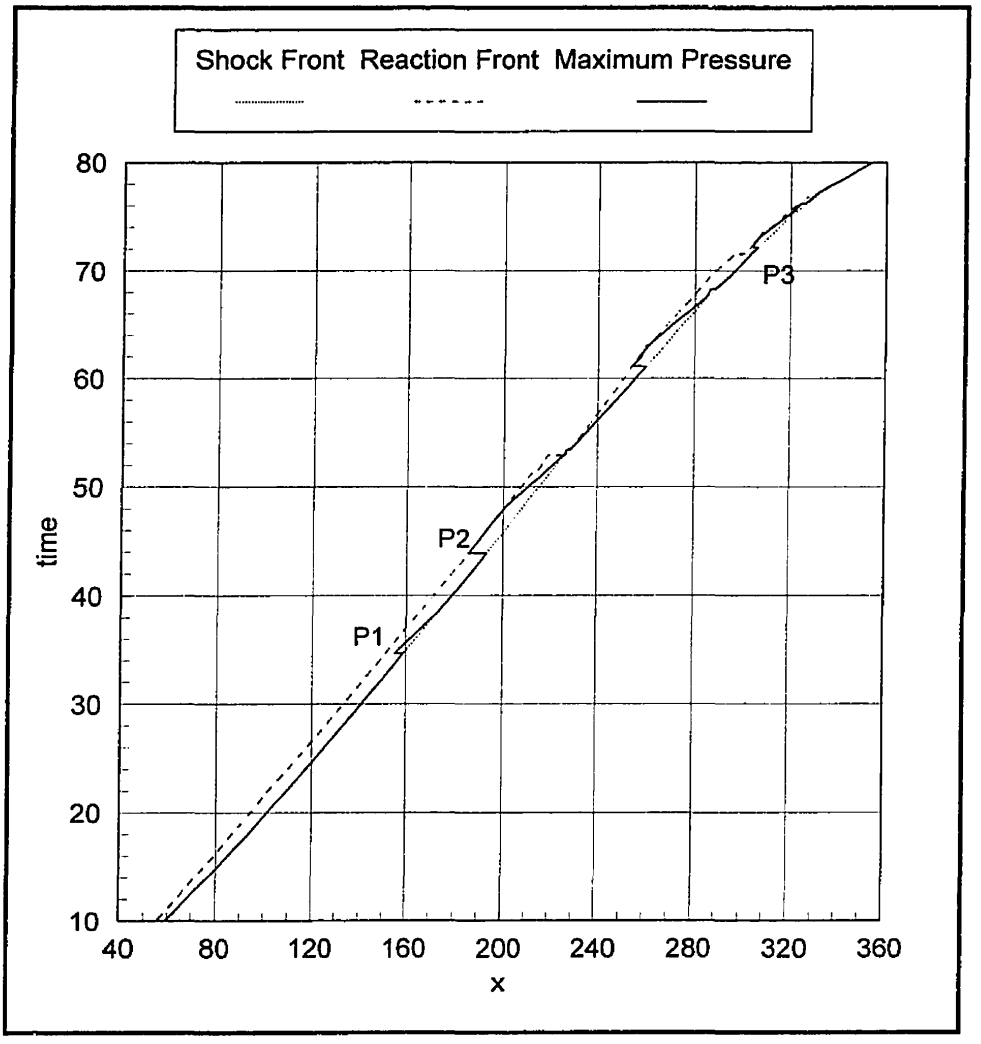

Figure 3.16. The relative propagation of the shock front, the reaction front, and the wave with maximum pressure ($Q/RT_o = 50$, $\gamma = 1.2$, $E_a/RT_o=24$, and $E_o/p_o=1695$).

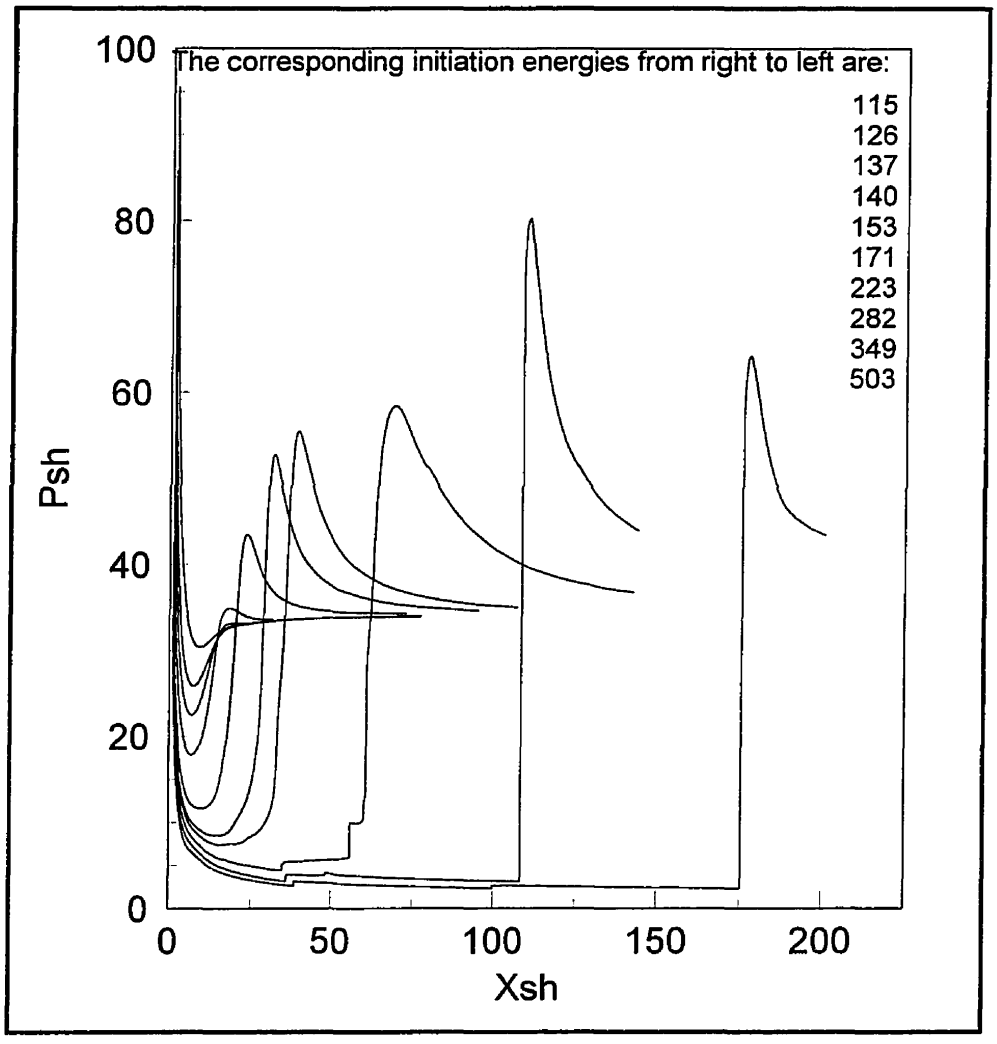

Figure 3.17. The shock evolution process for different initiation energies when the activation energy is low ($Q/RT_o = 50$, $\gamma = 1.2$, and $E_a/RT_o=15$).

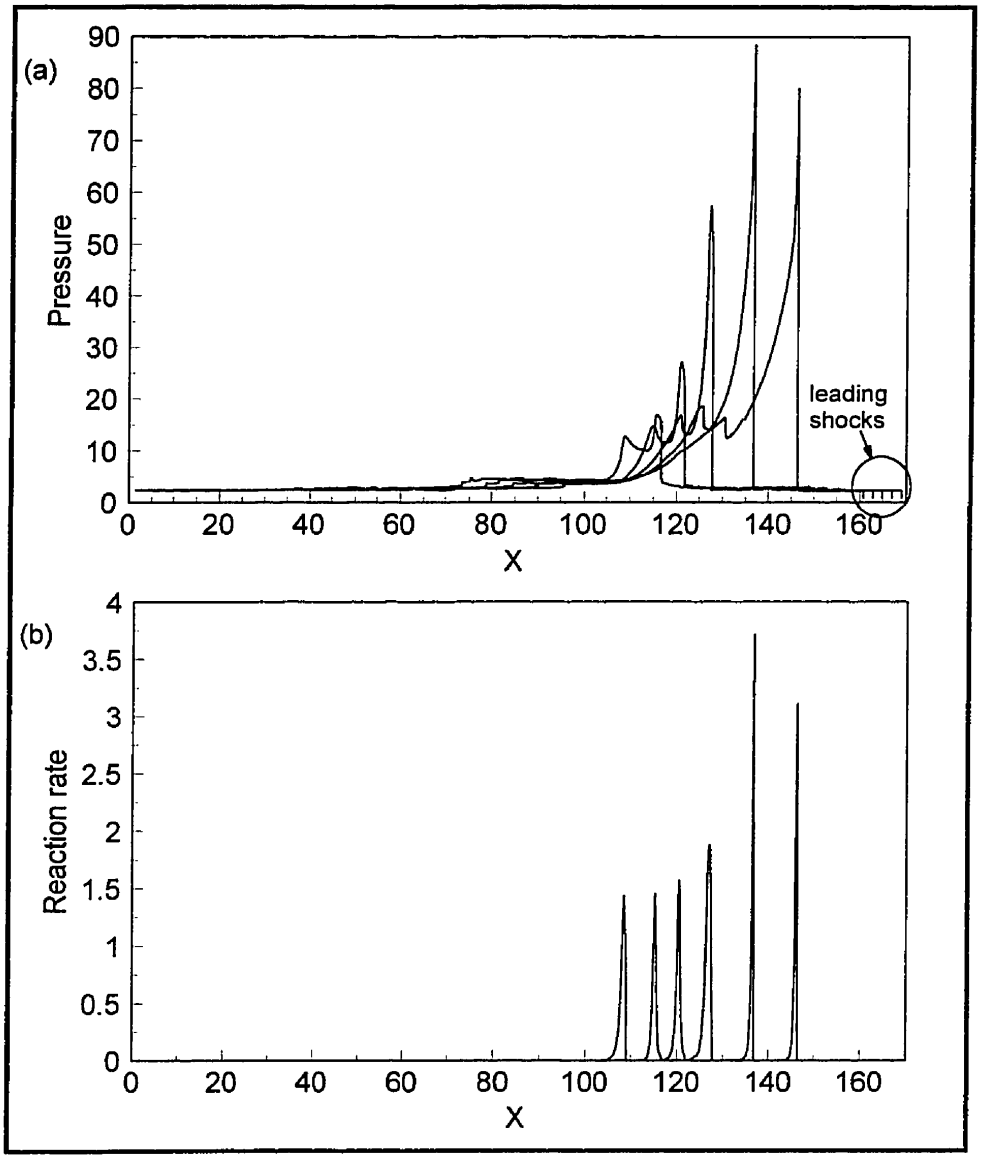

Figure 3.18. The formation of the detonation far behind the shock front for a low activation energy when initiation energy is very low (i.e., E_0/p_0=115). a - Pressure profiles, and b - Reaction rate profiles ($Q/RT_0 = 50$, $\gamma = 1.2$, $E_a/RT_0 = 15$).

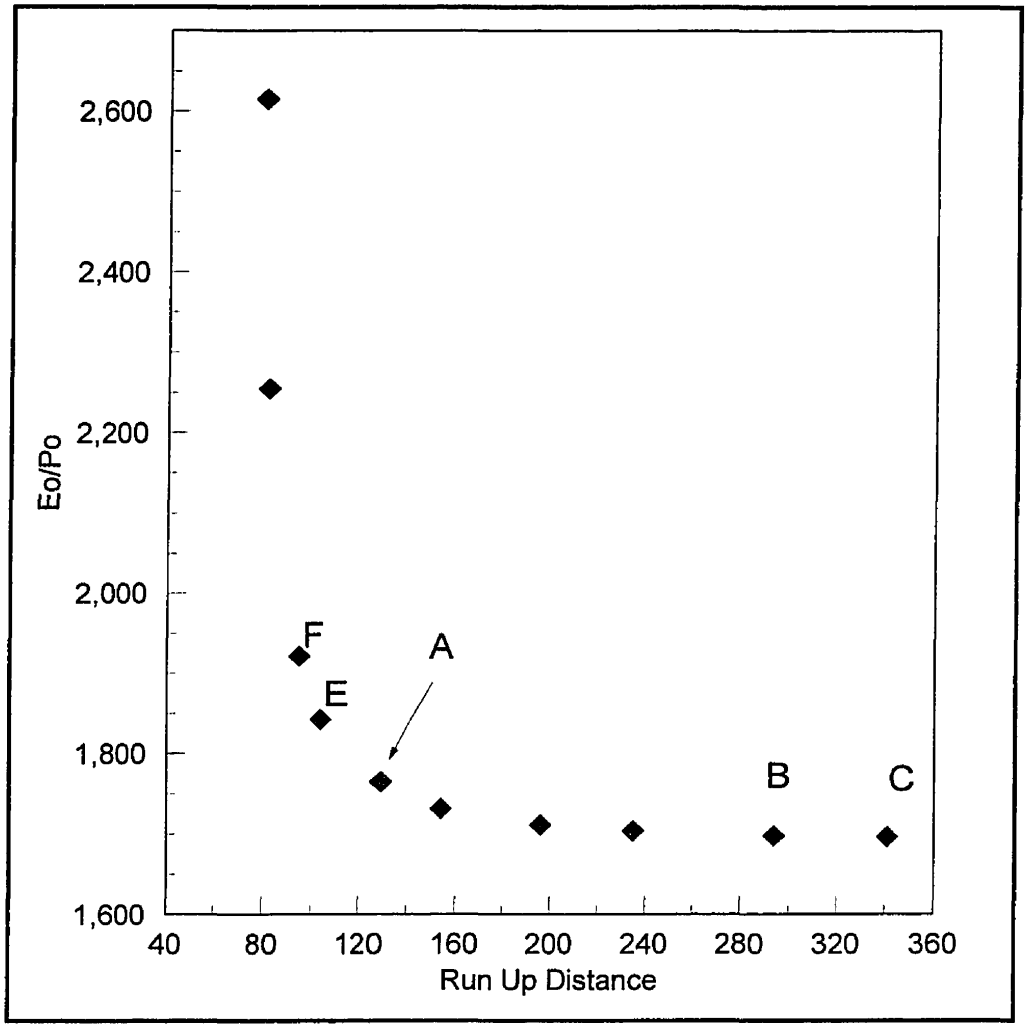

Figure 3.19. The variation of the run up distance with the initiation energy ($Q/RT_O = 50$, $\gamma = 1.2$, and $E_a/RT_O = 24$).

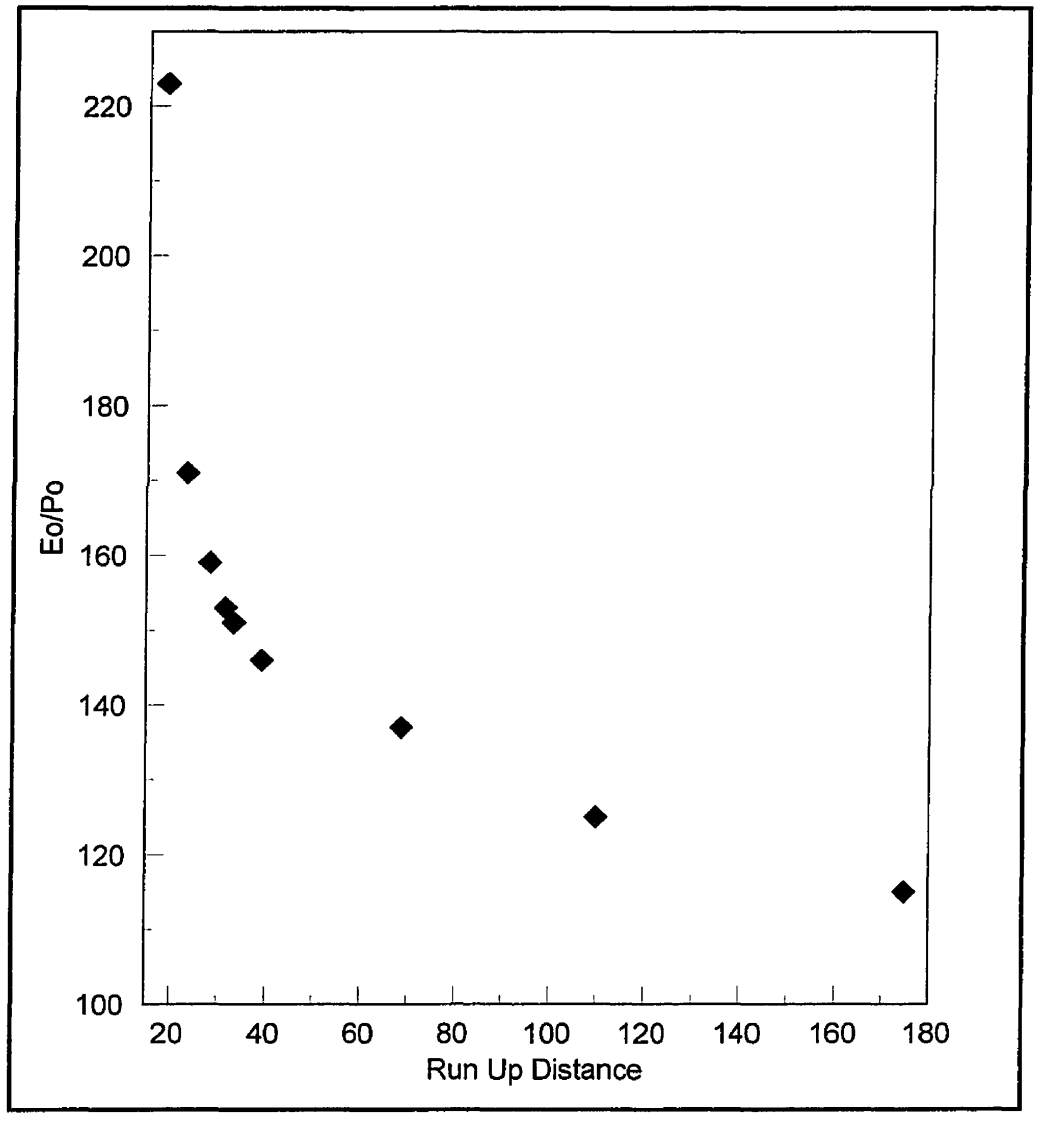

Figure 3.20. The variation of the run up distance with the initiation energy ($Q/RT_o = 50$, $\gamma = 1.2$, and $E_a/RT_o = 15$).

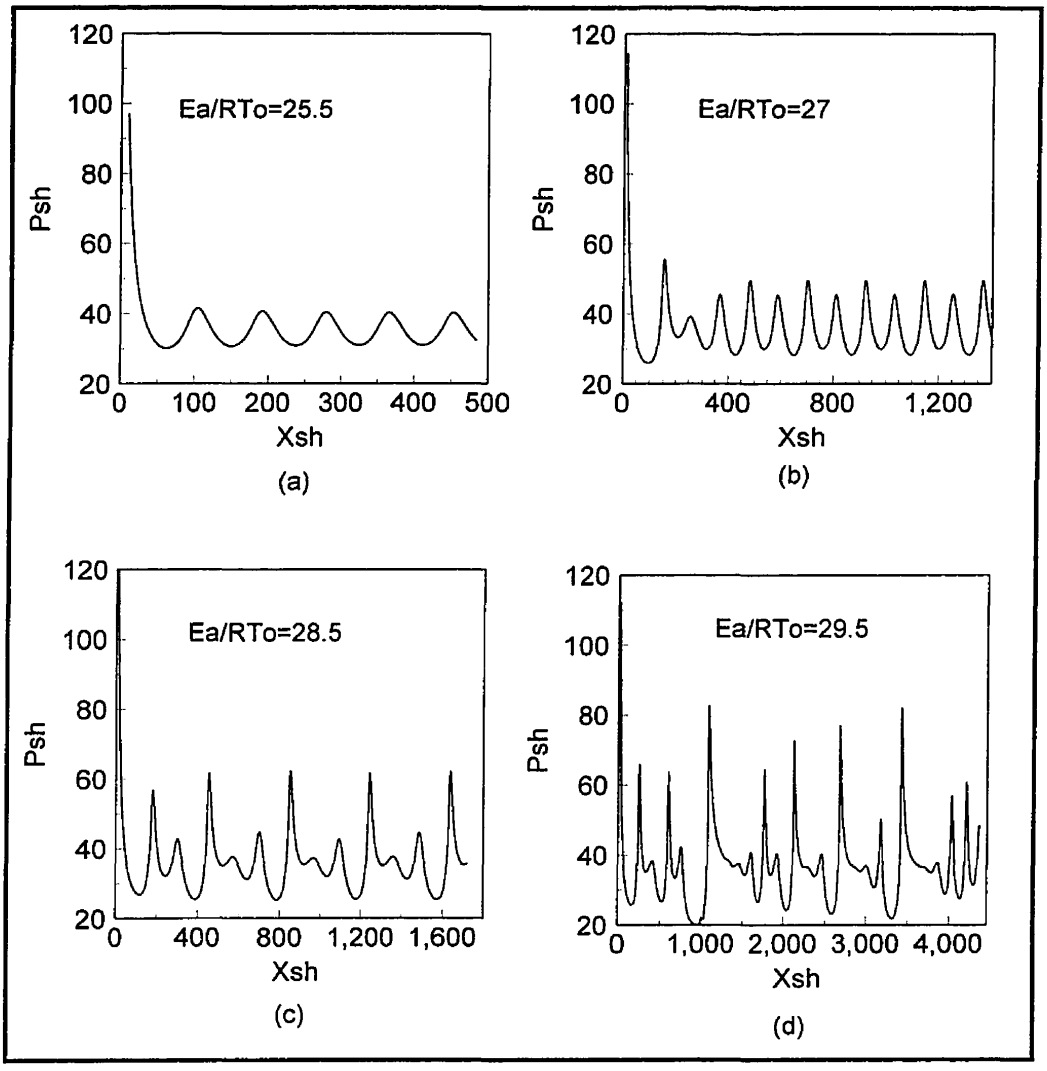

Figure 4.1. The oscillatory propagation of unstable detonation front for different activation energies. ($Q/RT_O = 50, \gamma = 1.2$).

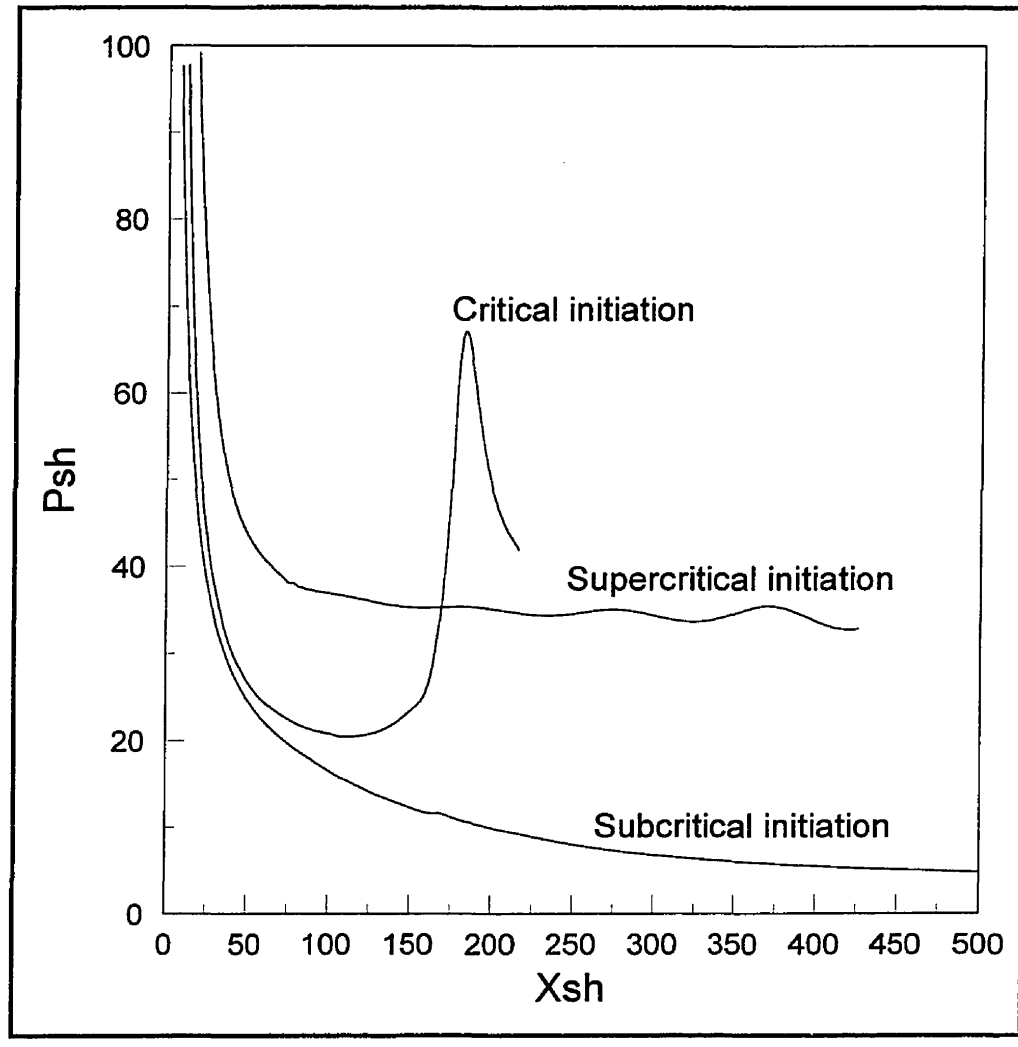

Figure 4.2. The three regimes of initiation for an unstable detonation. The corresponding initiation energies are 4700 for supercritical, 2895 for critical, and 2668 for subcritical initiation ($E_a/RT_o = 26$, $\gamma = 1.2$, and $Q/RT_o = 50$).

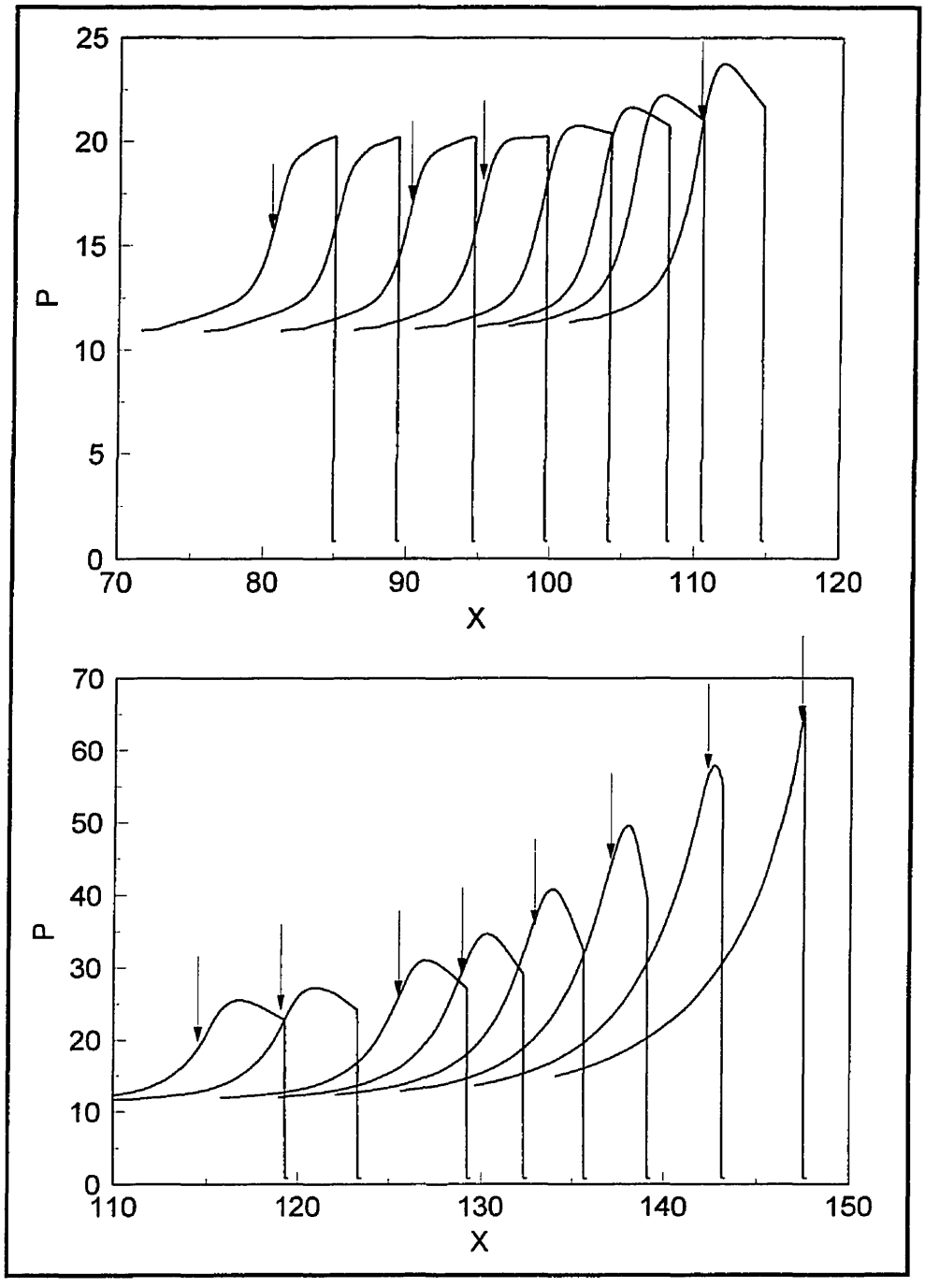

Figure 4.3. Pressure profiles in the quasi-steady period prior to the onset of an unstable detonation. Arrows show the location of the reaction front ($E_a/RT_0 = 26$, $\gamma = 1.2$, and $Q/RT_0 = 50$).

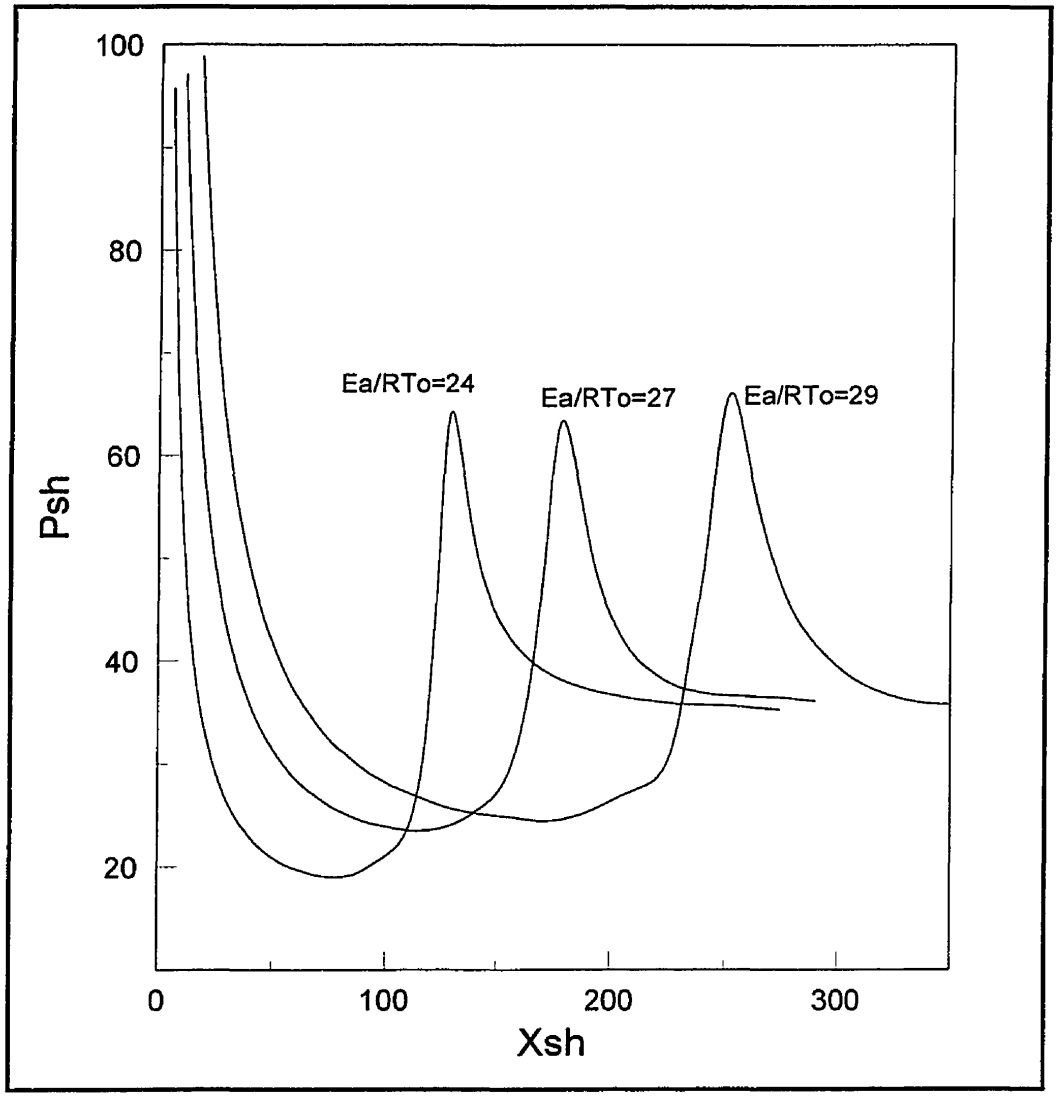

Figure 4.4. Comparison between the initiation processes in critical regime for three different activation energies ($Q/RT_0 = 50$, $\gamma = 1.2$). The corresponding initiation energies are 1766, 3700, and 5600 for $E_a/RT_0 = 24$, 27, and 29 respectively.

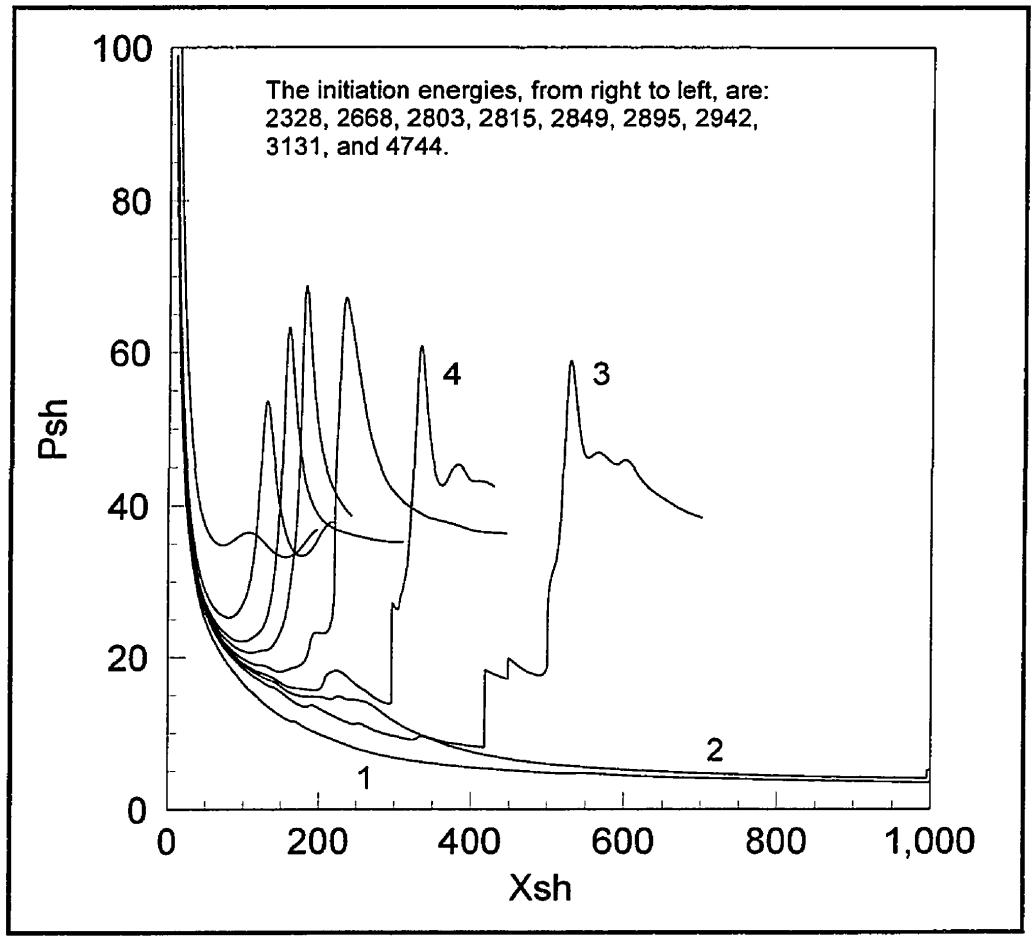

Figure 4.5. The initiation processes for different initiation energies ($Q/RT_o = 50$, $\gamma = 1.2$, and $E_a/RT_o = 26$).

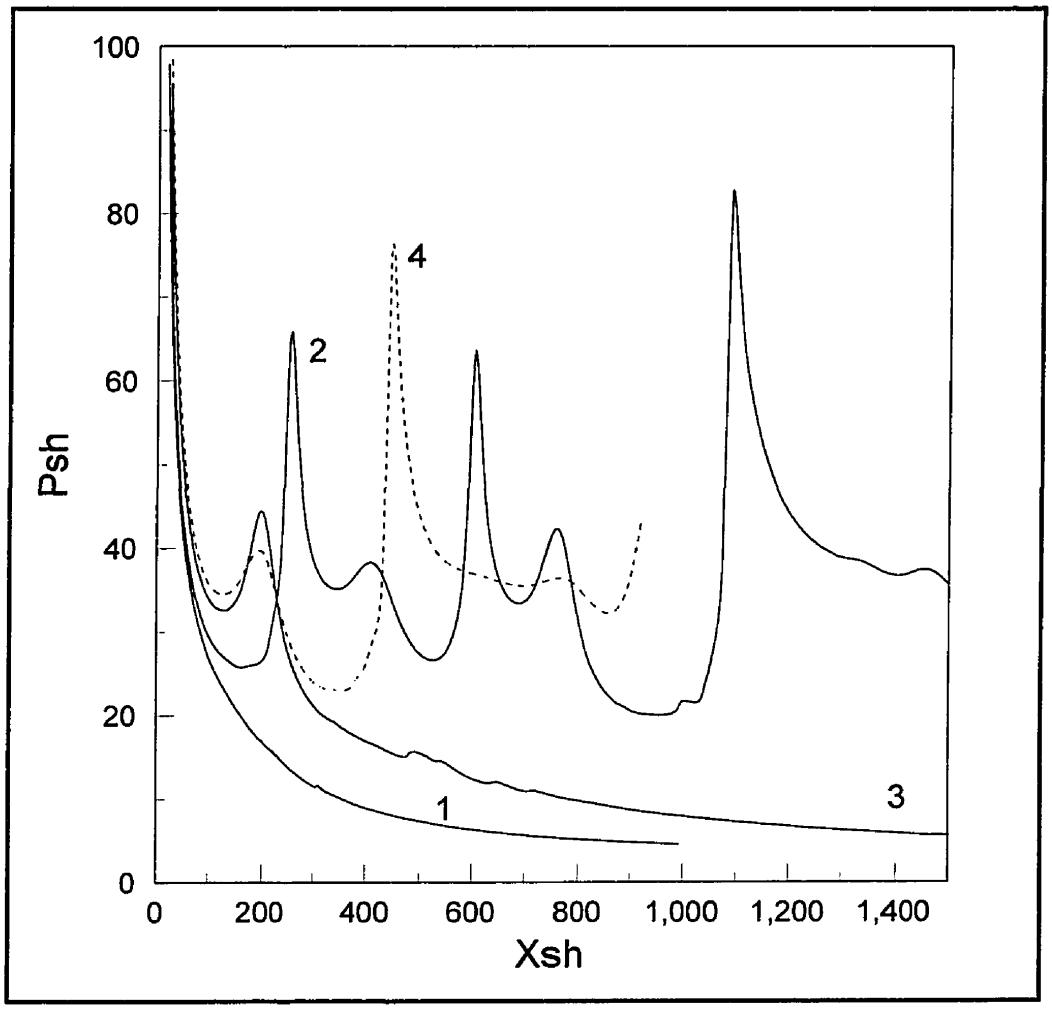

Figure 4.6. Different regimes of initiation for a very unstable detonation ($Q/RT_o = 50$, $\gamma = 1.2$, and $E_a/RT_o = 29.5$). The corresponding initiation energies are: $E_{o1} = 6066$, $E_{o2} = 6790$, $E_{o3} = 8000$, and $E_{o4} = 8790$.

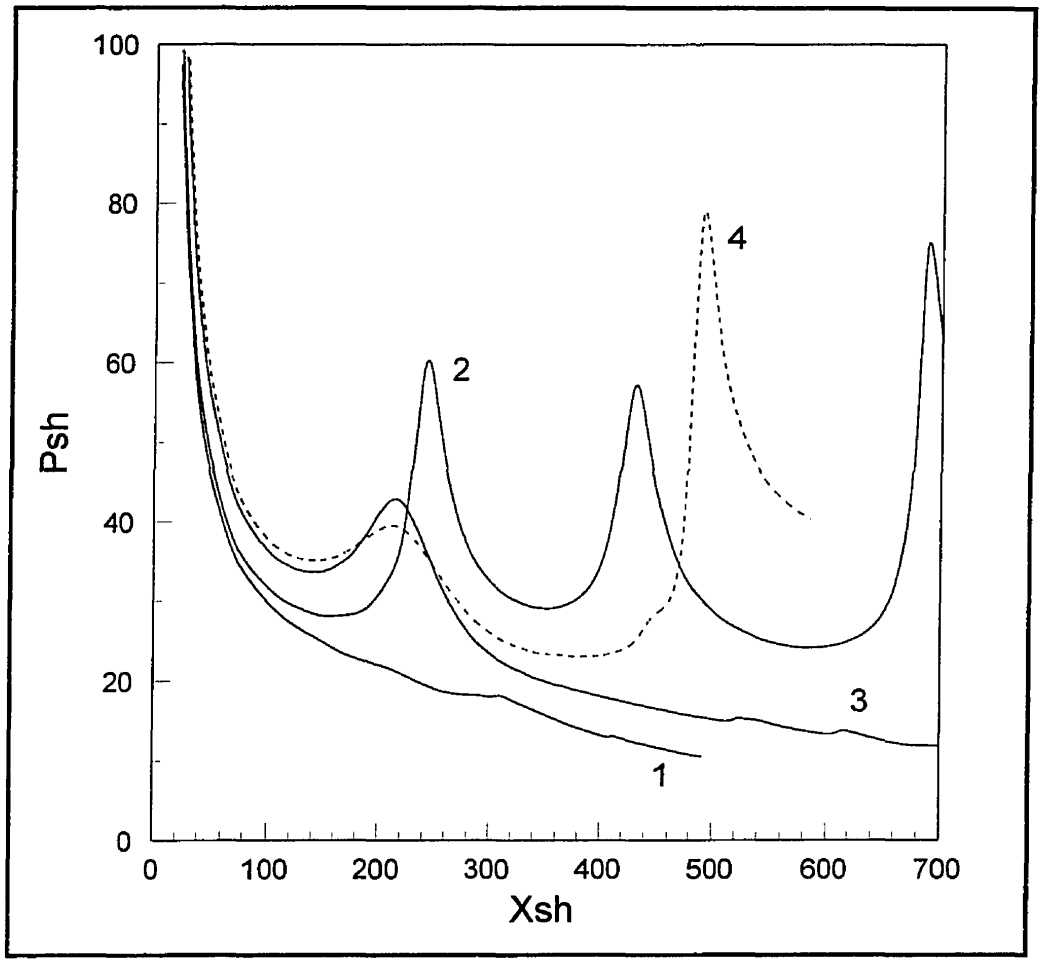

Figure 4.7. Different regimes of initiation for a very unstable detonation ($Q/RT_0 = 50$, $\gamma = 1.2$, and $E_a/RT_0 = 30$). The corresponding initiation energies are: $E_{01} = 6880$, $E_{02} = 7350$, $E_{03} = 8690$, and $E_{04} = 9260$.

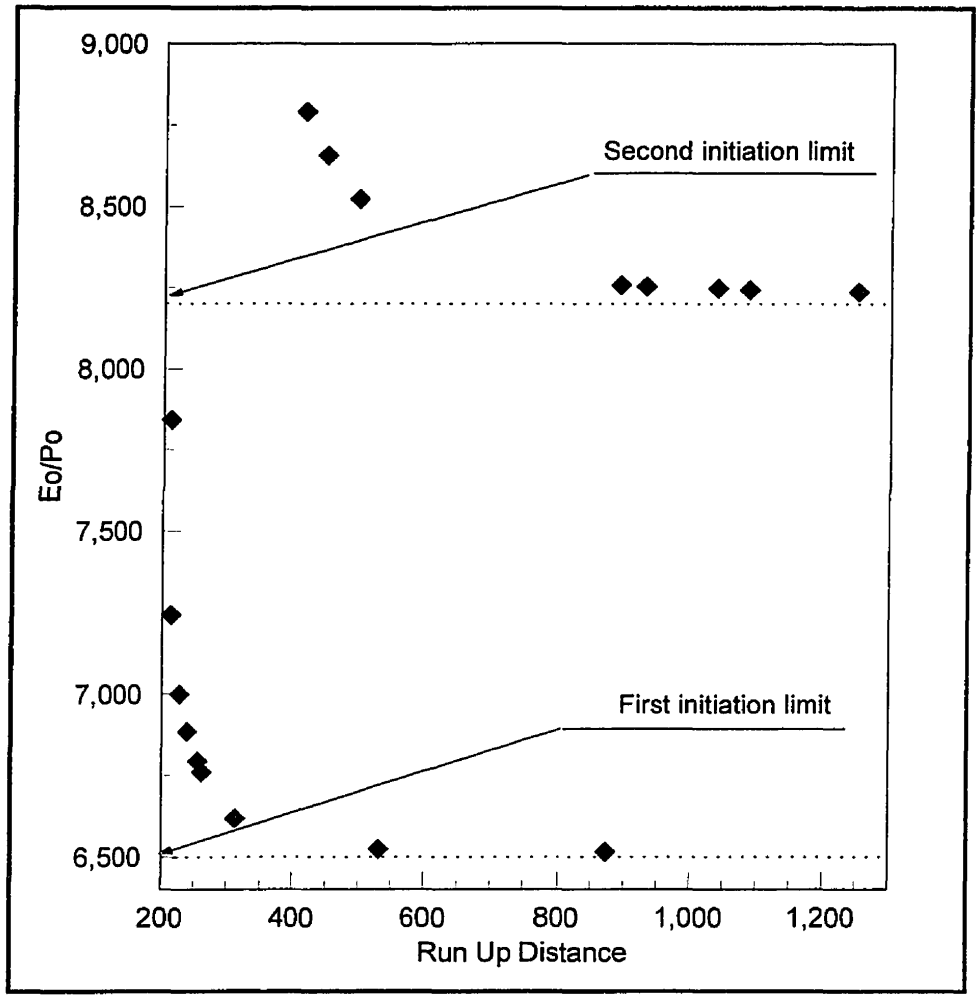

Figure 4.8. The variation of run up distance with initiation energy. Two lines show the asymptotic values of the critical initiation energies ($Q/RT_o = 50$, $\gamma = 1.2$, and $E_a/RT_o = 29.5$).

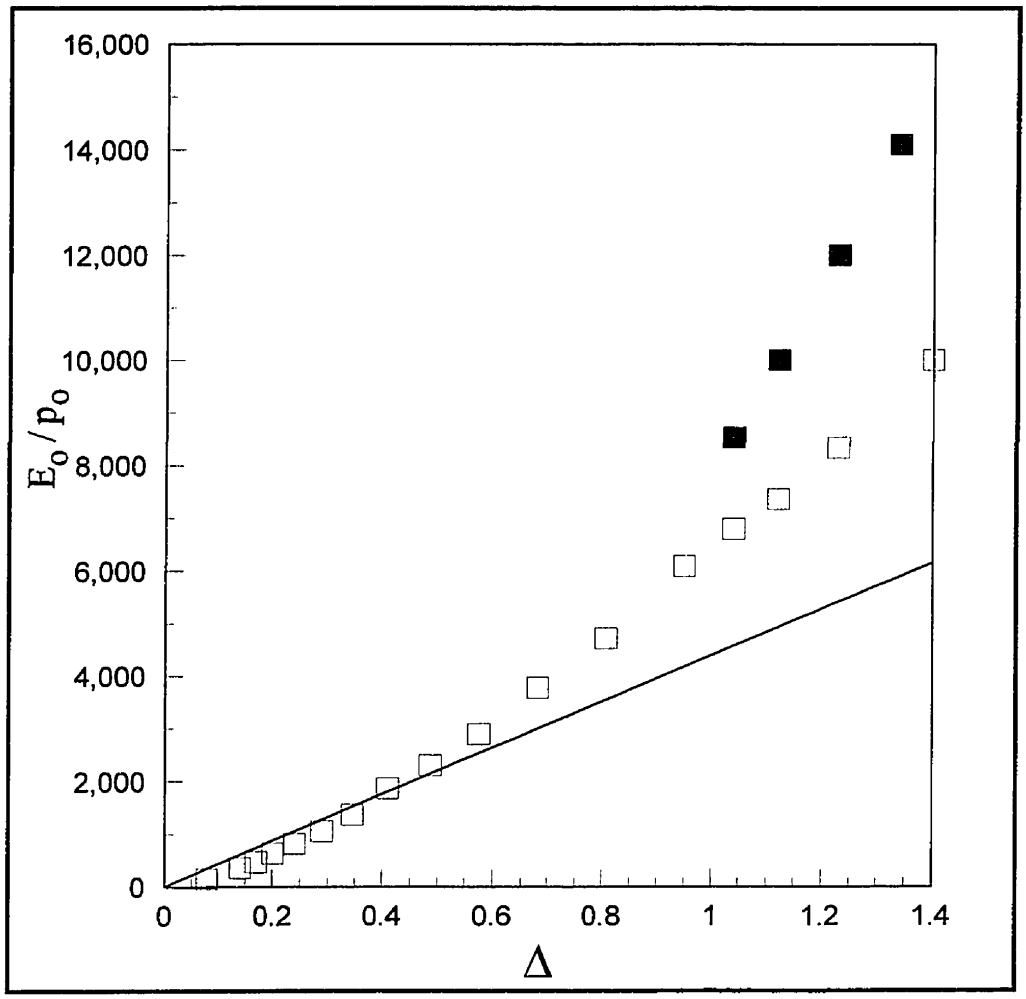

Figure 4.9. Variation of the critical initiation energy, determined by numerical simulation, with the ZND detonation induction length ($Q/RT_0 = 50$, $\gamma = 1.2$).

Note: the solid line shows the critical initiation energy calculated by Equation 4.1. Hollow squares show the critical initiation energy, and solid squares correspond to the second limit of initiation, both calculated via numerical simulation.

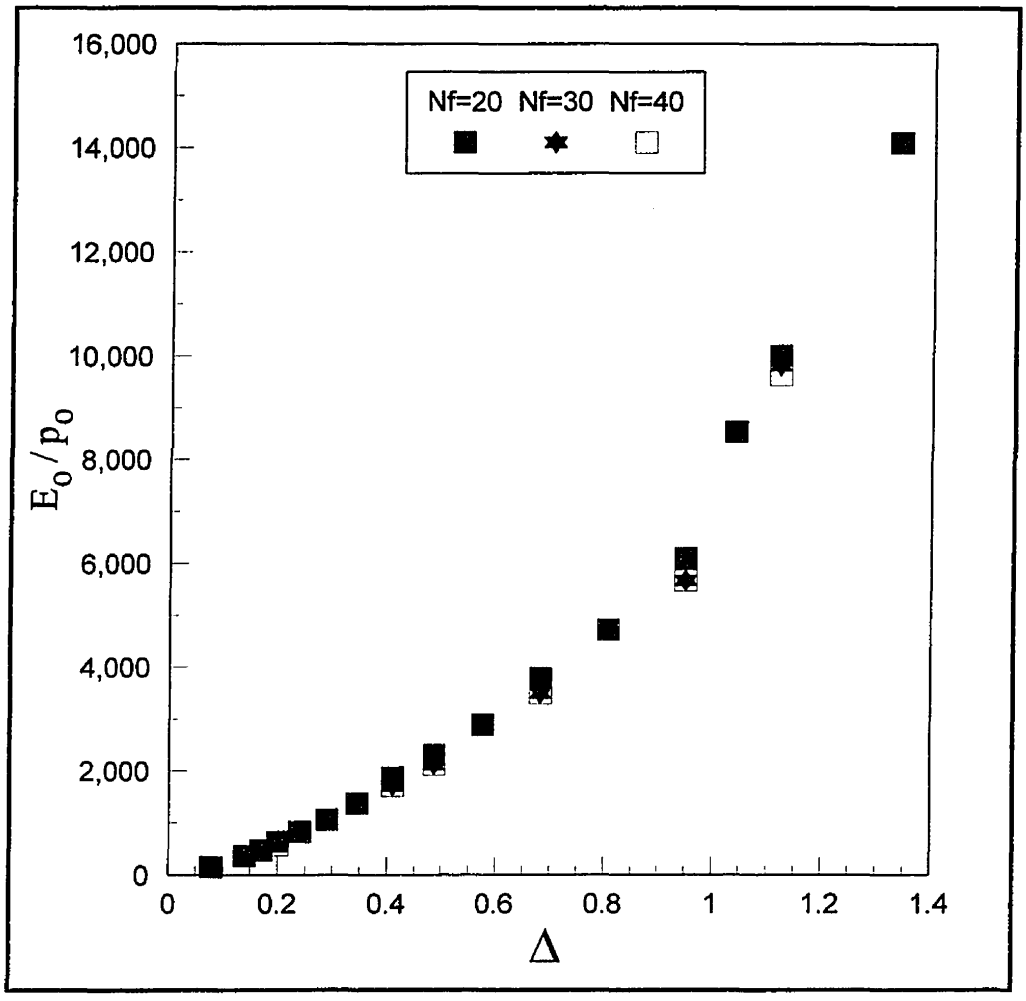

Figure 4.10. Variation of the critical initiation energy with the induction length of ZND detonation for three different mesh resolutions ($Q/RT_o = 50$, $\gamma = 1.2$).

Note: "Nf" refers to the number of fine meshes per half reaction zone length of ZND detonation of a mixture with: $Q/RT_o = 50$, $\gamma = 1.2$, and $E_a/RT_o = 25.5$.

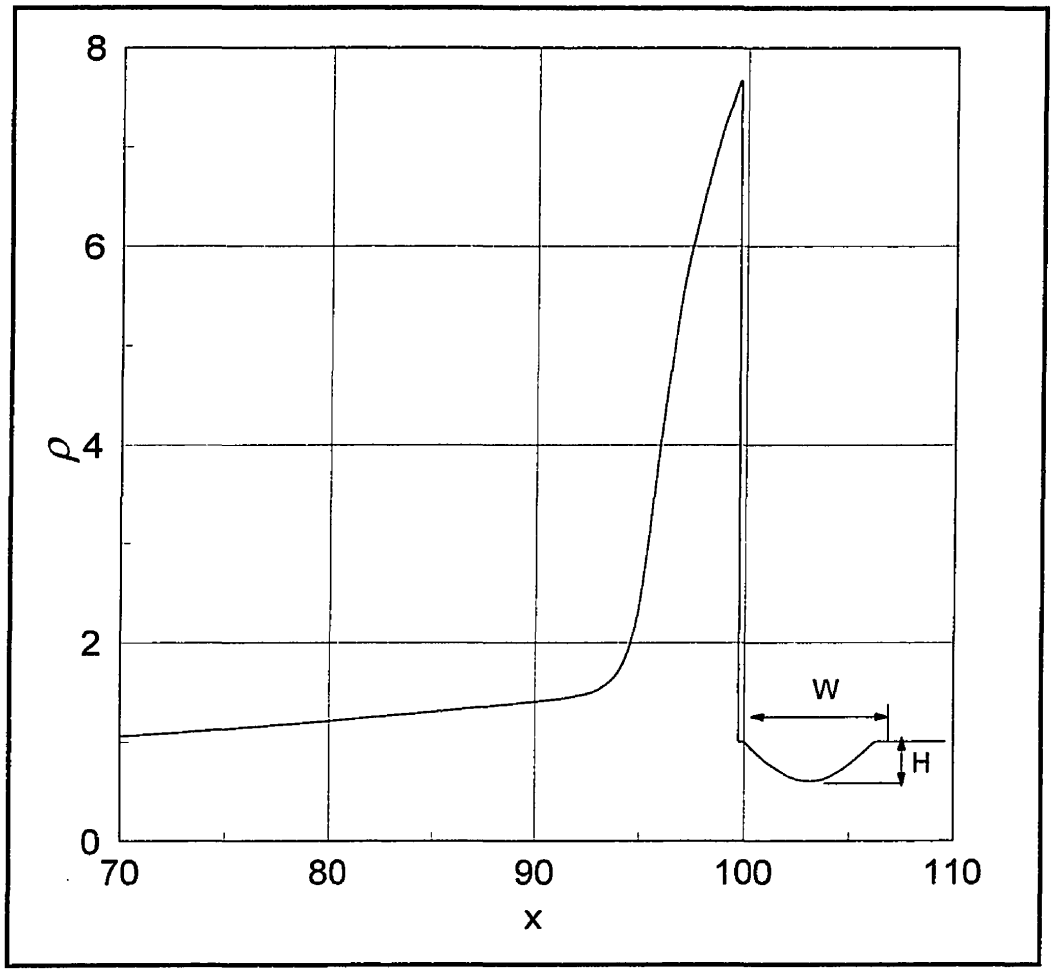

Figure 5.1. The characteristics of the density perturbation.
$H = (\rho - \rho_0)/\rho_0$, and $W = 0.5 * (D_{cj}/2) * \tau$

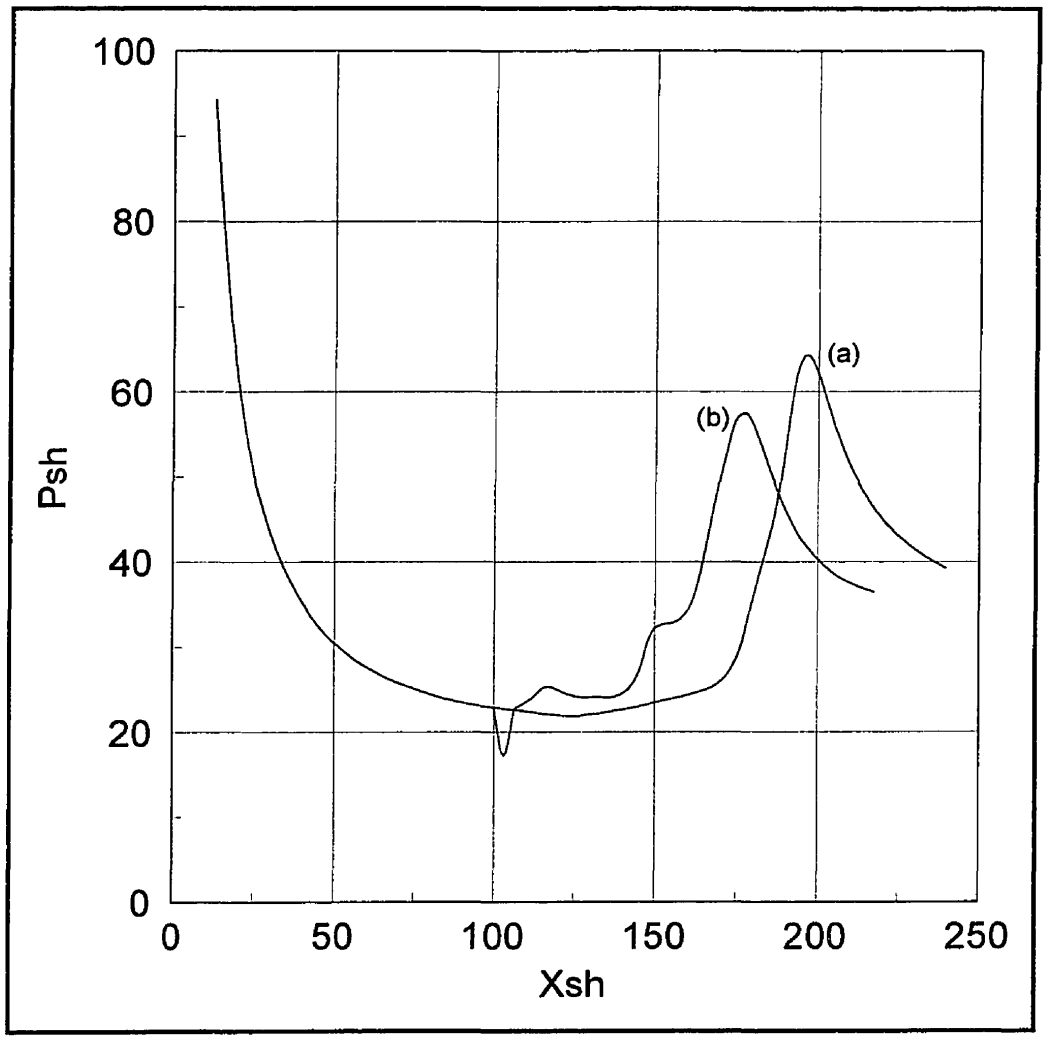

Figure 5.2. Comparison between the initiation processes: a - without, and b - with the presence of a density perturbation in the critical regime of initiation ($E_a/RT_o = 27$, $Q/RT_o = 50$, $\gamma = 1.2$, $E_o/p_o = 4320$, $W = 6$, and $H = 0.4$).

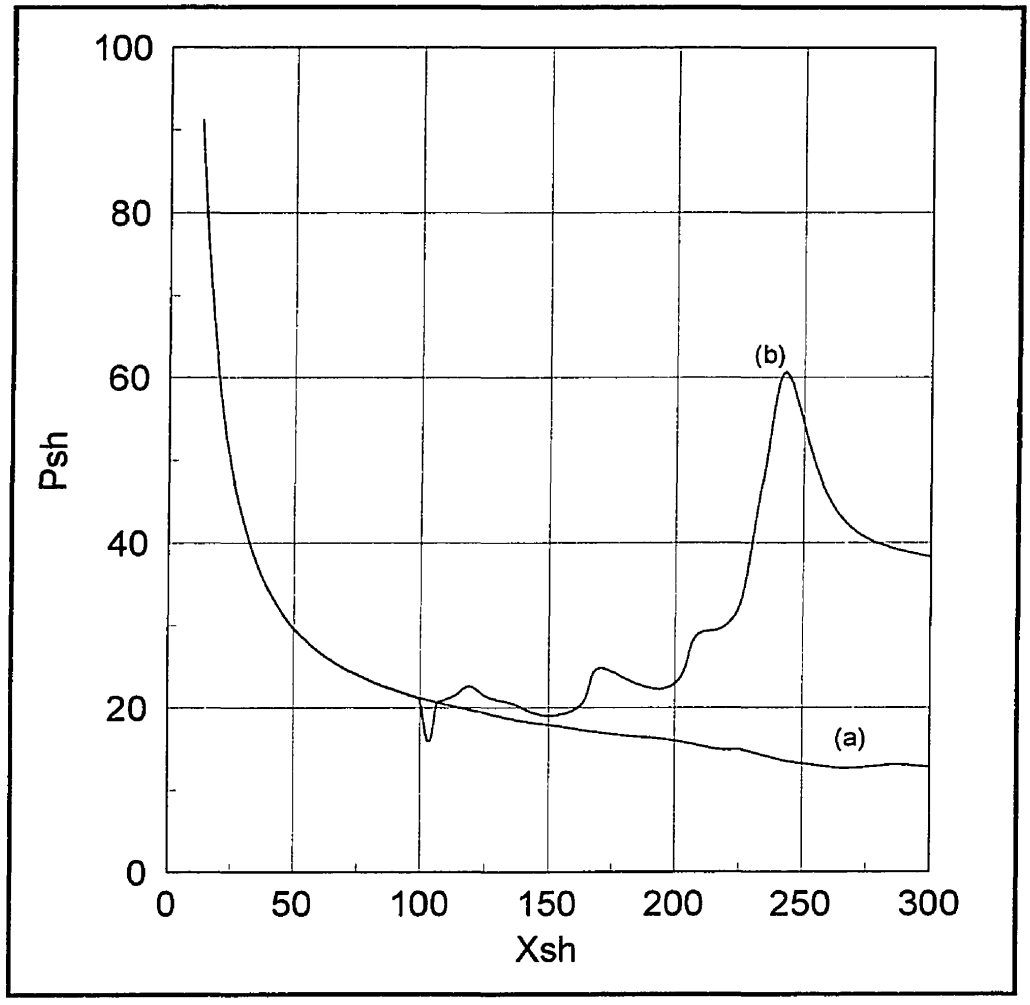

Figure 5.3. Comparison between the initiation processes: a - without and b - with the presence of a density perturbation in subcritical regime ($E_a/RT_o = 27$, $Q/RT_o = 50$, $\gamma = 1.2$, $E_o/p_o = 4100$, W=6, and H=0.4).

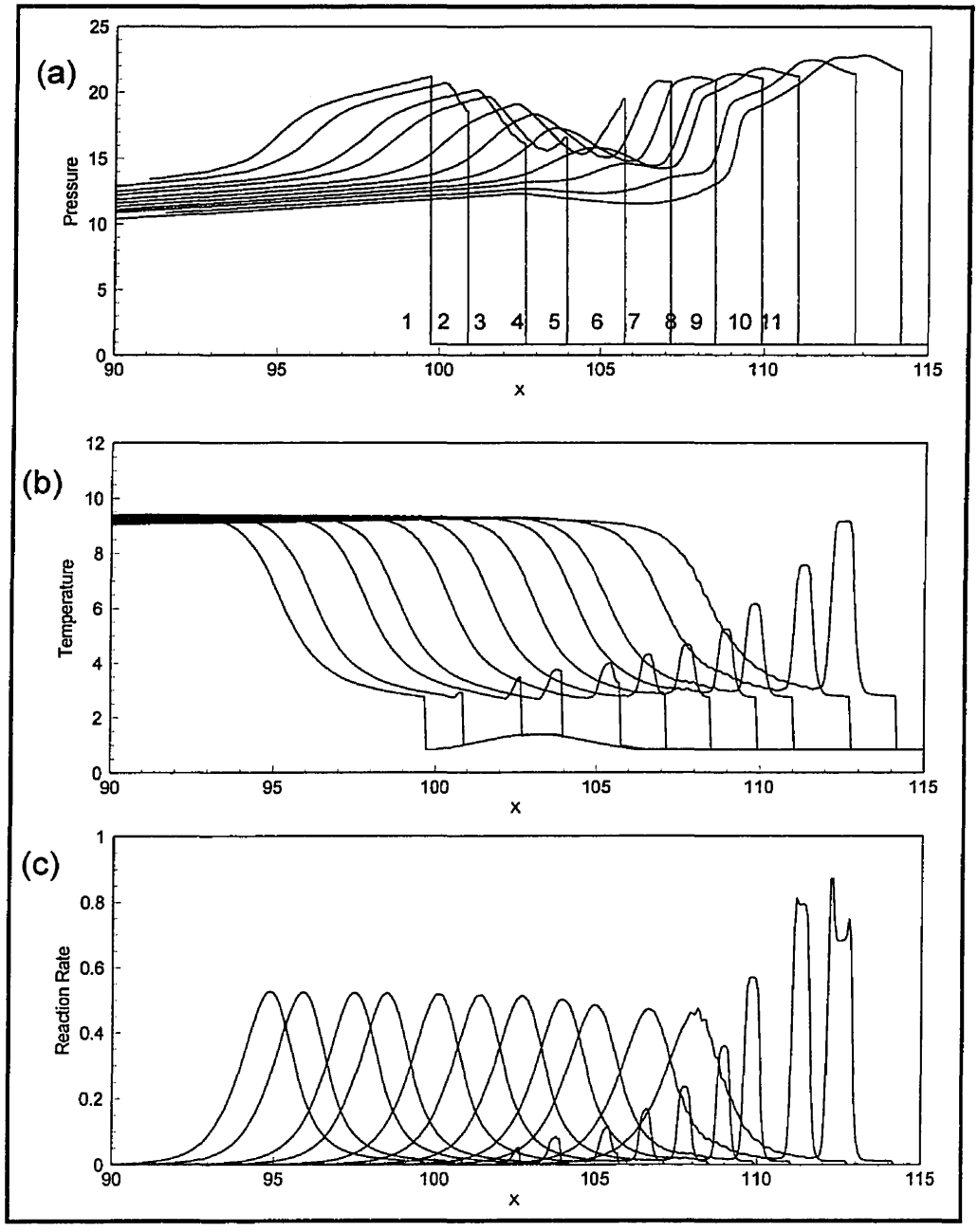

Figure 5.4. Pressure, temperature , and reaction rate profiles for initiation process in the presence of the density perturbation ($E_a/RT_o = 27$, $Q/RT_o = 50$, $\gamma = 1.2$, $E_o/p_o = 4100$, W=6, and H=0.4).

Note: The initiation energy is 5% less than the critical initiation energy.

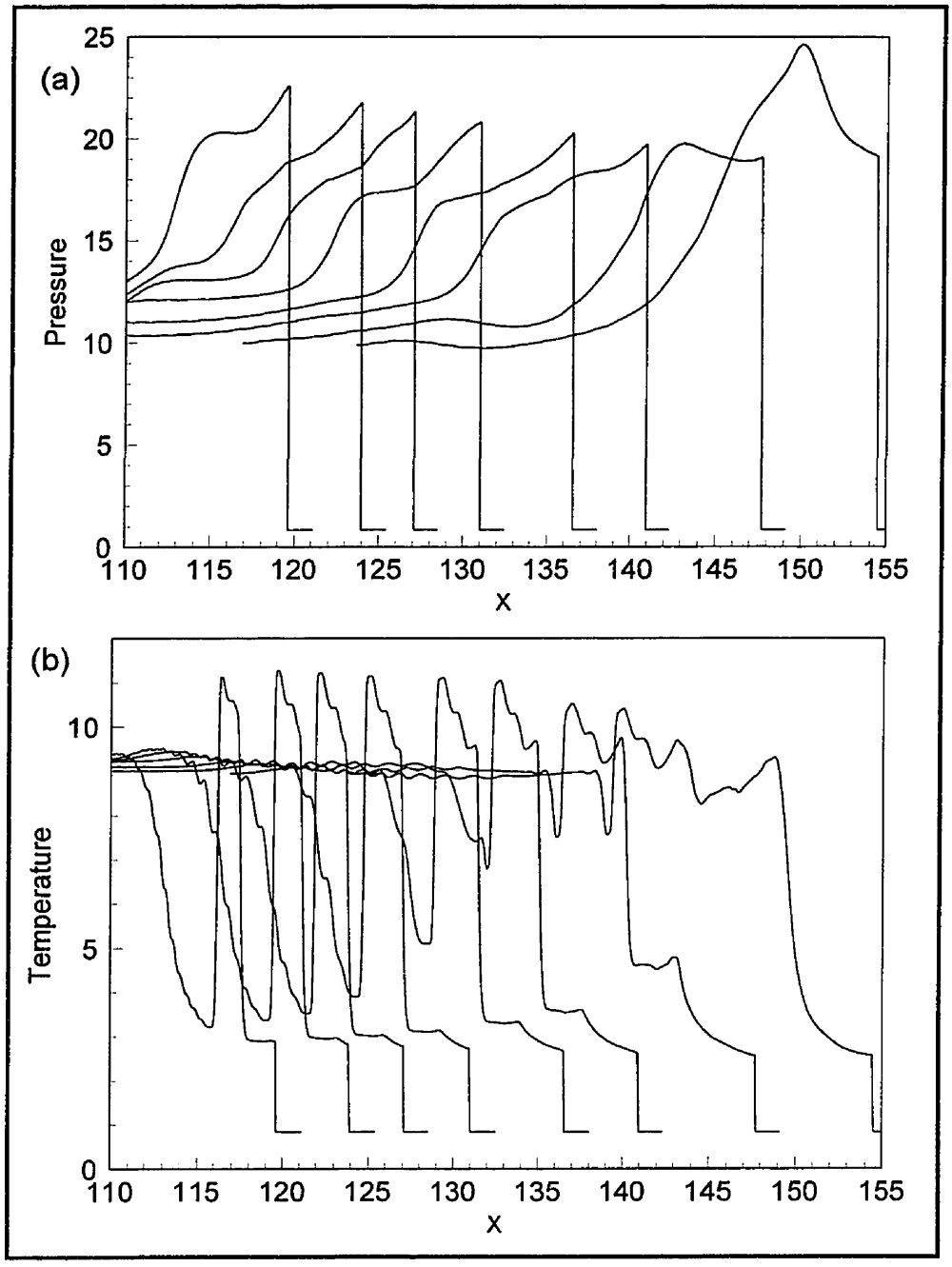

Figure 5.5. Pressure and temperature profiles for initiation process in the presence of the density perturbation ($E_a/RT_o = 27$, $Q/RT_o = 50$, $\gamma = 1.2$, $E_o/p_o = 4100$, W=6, and H=0.4).

Note: The initiation energy is 5% less than the critical initiation energy without hot-spot.

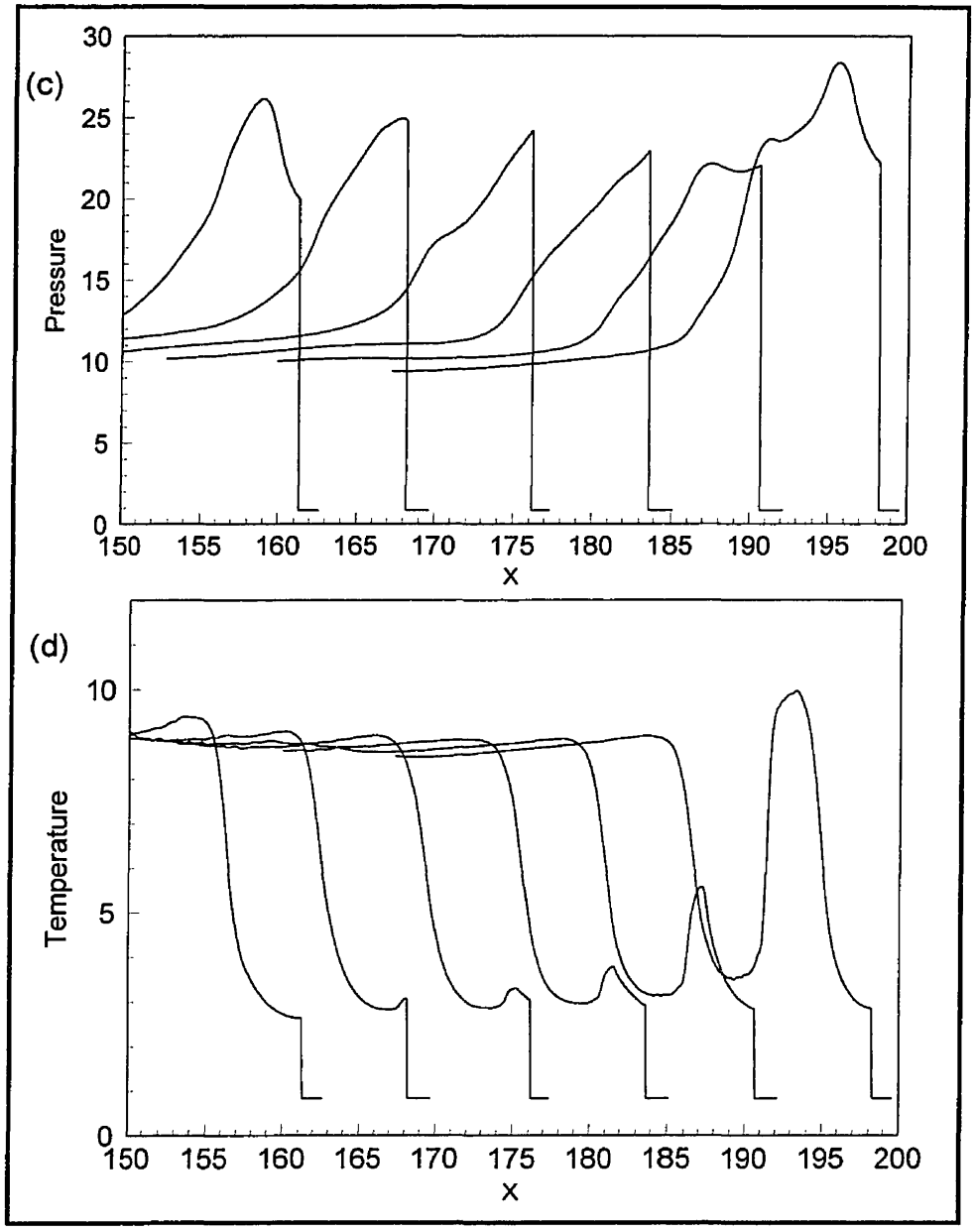

Figure 5.5. (Continued).

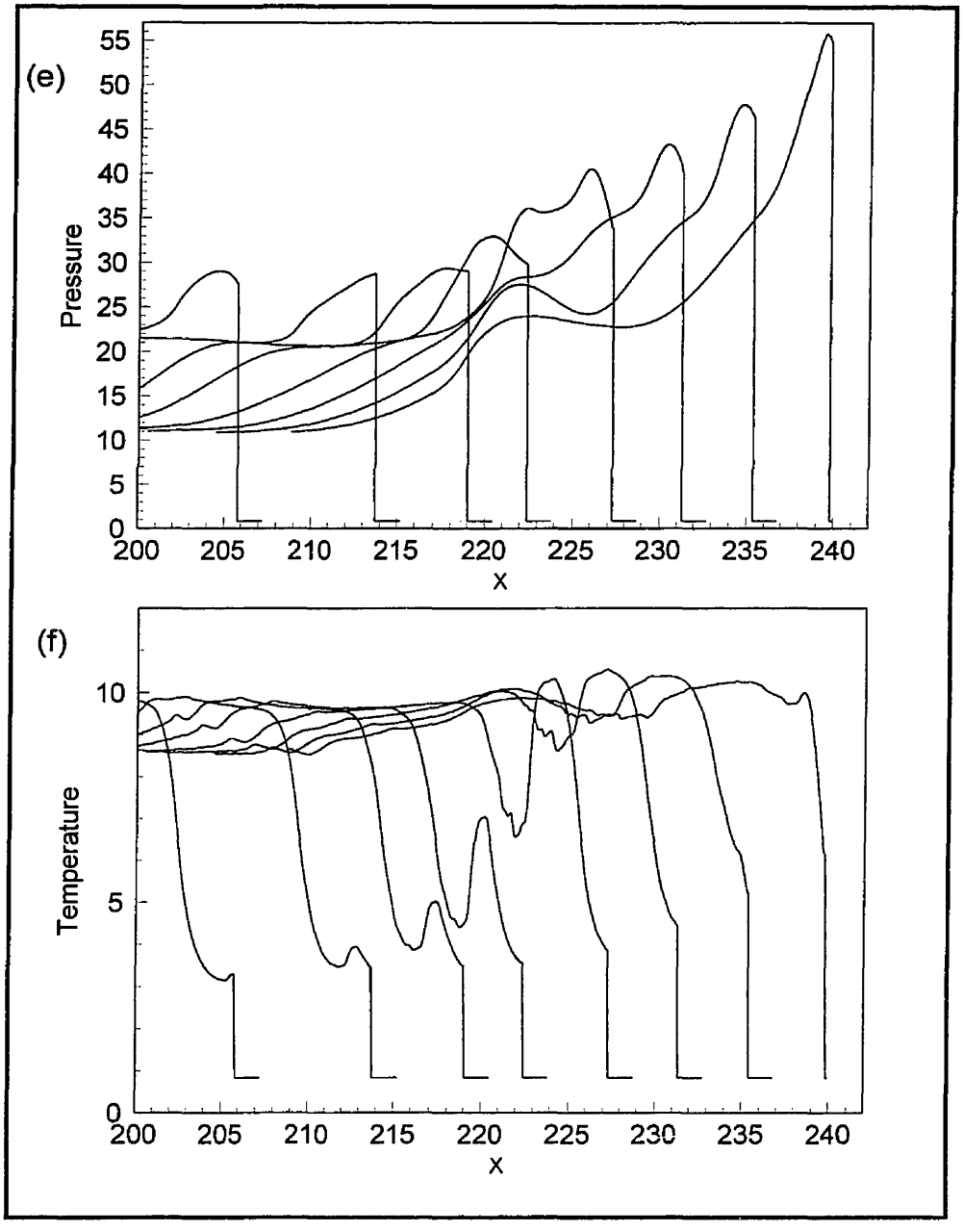

Figure 5.5. (Continued).

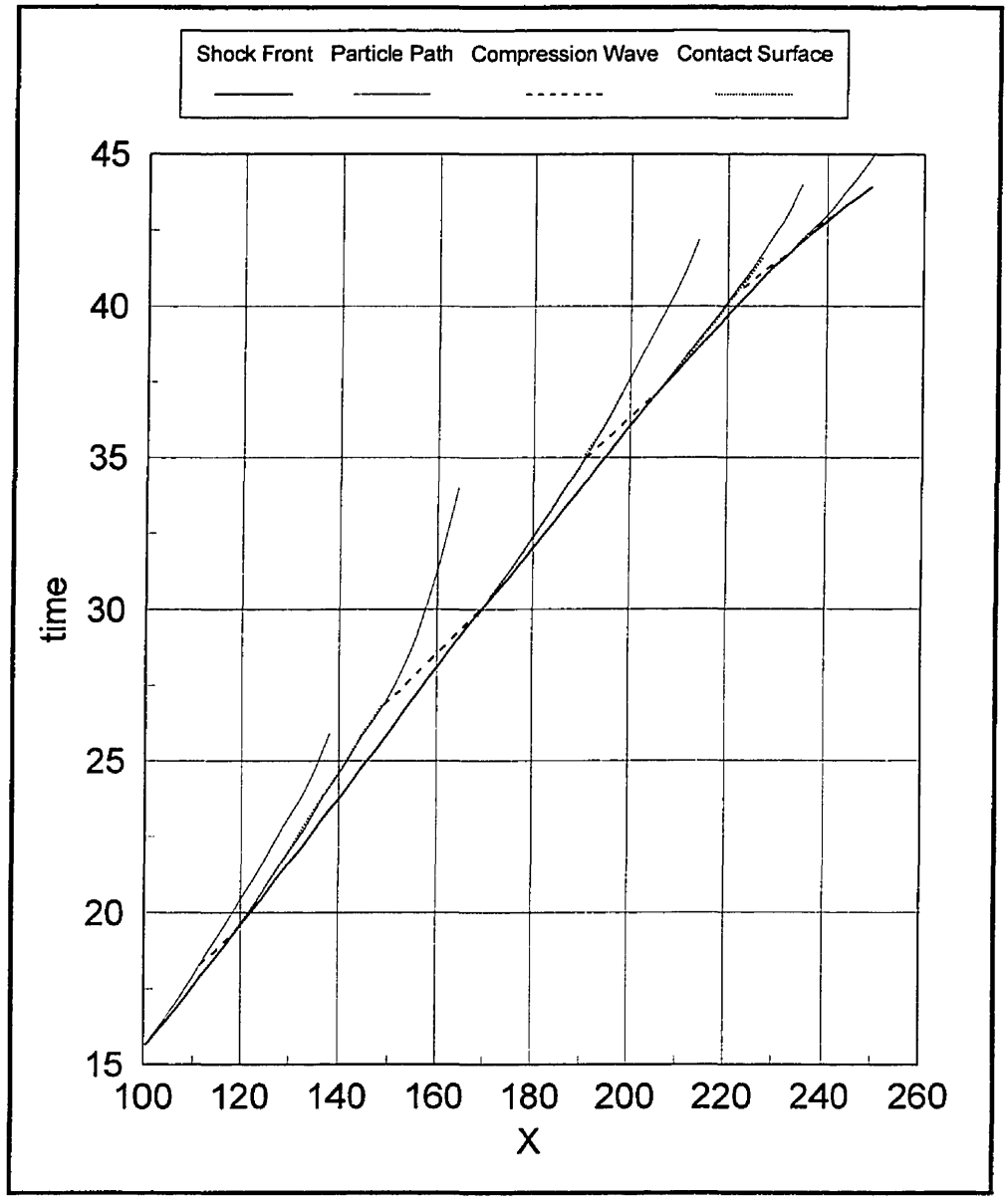

Figure 5.6. Wave diagram for the transition process and the multi-step shock merging mechanism of Fig. 5.3 ($E_a/RT_0 = 27$, $Q/RT_0 = 50$, and $\gamma = 1.2$).

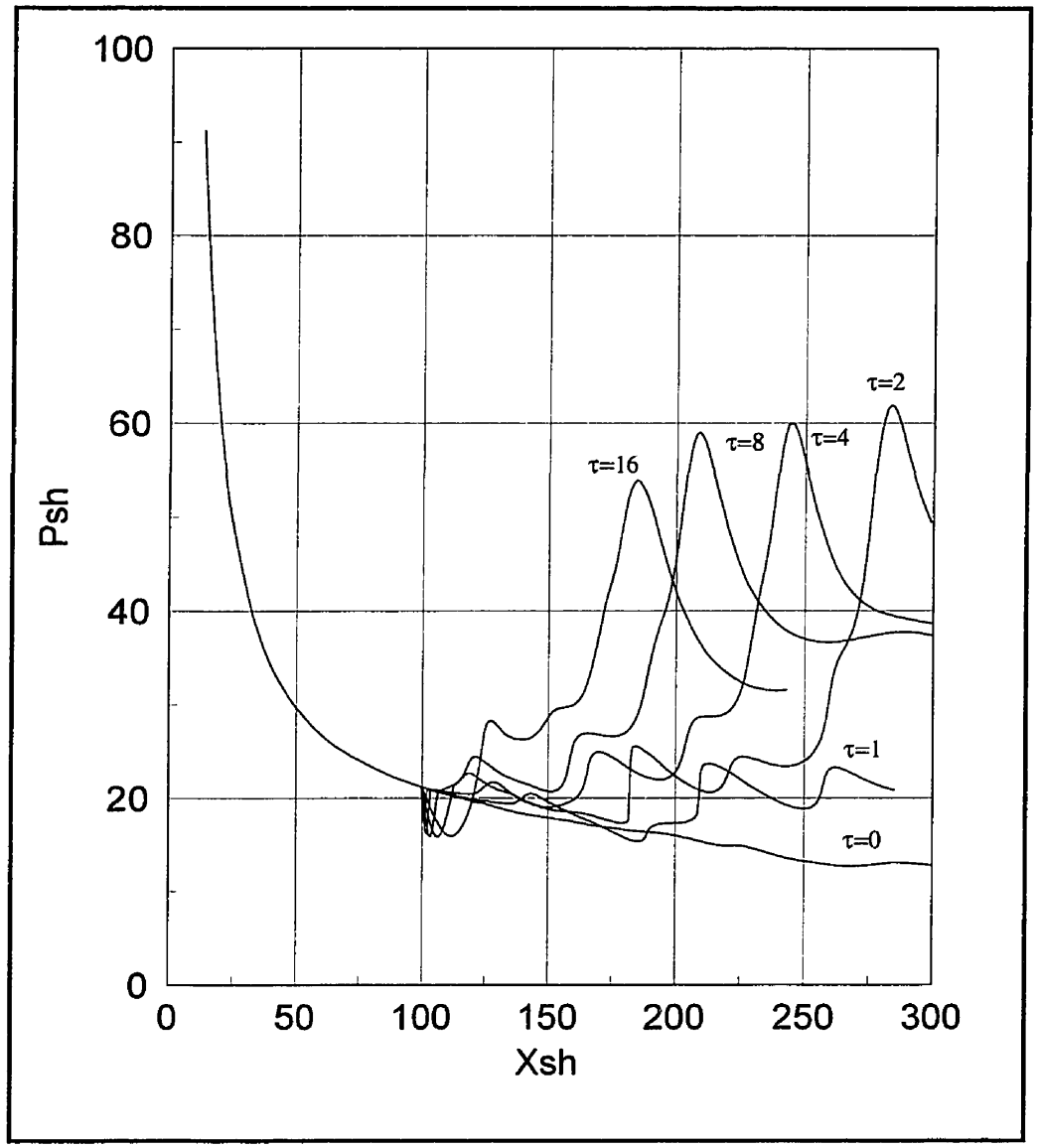

Figure 5.7. The effect of the width (W) of the density perturbation on the initiation process ($E_a/RT_o = 27$, $Q/RT_o = 50$, $\gamma = 1.2$, $E_o/p_o = 4100$, and $H = 0.4$).

$W = 0.5 * (D_{cj} / 2) * \tau$

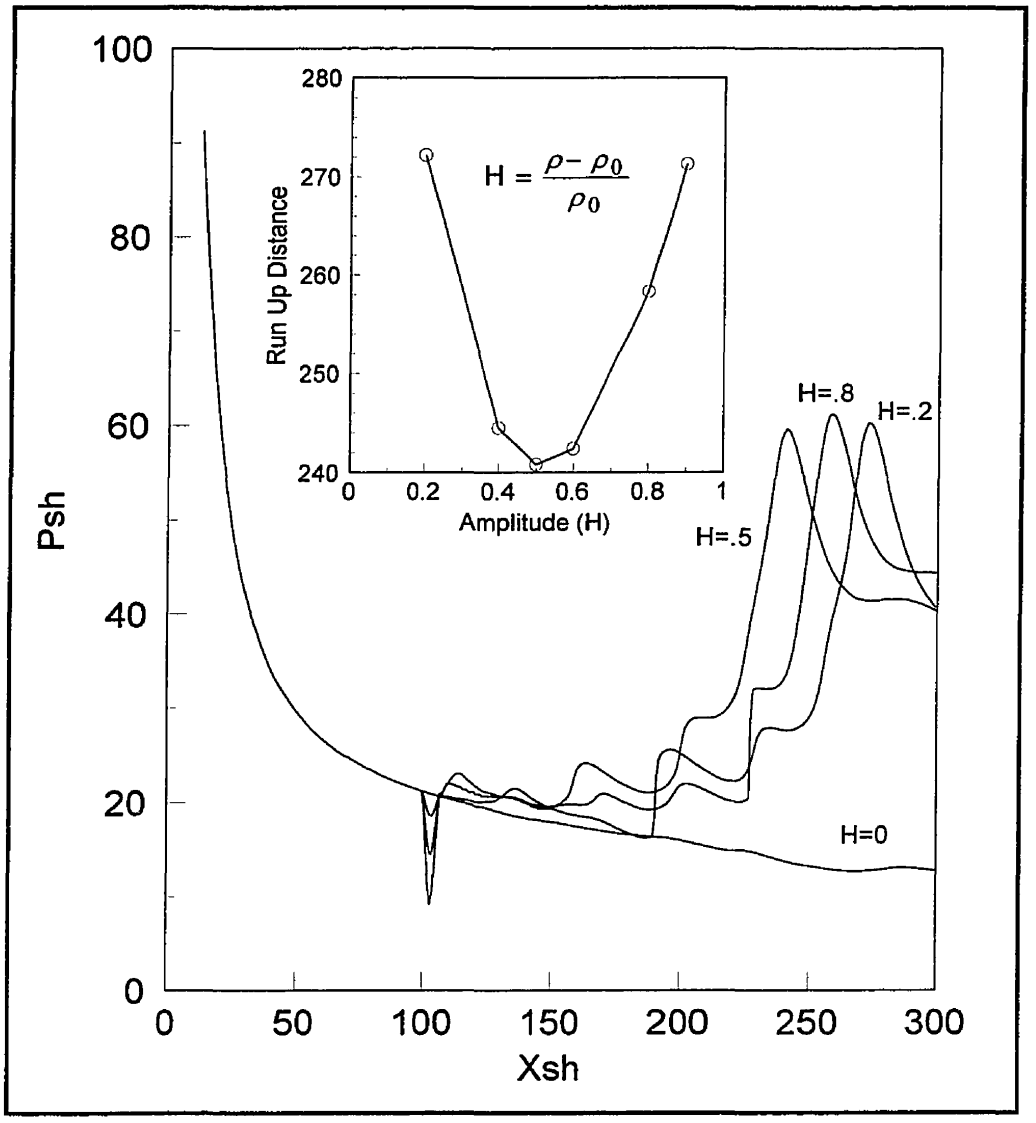

Figure 5.8. The effect of the amplitude of the density perturbation on the initiation process. The small plot shows the variation of run up distance with the perturbation amplitude ($E_a/RT_o = 27$, $Q/RT_o = 50$, $\gamma = 1.2$, $E_o/P_o = 4100$, and $W = 6$).

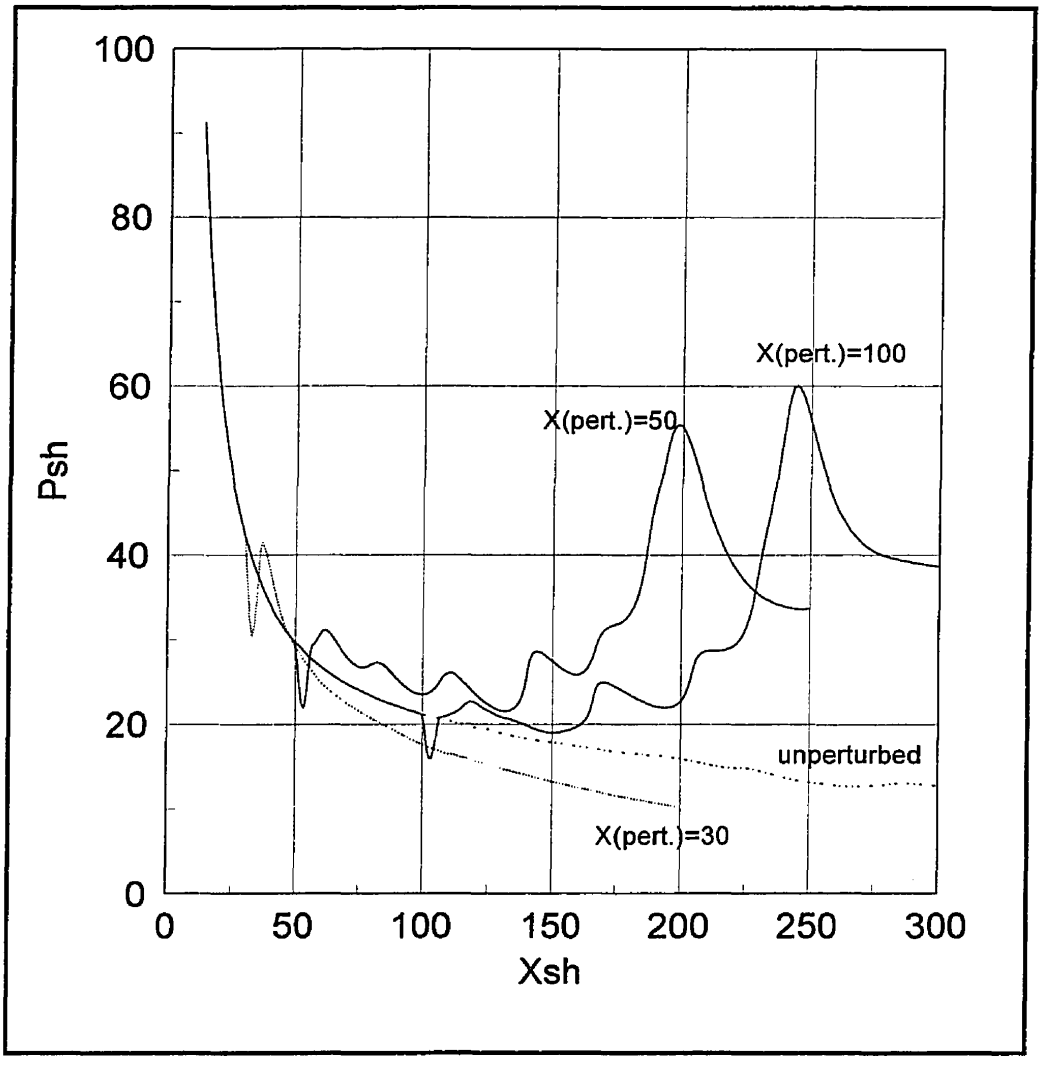

Figure 5.9. The effect of the location of the density perturbation on the initiation process ($E_a/RT_O = 27$, $Q/RT_O = 50$, $\gamma = 1.2$, $E_0/P_O = 4100$, $H = 0.4$, and $W = 6$).

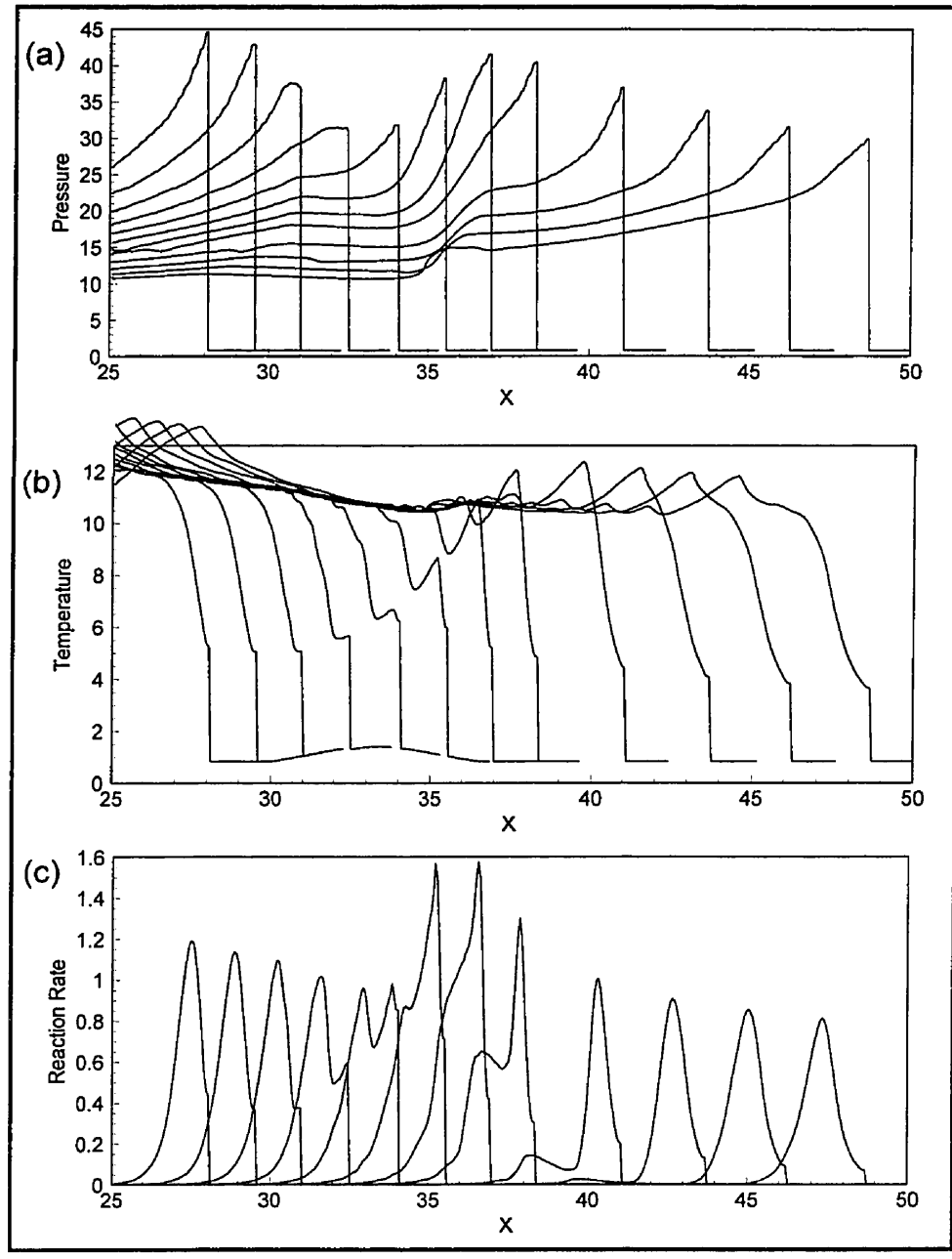

Figure 5.10. Pressure, temperature , and reaction rate profiles for initiation process in the presence of a single density perturbation located at x=30 ($E_a/RT_O = 27$, $Q/RT_O = 50$, $\gamma = 1.2$, $E_0/P_0 = 4100$, $H = 0.4$, and $W = 6$).

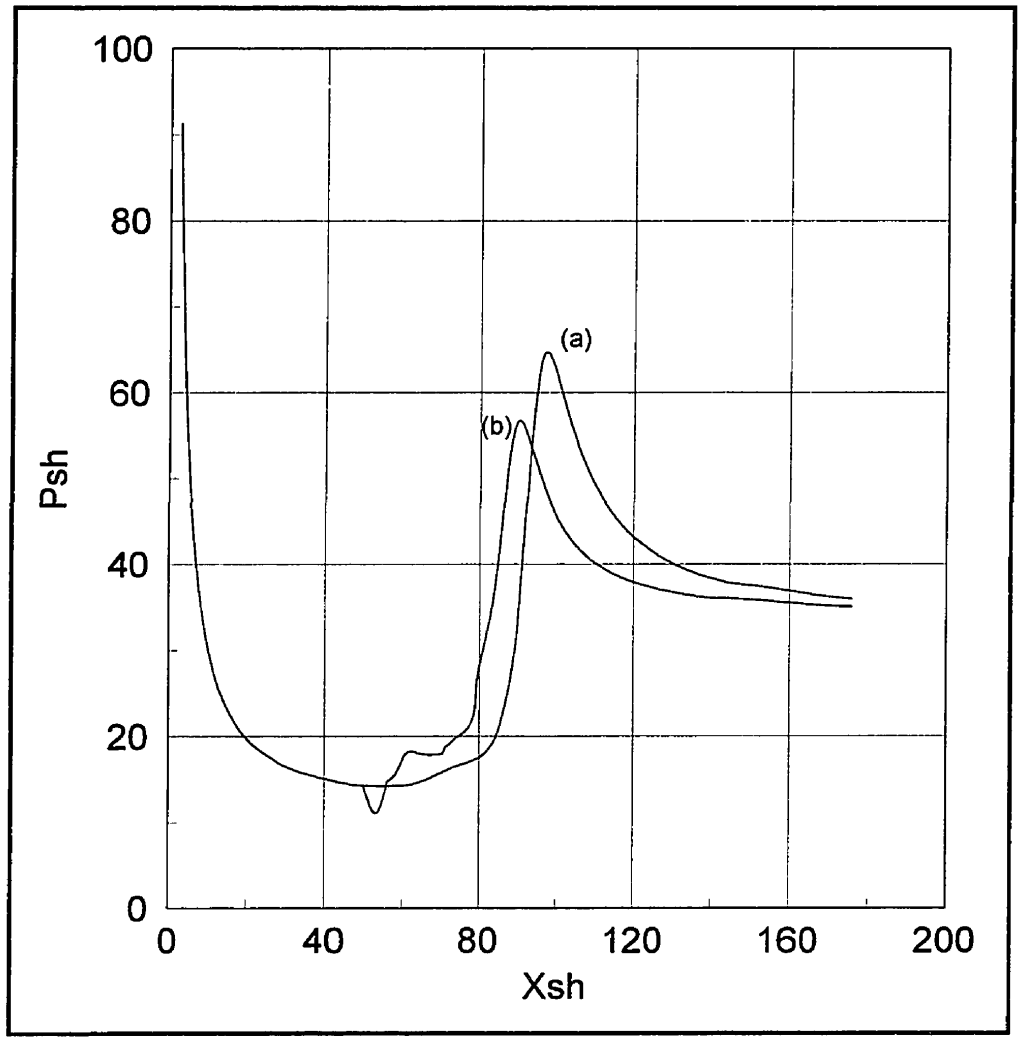

Figure 5.11. Comparison between the initiation processes with and without the presence of a density perturbation in critical initiation regime for a low activation energy ($E_a/RT_o = 21$, $\gamma = 1.2$, $Q/RT_o = 50$, $W = 6$, and $H = 0.4$).

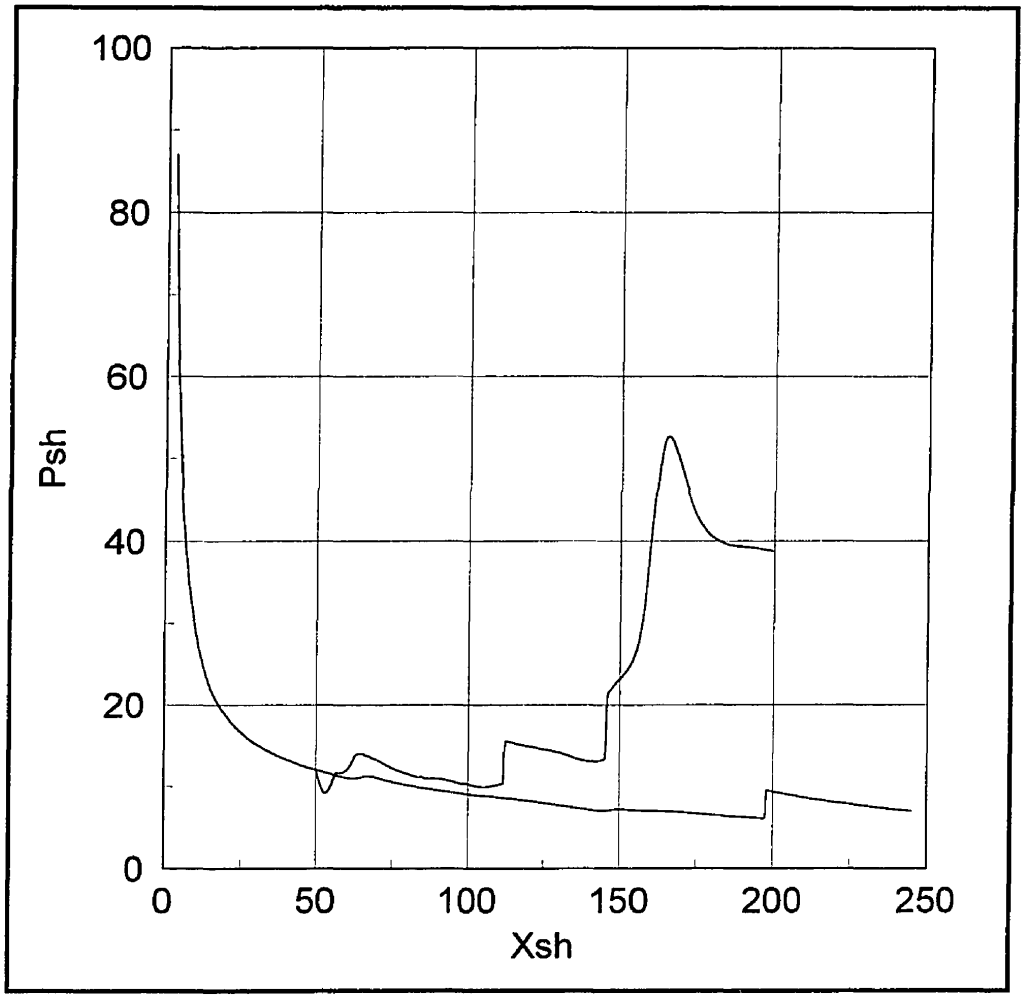

Figure 5.12. Comparison between the initiation processes with and without the presence of a density perturbation in subcritical initiation regime for a low activation energy ($E_a/RT_o = 21$, $\gamma = 1.2$, $Q/RT_o = 50$, $W = 6$, and $H = 0.4$).

IMAGE EVALUATION TEST TARGET (QA-3)

150mm

6″

APPLIED IMAGE, Inc
1653 East Main Street
Rochester, NY 14609 USA
Phone: 716/482-0300
Fax: 716/288-5989